Analysing the impact of the absence of CARD containing caspases on different forms of cell death

Ranja Salvamoser

ORCID ID # 0000-0002-1789-9898

Submitted in total fulfilment of the requirements of the degree Doctor of Philosophy

September 2018

The Walter & Eliza Hall Institute of Medical Research

Department of Medical Biology

Faculty of Medicine, Dentistry and Health Sciences

The University of Melbourne

Table of Contents

Abstract

Cell death is an important process during embryogenesis as well as tissue homeostasis in the adult. Apoptosis, pyroptosis and necroptosis are three of the major programmed cell death pathways. Dysregulation of either of these cell death pathways can promote the development of a variety of diseases, such as cancer or autoimmune pathologies.

Cysteine-dependent aspartate-specific proteases, known as caspases, exert key functions in all of these cell death pathways. Of note, certain caspases have been shown to play a role in more than one cell death pathway.

This thesis presents the functional analysis of different caspases, in particular caspase activation and recruitment domain (CARD) containing caspases and their contributions to the pyroptotic, apoptotic and other cell death pathways. We have generated a novel triple knockout mouse strain deficient for the CARD containing caspases-1, -11 and -12. We initially used this strain to improve our understanding on the contributions of caspases-1, -11 and-12 to sepsis and different forms of cell death. Previous studies have suggested a role for caspase-12 in endoplasmic reticulum (ER) stress-induced cell death. However, we were not able to attribute a role of caspase-12 to sepsis or ER stress-induced apoptosis *in vitro* and *in vivo*.
In Chapter 4 we present a study on the roles of different caspases as well as RipK3 during *Salmonella* infection *in vitro* and *in vivo*. There is evidence for a substantial functional overlap between different cell death pathways in the cellular response to pathogens, such as *Salmonella*. We examined this functional overlap of different cell death processes in the organismal and cellular response to infection by generating mice deficient for multiple caspases and also RipK3, an essential mediator of necroptotic cell death.
Upon infection with *S.* Typhimurium SL1344 strain, primary myeloid cells from caspase-1/11/12/8 RipK3$^{-/-}$ mice showed marked resistance to cell death and survived even at high bacterial loads for up to 24 hours. When infecting the caspase-1/11/12/8 RipK3$^{-/-}$ mice with the vaccine *Salmonella* Typhimurium strain, they were not able to clear the bacteria from primary organs.

Collectively, these findings provide evidence that there is substantial functional overlap between the different cell death pathways and hence the caspases involved in these processes in the cellular as well as organismal response to infection with *S.* Typhimurium and possibly other pathogens.

Lastly, I generated mice lacking all murine CARD containing caspases, i.e. caspase-1, -11, -12, -2 and -9. These preliminary analyses revealed no major defects when comparing the embryonic development of mice lacking caspases-1, -11, -12, -2 and -9 to wildtype.

Furthermore, we isolated haematopoietic stem and progenitor cells (HSPCs) from foetal livers derived from caspase-1/11/12/2/9 deficient mice and reconstituted lethally irradiated wildtype mice. Surprisingly, we did not find notable defects in the lymphoid and myeloid compartments in the caspase-1/11/12/2/9 deficient mice at steady state. In thymocyte cell death assays, cells from the quintuple caspase knockout mice still could undergo cell death, induced by the cytotoxic agent ionomycin, albeit at a delayed rate.

Declaration

This is to clarify that:

(i) This thesis comprises only of my original work towards the Doctor of Philosophy, except where indicated in the preface;

(ii) Due acknowledgement has been made in the text to all other materials used; and

(iii) The thesis is fewer than 100,000 words in length, exclusive of tables, figures, bibliographies and appendices.

Ranja Salvamoser

Preface

In accordance with the regulations of the University of Melbourne, I acknowledge that parts of this work presented in this PhD thesis involved collaboration with others.

Chapter 3 has been accepted and published online (to date) as the following paper in the journal of Cell Death & Differentiation,
2018 Aug 28. DOI: 10.1038/s41418-018-0188-2.

R Salvamoser, K Brinkmann, LA O'Reilly, L Whitehead, A Strasser, MJ Herold (2018). Characterisation of mice lacking the inflammatory caspases-1/11/12 reveals no contribution of caspase-12 to cell death and sepsis

Kerstin Brinkmann helped with the *in vivo* tunicamycin experiments and assessments (TUNEL staining and blood analysis, ALT, AST analysis) in Figure 5 and Supplementary Figure 4. Lachlan Whitehead wrote the scoring macro for the computational TUNEL scoring for Figure 5 in the publication and Supplementary Figure 4 and Lorraine O'Reilly generated rat monoclonal antibodies against caspase-1 and caspase-11 described in the Materials and Methods section. All other authors listed were involved in discussions of results and designing experiments. The other figures and data presented in the paper were exclusively obtained and analysed during my PhD.
The layout of the wider supplementary figures and tables of this publication were adapted to be in accordance to the thesis document outline guidelines. Overall, I assess my contributions to chapter 3 to be 90%.

Parts of the *in vitro* GPA work presented in Chapter 4 are the result of a collaboration with Prof. Clare Bryant and her laboratory at the Department of Veterinary Medicine in Cambridge, U.K. The initial *in vitro* phenotype discovery on our caspase-1/11/12/8 RipK3 knockout mice was made by me while visiting Prof. Bryant's lab. We followed up on this finding together with A/ Prof. Sammy Bedoui and Dr. Paul Whitney from the Peter Doherty Institute for Infection and Immunity, Melbourne.

All work with *Salmonella* was performed at the Peter Doherty institute. Some GPA experiments (Figure 4-1 and Figure 4-6) as well as the *in vivo* studies were carried out together with Paul Whitney. Paul Whitney infected all the mice used in this chapter (presented in Figures 4-2; 4-3, 4-4 and 4-5) and subsequent organ and blood processing and analysis presented in this data was carried out in collaboration. Additional experimental input, discussion of results and planning of the project was provided by the collaboration partner A/ Prof. Sammy Bedoui.
I generated the caspase-1/11/12/8 RipK3$^{-/-}$ mice as well as control mice by inter-crossing our caspase-1/11/12$^{-/-}$ mice with caspase-8 RipK3 knockout mice, generously provided by Prof. John Silke (member of my PhD committee).
The TRIF$^{-/-}$ mice as well as all *Salmonella* strains used came from A/Prof. Sammy Bedoui's laboratory.

Overall, I assess my contribution to chapter 4 to be 70%.

The work presented in chapter 5 was exclusively performed and analysed during my PhD and did not require further collaboration. The caspase-1/11/12$^{-/-}$ mice have been generated and characterised by me as described in Chapter 3. I generated the caspase-1/11/12/2/9 $^{-/-}$ embryos and mice by inter-crosses with the caspase-2$^{-/-}$ 9$^{+/-}$ mice that were already available in the Strasser lab.

This work has been supported by the Melbourne International Fee Remission Scholarship (MIFRS) and the Melbourne International Research Scholarship (MIRS).

Acknowledgements

I want to honour all the mice that involuntarily gave their lives for my research over the past 4 years. One of the toughest challenges was taking so many lives of these intelligent little creatures. I do not take this light heartedly and hope that the sacrifices made were not in vain and will benefit the scientific community.

My supervisors/ mentors:
Firstly, thank you to Marco Herold for the past 4 years. It sure was a rollercoaster ride for the both of us with regards to scientific discoveries, mistakes I made and growing as a team. I am aware that I am very stubborn and defensive and a challenge to work with at times, nonetheless you kept your cool and humour in every meeting and even if you probably were sometimes close, you never gave up on me. I think it's safe to say that this was my biggest learning curve (as predicted by Andreas in year 1). On a scientific as well as personal level. Thank you for your support, with regards to research but most importantly mentally when I was struggling. Thank you for getting me through my PhD, I'm not sure too many other supervisors would have managed as well and friendly as you did. Also, I will never misspell ASSAY again ☺ .

Andreas, thank you for the support, sometimes tough but constructive criticism and most of all kind words to help me through. I highly appreciate that I always feel welcome in your office with any problem and you take time out of your busy schedule to listen and talk things through.

Of course, thank you both for the amazing mentoring and helping me become an actual scientist and always supporting any research ideas or findings one of which now turned into what I think is an exceptionally interesting project.

The Herold lab team and MGC, always warm and welcoming and a healthy work environment.

My PhD committee: John Silke, James Vince and Marc Pellegrini. Thank you for your time, scientific input and discussions throughout my time and to all my projects.

Paul Whitney for all the fun hours in the lab, the patience and support, input on the project and good laughs.

My family, my incredible mum Birgit, who would give the last shirt off her back for us 3 kids. Thank you for pushing me to get back on that plane every time I wanted to quit, letting me travel the world even though you miss me every day and always being there for me. I could not be more proud of you and how you raised us and supported all our career goals (mostly by yourself) with everything you have! I am so proud of you every day, mum, and I cannot tell you that enough!
My two brothers, you guys are awesome and very loved!

All family and friends, the ones I left behind in Europe and who are always patiently waiting for me and the new friends I made during my time here.

And of course my Aussie family: Simon and Heather. Simon, you are an amazing friend in every way possible, this all was only possible thanks to you! Heather, thank you for everything and all you love and care over the years! xx

And thanks Hans, for making me the most resilient, determined and stubborn person out there, other than yourself.

Thanks to whomever I forgot to mention.

List of Figures

List of Tables

List of Abbreviations

AIDS	Acquired Immune Deficiency Syndrome
ADP	Adenosine Di-Phosphate
ALR	AIM-Like Receptors
APAF-1	Apoptosis-Protease Activating Factor 1
ASC	Apoptosis-associated Speck-like protein containing CARD
AV	Annexin V
ATP	Adenosine Tri-Phosphate
BCL-2	B Cell Lymphoma 2
BH3	BCL-2 Homology 3
BID	BCL-2 homology domain 3 (BH3) Interacting Domain
BMDM	Bone Marrow-Derived Macrophage
CAD	Caspase-Activated DNase
CAPS	Cryopyrin-Associated Periodic Syndrome
CARD	Caspase Activation and Recruitment Domain
Caspase	Cysteine-dependent ASPartate specific proteASE
cDNA	complementary Deoxyribonucleic Acid
CFU	Colony Forming Unit
COP	CARD-Only protein
DAMP	Damage-Associated Molecular Pattern
DD	Death Domain
DED	Death Effector Domain
DISC	Death Inducing Signalling Complex
DMEM	Dulbecco's Modified Eagle's Medium
DMSO	Dimethyl Sulfoxide
DNA	Deoxyribonucleic Acid
ELISA	Enzyme-Linked Immunosorbent Assay
ER	Endoplasmic Reticulum
ES	Embryonic Stem cells
FCS	Foetal Calf Serum
FADD	Fas-Associated protein with Death Domain
H&E	Haematoxylin and Eosin

HMGB1	High Mobility Group Box-1
HSPC	Haematopoietic Stem and Progenitor Cells
H_2O	Water
iBMDM	immortalised Bone Marrow-Derived Macrophage
ICE	Interleukin-1β Converting Enzyme
IL	Interleukin
iNTS	invasive Non-Typhoidal Serovars
i.p.	Intraperitoneally
i.v.	Intravenous
kb	Kilobases
kD	Kilo Daltons
KO	Knockout
LDH	Lactate Dehydrogenase
LPS	Lipopolysaccharide
M-CSF	Macrophage Colony Stimulating Factor
MDF	Mouse Dermal Fibroblast
MEF	Mouse Embryonic Fibroblast
MLKL	Mixed-Lineage Kinase Domain-Like protein
MOI	Multiplicity Of Infection
MOMP	Mitochondrial Outer Membrane Permeabilisation
mRNA	messenger RNA
NF-κb	Nuclear Factor kappa-light-chain-enhancer of activated B cells
NLR	Nod-Like Receptor
Nlrc	NLR family CARD domain-containing protein
Nlrp	NACHT, LRR and PYD domain-containing protein
NOD	Nucleotide-binding Oligomerisation Domain
NTS	Non-Typhoidal Serovars
PAMP	Pathogen Associated Molecular Pattern
PARP-1	Poly (ADP-ribose) Polymerase-1
PBS	Phosphate Buffered Saline
PCD	Programmed Cell Death
PCR	Polymerase Chain Reaction
POP	Pyrin-Only Proteins

PRR	Pattern Recognition Receptor
PYD	PYRIN Domain
RLR	RIG-I-like Receptors
RipK	Receptor-Interacting serine/threonine Protein Kinase
TLR	Toll-Like Receptor
TNF	Tumor Necrosis Factor
TNFR1	Tumor Necrosis Factor Receptor 1
TRADD	Tumor Necrosis Factor Receptor type 1-associated Death Domain protein
TRIF	TIR-domain-containing adapter-inducing interferon-β
wt	Wildtype
µg	microgram
µL	microliter
µM	micromolar
α	alpha
β	beta
γ	gamma

Chapter 1: Literature Review

1.1 Introduction: Caspases and their roles in cell death and inflammation

1.1.1 Caspases

Cystein-dependent ASpartate-specific ProteASEs, denoted caspases, are a family of conserved proteolytic enzymes that are involved in several programmed cell death processes and inflammation. Caspases are initially synthesised in the cell as inactive preforms, the so-called zymogens or pro-caspases [1, 2].

The discovery of Interleukin-1β-Converting Enzyme-1 (for its ability to cleave IL-1β), often called ICE and now caspase-1, marked the beginning of research on caspases. However, it was not until shortly afterwards, where studies in the nematode *Caenorhabditis elegans* on a protein called CED-3 actually revealed the role of caspases in cell death [3]. The discovery of CED-3 sparked interest in the field and in the following years a large number of related proteases were cloned and characterised. These proteases were then termed caspases as their common function as Cysteine-dependent ASPartate-specific proteinASES became clearer.

At first it was assumed that caspases are only involved in apoptosis and in the processing of pro-IL-1β in inflammation, however subsequent studies revealed broader functions for caspases in various cellular processes, including the control of cell cycling, cell motility and cell differentiation [2, 4].

Mammalian caspases have often been clustered into different groups based on various criteria, such as based on amino acid sequence similarity [1], according to structural similarities or based on similar/shared functions [2].
According to function caspases are often classified as: (1) initiator caspases (caspases-8, -9 and -10), which proteolytically activate the effector caspases during apoptosis; (2) effector caspases (caspases-3, -6 and -7) that play critical roles in the dismantling of the dying cells during apoptosis, (3) and the inflammatory caspases (caspase-1, -4, -5, -11 and -12) which promote cytokine secretion and/or trigger pyroptotic cell death (see below; Figure 1-1) [5].

However, clustering caspases based on their biological function can be misleading, suggesting the role of a certain caspase to be restricted to one category (i.e. apoptosis or inflammation). Some candidates, such as caspase-8, can also have non-apoptotic attributes. Caspase-8, known for its function in the extrinsic apoptotic pathway, has in recent years been shown to also be involved in inflammation [6, 7].
Furthermore, it is difficult to group caspase-2 based on function, since this caspase is still poorly understood. Both, apoptotic but also non-apoptotic roles for caspase-2 have been suggested, such as in maintaining genome integrity, ageing, cell cycle regulation and tumour suppression [8, 9, 10, 11].
Also, the functional clustering strategy makes it difficult to group caspase-14, because this caspase is not involved in apoptotic processes or inflammation but has a highly specific role in keratinocyte differentiation [12].
In general, the functions of caspases-2, -12 and -14 are still only relatively poorly understood [5].

Understandably, the functional clustering was often applied for simplicity; nevertheless a different, more accurate approach should be applied in the future taking into account the emerging data on caspase function in the recent years (e.g. the newly emerging functions of caspase-8 in inflammation [6, 7]).
Conceivably a more accurate approach of classifying caspases is by their overall structure.

According to structure, caspases can first be divided into those that have a short pro-domain, including caspases-3, -6, -7 -14 (Figure 1-1) and those that have long pro-domains, including caspases-1, -2, -4, -5, -8, -9, -10, -11 and -12 [13].

There are two types of pro-domains in caspases that are related to each other in structure, the CARD domain that is present in caspases-1, -2, -4, -5, -9, -11 and -12, and the DED domain that is present in caspases-8 and -10 [13]. Thus, one could further sub-divide the members of the caspase family with long pro-domains into DED-containing (caspase-8 and -10) and CARD containing (caspase-1, -2, -4, -5, 9, -11, -12) members.

The CARD and DED domains play critical roles in the activation of the caspases with long pro-domains (see also below) [14, 15]. Human caspases-8 and -10 show high homology in their protein sequence [16].

It is also noteworthy that there are differences in the nomenclature and numbers of caspases between humans and mice. In humans, 12 caspases have been identified so far: caspases-1 to 10, caspase-12 and caspase-14 [17, 18]. Mice encode for caspases-1, -2, -3, -6, -7, -8, -9, -11, -12 and -14 [13].The human caspases-4 and -5 are considered to be orthologues of mouse caspase-11 [19] and *caspase-10* is absent in the murine genome [20].

Mammalian *caspase-13* has been removed from the list of human and murine caspases as it was suggested to be a bovine-specific gene [20, 21].

All caspases are synthesised as so-called zymogens that have no or only marginal enzymatic activity. Producing an enzymatically inactive pro-form of a protease allows elaborate regulation of the activation of caspases in response to diverse stress stimuli and signalling pathways [22, 23, 24]. The caspase zymogens are comprised of a long or short pro-domain (see above), a large (p20; i.e. ~20 kDa) and a small (p10; i.e. ~10 kDa) subunit. [1, 2] (Figure 1-1).

The exact mechanism of caspase activation in apical and inflammatory caspases has not been fully resolved yet. However, it is widely accepted that caspases with long pro-domains (e.g. initiator caspases and inflammatory caspases) are activated by proximity-induced dimerisation [5, 22, 23, 25].

Initiator caspases exist as monomers and it is generally accepted, that they only require dimerisation (via platforms) to assume an active conformation [26, 27]. This model suggests that the increase in local monomer concentration drives dimerisation and thereby activation. Apical caspase activation requires large complexes with specific adaptor proteins, which recruit the pro-caspases and cause their activation. This first became apparent with the finding of the apoptosome, in which complexes between APAF-1 and cytochrome C recruit and facilitate the activation of caspase-9 [28]. The binding of pro-caspase-9 to APAF-1 is mediated by homotypic interaction of CARD domains that are present in both proteins [27, 29].

The more puzzling part of the apical caspase activation event appears to be the importance of the proteolytic cleavage that follows dimerisation with some data suggesting that the cleavage step is not absolutely essential for activation [25, 30, 31].

Caspase- 8 is responsible for triggering the extrinsic apoptotic pathway. Consistent with the caspase-9 activation model, the proximity-induced dimerisation is the commonly accepted key event for caspase-8 activation [5, 27].The activation of caspase-8 (and caspase-10) is driven by the adaptor protein FADD (sometimes also TRADD) through homotypic interactions of death domains (DD) that are present in both proteins. This interaction and caspase-8 or -10 activation occurs within the so-called death inducing signalling complex (DISC) that is formed upon stimulation of so-called death receptors, i.e. members of the TNF receptor family that contain an intracellular death domain (e.g. FAS, TNF-R1, TRAIL-R1) [5, 32, 33].However, again, the exact implications of the cleavage event remain in dispute. [25, 34, 35]. Once fully active, apical caspases can provoke effector caspase activity [22, 27, 36].
Effector caspases (caspase-3, -6 and -7) exist as preformed dimers in the cytosol that are being held inactive by a linker separating the large and small chain. To become activated a cleavage at specific aspartate residues in the linker region between the p10 and p20 subunit has to occur followed by a rearrangement event. This proteolytic activation is carried out by an activated initiator caspase, such as caspase-8 or -9 [37, 38, 39]. The p20 and p10 fragments assemble into active tetrameric ($p20_2p10_2$) effector caspases [14, 40]. Once effector caspases are catalytically active,

they can bind and cleave hundreds of substrate proteins, and thereby cause cellular demolition [41].

The inflammatory caspases, caspases-1, -4, -5, -11 and possibly -12, play critical roles in inflammation, pyroptotic cell death and the innate immune response against microbes. All inflammatory caspases carry a large N-terminal CARD domain [42]. The inflammatory caspases in mammals are all encoded by genes clustered on a single locus encompassing caspases-1, -4, -5 and-12 in humans and caspases-1, -11 and -12 in mice (see Figure 1-2). Based on amino acid sequence, the human caspases-4 and -5 appear to be the orthologues of murine caspase-11 and must have resulted from the duplication of an ancestral gene [43]. The major (direct or indirect) substrates of caspases-1, -4, -5, and -11 are the pro-forms of the cytokines IL-1β and IL-18, which both play critical roles in inflammation [19, 44, 45, 46]. Caspase-1 can also cleave and thereby activate gasdermin D, which then drives pyroptotic cell death [47, 48].
Caspase-1 is activated within the so-called inflammasome, a structure containing several adaptor proteins, some of which, like caspase-1 itself, contain a CARD domain (described in more detail below) [49, 50]. Only recently it was shown that the murine caspase-11 and the human caspases-4 and -5 can directly bind cytosolic LPS which triggers their oligomerisation and activation [51]. Of note, no interaction between LPS with other CARD containing caspases was detected [51].
The processes underlying the activation of caspase-12 are still only poorly understood [52].

Interestingly, certain caspases can play roles in both inflammation as well as cell death. Therefore, the clustering of caspases based on a single function might be misleading and thus outdated. As mentioned above, caspases-1, -4, -5 and -11 play roles in both inflammation (processing of the pro-forms of IL-1β and IL-18) and pyroptotic cell death (via proteolytic activation of gasdermin D). Moreover, caspase-8 is critical for initiation of apoptosis after stimulation of so-called death receptors (e.g. FAS, TNF-R1) but it is also critical to prevent necroptotic cell death and it can become activated during inflammation within the Nlrc4 inflammasome and thereby contributes to the maturation and secretion of IL-1β [6, 53]. This suggests that the roles of certain caspases in immune defence against pathogens and possibly other

physiological processes may be highly complex. Therefore, a caspase clustering simply by function should be avoided in the future and a more accurate approach, such as structural grouping should be applied.

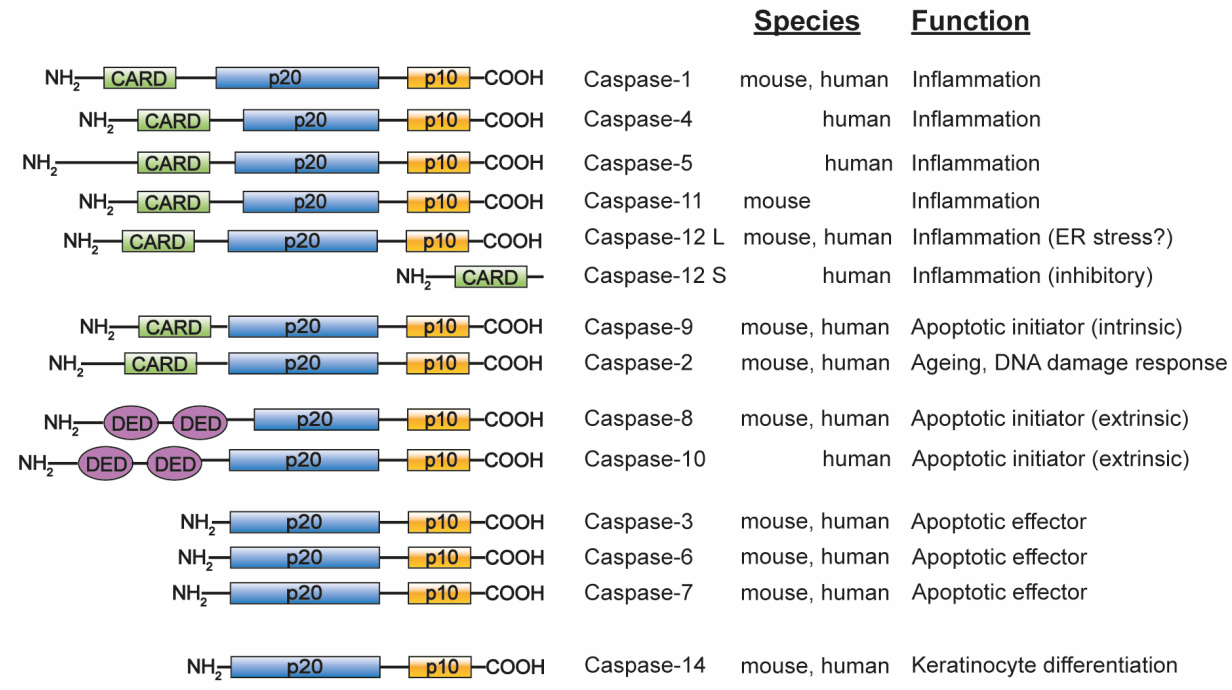

Figure 1-1: Human and murine caspases grouped according to their domain structure.

Different domains are highlighted with the CARD domain in green boxes and the DED domains in purple ovals. The p_{10} subunit indicated in orange, large p_{20} subunit depicted as blue box.

Figure based on Shalini, S. et al. Old, new and emerging functions of caspases. *Cell Death and Differentiation* 2015; **22** (4)**:** 526-39.

1.1.2 The functions of the long pro-domains in the activation of caspases

As mentioned above, different albeit structurally related motifs, collectively known as the death domain super-family, can be found in pro-domains of distinct caspases and their activators/adaptors. The death domain superfamily comprises the death domain (DD; e.g. found in FADD and the death receptors), death effector domain (DED; e.g. found in FADD and caspase-8), the caspase-activation and recruitment domain (CARD; e.g. found in APAF-1 and caspase-9) and the pyrin domain (PYD; e.g. found in ASC) [54]. The unifying feature of all members of the death domain super-family is a six helical bundle fold that is essential for their protein-protein interactions [33, 55].

CARD domains are found in caspases-1, -2, -4, -5, -9, -11 and -12 and in some of their activators/adaptors. CARD domains are interaction motifs that play a role in signal transduction during apoptosis, pyroptosis and inflammation. These domains constitute the building blocks for the assembly of multimeric protein complexes. As a result of direct interactions mediated by CARD domains large protein complexes can be formed, such as the apoptosome or the inflammasome. This can lead to proximity-induced activation of initiator or inflammatory caspases [22, 49, 56]. In regard to CARD domain containing caspases, the mechanisms of activation of caspase-12 is not fully understood and although caspase-2 has been implicated in the control of mitosis and the response of cells to defects in the alignment of chromosomes interactions, more work is needed to fully understand its function and regulation [9].

Two death effector domains (DED) are present in caspases-8 and -10 and one DED is present in their adaptor FAS-associating death domain-containing protein (FADD) [33, 54]. The DED domain, similar to the CARD, functions as a homotypic interaction module, playing a crucial role during death receptor-induced apoptosis signalling. Upon ligand (FAS ligand, FASL) binding, the surface receptor FAS becomes aggregated and this causes recruitment of the adaptor proteins FADD (and in the case of TNFR1 stimulation also TRADD) via homotypic interactions of the DD

present in the intracellular region of the death receptors and the DD present in the adaptor proteins [54]. The aggregation of FADD at the cytosolic aspect of the ligated death receptors promotes recruitment of caspase-8 (and in humans also caspase-10) via homotypic interactions of death effector domains (DED) that are present in both FADD and the pro-domains of these caspases [33]. This forces a conformational change in caspase-8 (or caspase-10) that causes the activation of these proteases and this can be followed by autocatalytic processing (see above) [35].

The pyrin domains (PYD) are present in proteins that act as activators or regulators of the inflammasome. Inflammasomes serve as multimeric protein platforms and are crucial components of the innate immune system in response to danger signals and pathogens.

Pyrin domains are present in many AIM-like receptors (ALR) or Nod-like receptors (NLR) (e.g. Nlpr1, Nlrp2, Nlrp3, Aim2) and also in the adaptor protein ASC [57]. The adaptor protein ASC contains both a CARD and a PYD domain and thereby can link CARD containing pro-caspase-1 to the pyrin containing ALR or NLR [58] during inflammasome assembly. The assembly of this multi-protein complex is critical for inflammasome formation and the activation of caspase-1 [57].

Apart from its important roles in pattern recognition receptors (PRRs) and ASC during inflammasome assembly, some pyrin-containing NLRs, like Nlrp12 and Nlrp4, have been shown to act as regulators during NF-κb signalling [59, 60].

Furthermore, some primate-specific proteins exist, that consist of only the pyrin domain and are thus termed pyrin-only proteins (POPs) [61]. These proteins can act as negative regulators in NF-κB signalling and inflammasomes assembly for example by binding to the sensor, thereby inhibiting inflammasome assembly and zymogen activation [62, 63, 64, 65].

However, the exact function of POPs is still poorly defined and requires further investigation.

1.1.3 Caspase-12 and the CARD-only protein family (COP)

Caspase-12 is a CARD containing protein encoded on murine chromosome 9 downstream of the *caspase-1* and *-11* genes and in the human genome this gene is located on chromosome 11 together with the genes for caspases-1, -4 and -5 (see Figure 1-2) [52]. In humans, two different forms of caspase-12 exist: the full-length form of the protein (Casp12l), and a truncated short form (Casp12s) that is caused by a single nucleotide change that gives rise to an early stop codon. The short form is found in the Caucasian and Asian (or new world) populations, whereas the full-length caspase-12 is only present in sub-Saharan African populations. Overall about 20% of people with an African background express full-length caspase-12 [66, 67]. It has been proposed that the mutation preventing the expression of full-length caspase-12 must have occurred before the migration of humans out of Africa, and that this was followed by selective pressure either for a function that is uniquely exerted by caspase-12 short or against a function provided by full-length caspase-12. Expression of a proteolytically inactive form of this putatively inflammatory caspase was postulated to be advantageous as humans were confronted with different pathogens and possibly other environmental factors when entering Asia and Europe [67].

The most frequent variant of caspase-12 in Caucasians and Asians contains a premature stop codon (TGA) instead of an Arginine (CGA) at amino acid position 125 in exon 4 [66].

The short form of caspase-12 consists mainly of the CARD motif and can therefore be grouped as a member of the CARD-only protein (COP) family [68]. Being co-located with the genes for caspases-1 and -11 in mice or the genes for caspases-1, -4 and -5 in humans, a function of caspase-12 in inflammation and the response to microbial infection seems likely. Consistent with this hypothesis, regulated expression of the gene for caspase-12 has been demonstrated in human retinal pigment epithelial cells when stimulated with pro- or anti-inflammatory stimuli [69]. One study has suggested that caspase-12 acts as a caspase-1 inhibitor thereby restricting the development of sepsis [70]. Since most humans express a catalytically inactive form of

caspase-12, (expressing the CARD domain but lacking the active centre) might suggest that they are more protected from sepsis, while sub-Saharan Africans express full-length caspase-12 and hence have a stronger sepsis phenotype. However this inhibitory function of caspase-12 on caspase-1/inflammasome could not be reproduced by an independent follow-up study [71].

As mentioned above, the short form of caspase-12 that is expressed in most humans shares structural similarities to other CARD-only proteins (COPs). To date this protein family is comprised of five members: COP1/Pseudo-ICE, INCA, ICEBERG, Nod2-S and caspase-12s [68]. All members of this group except for Nod2-S are found within the inflammatory gene locus (Figure 1-2) and COP1/Pseudo-ICE, INCA and ICEBERG share a high amino acid identity with the CARD domain in caspase-1 [65, 68, 72]. Interestingly, COPs appear to be a recent evolutionary development, since these proteins are only found in higher primates but are absent in mice or rats. The genes encoding these proteins most likely emerged by gene duplication events of *caspase-1* [72, 73].

COPs lack enzymatic activity and are thought to function as dominant negative regulators during the inflammatory and innate immune response in humans and other primates [65, 72, 73, 74]. Since COPs show amino acid sequence similarity to the CARD domain of caspase-1, these proteins have the ability to bind to pro-caspase-1 thereby preventing inflammasome assembly and its activation [65]. Additionally, ICEBERG and COP/ Pseudo-ice have been shown to interact with active caspase-1 and thereby block IL-1β production [74, 75].

Even though the COPs are thought to have a role in regulating inflammatory responses and immune responses against microbes, only very few studies have been reported on their functions within the whole animal, such as through analysis of knockout mice. Should the COPs be confirmed to function as potent negative regulators of inflammation, they might be of interest for the development of novel therapies, for example by generating low molecular weight compounds that can mimic the function of these proteins, akin to the BH3 mimetic drugs that mimic the function of BH3-only proteins to inhibit the pro-survival BCL-2 proteins and are

showing success in the treatment of certain cancers, such as chronic lymphocytic leukaemia (CLL) [72].

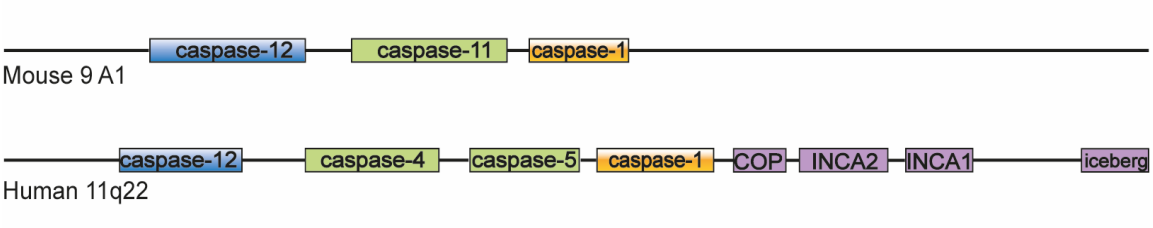

Figure 1-2: Comparison of the inflammatory gene locus in mouse and human.
Caspases-4 and -5 in the human genome locus are thought to be the result of a gene duplication event of an ancestral gene of *caspase-11* gene. Purple boxes represent genes coding for CARD-only proteins.
Figure adapted from Martinon F, Tschopp J. Inflammatory caspases and inflammasomes: master switches of inflammation. *Cell Death and Differentiation* 2007; **14**(1)**:** 10-22.

1.2 Major programmed cell death pathways

1.2.1 Apoptosis

Programmed cell death (PCD) is an evolutionary conserved process important for tissue homeostasis and the removal of unwanted cells [76]. When apoptosis was initially discovered by Kerr, Wyllie and Currie in 1972, it was thought to be the only form of PCD [77]. However, in recent years several other pathways of programmed cell death, such as pyroptosis, necroptosis and autophagy have broadened the spectrum. Hallmarks of apoptosis include chromatin condensation, inter-nucleosomal DNA cleavage, PARP cleavage, phosphatidylserine exposure and eventually cell shrinkage and the formation of "apoptotic bodies" [78]. Two apoptotic pathways have been identified, the so-called BCL-2 regulated (also called intrinsic, stress-induced or mitochondrial) and the death receptor activated (also called extrinsic) pathways (Figure 1-3a and b). The BCL-2 regulated apoptotic pathway is activated in response to developmental cues, growth factor/nutrient deprivation, DNA damage, ER stress or a broad range of cytotoxic drugs. The death receptor apoptotic pathway can be activated by certain members of the TNF family of extracellular ligands, such as FAS ligand (FASL), TNF or TRAIL [79, 80].

The BCL-2 regulated apoptotic pathway is controlled by the BCL-2 family proteins that can be divided into three sub-groups: the pro-apoptotic BH3-only proteins (BIM, BID, PUMA, NOXA, BMF, HRK, BIK and BAD) that initiate apoptosis signalling, the pro-apoptotic effectors of apoptosis (BAX, BAK, BOK), which have 4 BH (BCL-2 homology domains) and the anti-apoptotic members (BCL-2, BCL-XL, BCL-W, MCL-1, A1/BFL-1 and possibly BCL-B) that are critical for cell survival [81, 82, 83]. In healthy cells, BAX and BAK are kept in check by the pro-survival BCL-2 family members [84]. In response to cell stress, the pro-apoptotic BH3-only proteins become upregulated (transcriptionally and/or post-transcriptionally) and initiate apoptosis signalling either indirectly by inhibiting the function of the anti-apoptotic BCL-2 family

members, thereby liberating BAX and BAK, and/or by directly activating these effectors of apoptosis [85, 86]. Once active, BAX and BAK form pores in the outer mitochondrial membrane (MOMP = mitochondrial outer membrane permeabilisation), thereby inducing the release of cytochrome C and other apoptogenic factors (e.g. SMAC/DIABLO) from the inter-mitochondrial space into the cytosol. Cytochrome C together with Apaf-1 form a protein scaffold known as the apoptosome that facilitates the activation of the initiator caspase-9, through a conformational change which is followed by auto-proteolysis [27, 87]. Active caspase-9 can then proteolytically activate the effector caspases, caspases-3, -6 or -7. These effector caspases can cleave hundreds of cellular proteins and thereby unleash the demolition of the doomed cells.

The death receptor pathway is initiated when ligands of the tumour necrosis factor family bind to their cognate receptors, the death receptors that are members of the TNF receptor family. Ligation of death receptors causes assembly of an intracellular death inducing signalling complex (DISC) that drives activation of the initiator caspase-8. Like activate caspase-9, active, caspase-8 can proteolytically activate the effector caspases-3, -6 and -7 [88], which then cleave hundreds of cellular proteins to cause cell demolition. In certain cell types (called type 1), such as thymocytes or mature lymphocytes, direct activation of the effector caspases by caspase-8 is sufficient for efficient induction of apoptosis [89]. In so called type 2 cells (e.g. hepatocytes, pancreatic ß cells) this extent of caspase activation is insufficient for cell killing and efficient induction of apoptosis requires an amplification loop that involves caspase-8 mediated proteolytic activation of the pro-apoptotic BH3-only protein BID. Activated BID, called tBID, activates the apoptosis effectors BAX and BAK, either directly or indirectly by binding to the anti-apoptotic BCL-2 family members, thereby unleashing BAX and BAK (see above) [89]. This causes MOMP and increased activation of the effector caspases by caspase-9 (see above). Effector caspases cleave hundreds of cellular proteins and this causes directly or indirectly, for example via proteolytic activation of the DNAse CAD, the dismantling of the cells undergoing apoptosis [80, 90, 91]. Throughout this killing process, the integrity of the plasma membrane is maintained. The dying cells are broken down into small apoptotic bodies only at a late stage and this probably occurs only in tissue culture,

whereas within an organism cells are engulfed by phagocytes at an early stage of apoptosis (prior to the formation of apoptotic bodies). Apoptotic cells are recognised and engulfed by phagocytes or other neighbouring cells after the exposure of so-called "eat me signals", which includes the exposure of phosphatidylserine (PS) on the outer leaflet of the plasma membrane [92]. Cells dying via apoptosis are cleared rapidly and in a "clean manner", thereby avoiding an inflammatory response [93, 94, 95].

1.2.2 Necroptosis

Necroptosis is a genetically encoded regulated form of necrotic cell death, whereby dying cells release their cell content and in doing so can induce an innate immune response (Figure 1-3c). The key players in necroptosis are the kinases RipK1 and RipK3 and MLKL, the effector of cell killing in this pathway [96, 97, 98].

Necroptosis can be induced by the ligation of death receptors (e.g. TNF-R1, FAS) or pathogen recognition receptors (e.g. TLR3, TLR4) or stimuli that activate intracellular receptors that respond to constituents of intracellular pathogens. These stimuli cause the activation of the kinase activity of RipK1. RipK1 can then phosphorylate RipK3 causing its auto-phosphorylation and oligomerisation [98, 99]. This is followed by another phosphorylation step by which RipK3 activates MLKL [100, 101]. Once phosphorylated, MLKL undergoes conformational changes and translocates to the plasma membrane where it integrates into the membrane and causes its rupture and hence cell lysis with release of cellular content into the extra-cellular space, thereby causing inflammation [102, 103, 104, 105, 106, 107, 108].

1.2.3 Pyroptosis (and inflammation)

Organisms have evolved multiple processes to protect themselves against harmful pathogens. These processes include responses of both the innate and adaptive immune systems that function to recognise and react to pathogens and tissue damage. The formation of inflammasomes and ensuing pyroptotic cell death and production of the inflammatory cytokines IL-1β and IL-18 in innate immune cells has been described as a frontline response of the host immune defence that is crucial for pathogen clearance and wound healing [109].

The pyroptotic cell death pathway is activated by the human caspases-1, -4 and -5 or the murine caspases-1 and -11 [110, 111] (Figure 1-3 d and e). Upon sensing molecular constituents from microbes or infected neighbouring cells, caspase-1 and/or caspases-4, -5 and -11 are activated. These caspases are capable of proteolytic processing of the inert precursors of the cytokines thereby cause an inflammatory response to attract other immune cells to the site of infection to promote clearance of the pathogens and infected cells [19, 45, 110, 111]. Caspases-1, -4, -5, and -11 can also trigger pyroptotic cell death. This is achieved by proteolytic activation of gasdermin D, the N-terminal fragment of which translocates to the plasma membrane to cause cell lysis via pore-formation [47]. In contrast to apoptosis, this pyroptotic cell death causes inflammation [112, 113, 114].

Inflammasomes are macromolecular protein scaffolds that facilitate the activation of inflammatory caspases, such as caspase-1. Inflammasomes contain any of the (NOD)-like receptors, NLRs (e.g. AIM2, Pyrin, Nlrp1, Nlrp3, Nlrc4), caspase-1 and in some cases the adaptor protein apoptosis-associated speck-like protein containing a caspase-recruitment domain (ASC). ASC consists of an N-terminal pyrin and a C-terminal CARD domain, which are both necessary to form a link between Pyrin-containing NLRs and the CARD-domain of caspase-1 in order to form the inflammasome [42, 111]. Specific homotypic protein-protein interactions between the Pyrin domains as well as homotypic CARD domain interactions are crucial for the assembly of the inflammasomes. The formation of this complex is thought to serve

in a similar function to the "apoptosome" (APAF-1, cytochrome C and caspase-9) for the activation of caspase-9. The caspase zymogens are recruited via their CARD domains and activated by induced proximity mediated oligomerisation. The best studied inflammasome to date is the Nlrp3 inflammasome, consisting of caspase-1, Nlrp3 and adaptor protein ASC [49].

Cells of the innate immune system are able to recognise so-called damage - associated molecular patterns (DAMPS) and pathogen-associated molecular patterns (PAMPs) via their pattern recognition receptors (PRRs) [49, 115]. PAMPs are conserved microbial signature molecules, such as LPS as a component of Gram-negative bacterial cell walls or viral RNA [116]. DAMP specific PRRs become activated upon sensing host derived danger signals, such as uric acid, ATP or cytokines which are released upon insults to the host (microbial or non-microbial) [116, 117, 118].

The activation of caspases-1 and -11 (human caspase-4, -5) requires a two-step stimulation process. A first so-called priming signal is sensed by membrane bound PRRs, and this is followed by a second cytosolic signal that is sensed via intracellular PRRs (called the activation step) [49, 117]. The receptors crucial for both of these steps can be found on the membrane of a cell, in lysosomal or endosomal compartments or in the cytoplasm. PRRs can be divided into the Toll-like receptors (TLRs), RIG-I-like receptors (RLRs), cytoplasmic DNA sensing AIM2-like receptors (ALR) and nucleotide-binding oligomerisation domain (NOD)-like receptors (NLRs) [49, 119].
These sensor proteins differ in their localisation within a cell [120]. TLRs are found in the plasma membrane of a cell or on endosomes and respond to extracellular stimuli, whereas RLRs, ALRs and NLRs reside in intracellular compartments [49, 119].
Once a priming signal (signal 1) is sensed and intracellular signalling pathways are stimulated, the activation signal (signal 2) causes the activation of either caspase-1 or murine caspase-11 (human caspases-4 and -5). Pyroptosis can be caspase-1-dependent, via the so-called canonical pathway or caspase-1-independent, via the non-canonical pathway [49, 109, 121, 122] (see Figure 1-3). The non-canonical inflammasome pathway has been reported to be activated by intracellular LPS [121]. The expression of pro-caspase-11 and other components of the inflammasome components, such as Nlrp3, as well as the expression of the inactive precursors of

IL-1β and IL-18 are induced once NF-κB signalling is triggered via a PRR [121, 123, 124]. The second signal in the non-canonical pyroptotic pathway is provided by cytosolic LPS that is released by Gram-negative bacteria [122, 125]. It has been reported that LPS directly binds to the zymogen of caspase-11. This suggests that this caspase can function both as a cytosolic sensor of a pathogen derived signal and as an initiator caspase. Once active, caspase-11 will trigger pyroptosis via cleavage of gasdermin D (see above) and promote the secretion of certain cytokines (IL-1α and HMGB1) [114, 118, 121]. Moreover, caspase-11 can trigger the activation of the caspase-1-dependent inflammasome in a manner yet to be identified.

The expression of caspase-1 for canonical inflammasome signalling does not require a priming signal; the zymogen of this caspase is constitutively expressed in several cell types, particularly those of myeloid origin [126]. However, the priming signal is necessary for the synthesis of other components of this pathway, such as intracellular NLRs and the precursors of the cytokines, IL-1β and IL-18 [49]. Once a second DAMP or PAMP is sensed inside a cell, the formation of an inflammasome is triggered. Such inflammasome assembly drives caspase-1 activation via conformational changes that are often followed by autocatalytic cleavage [22, 111, 127]. Active caspase-1 can directly process pro-IL-1β [128] and pro-IL-18 into their active forms and thereby promote their secretion. Active caspase-1 can also cleave gasdermin D [129]. The N-terminal fragment of gasdermin D can oligomerise to form pores in the plasma membrane causing cell lysis and a form of cell death that is highly pro-inflammatory [47, 112, 130].

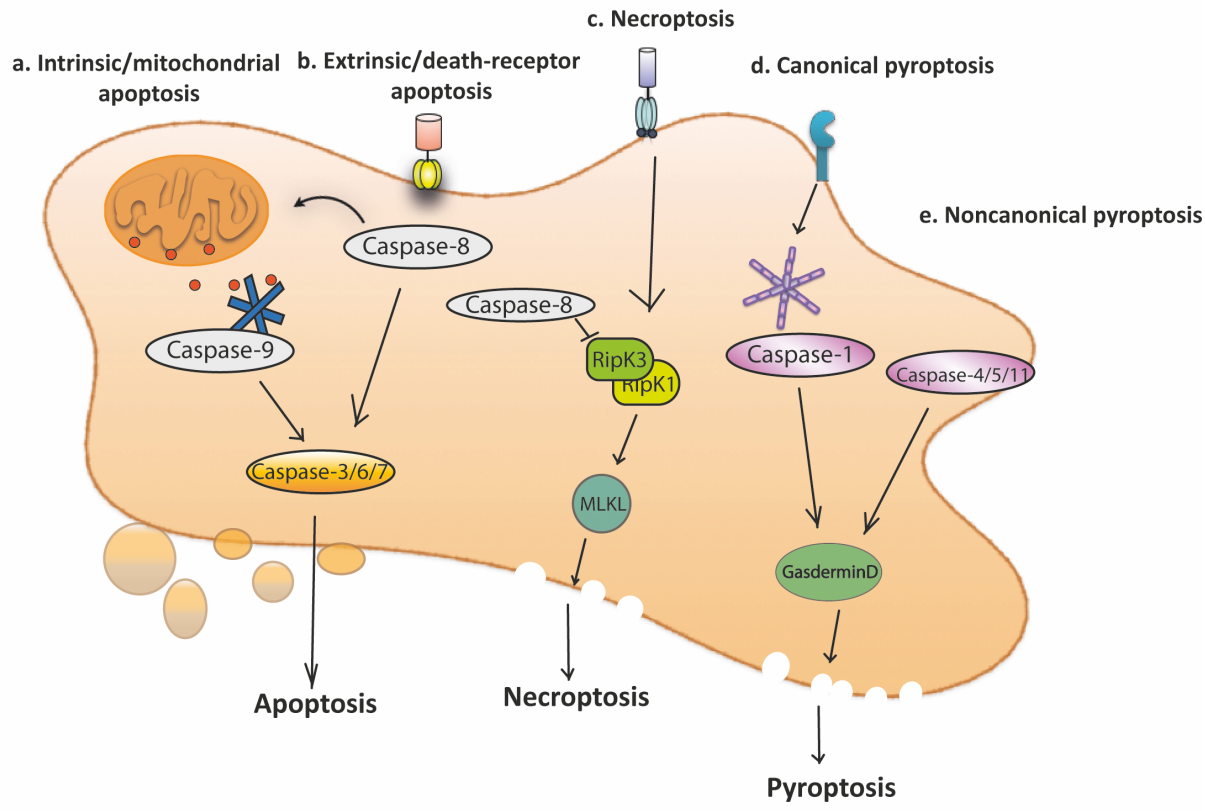

Figure 1-3: Overview of programmed cell death pathways and their main components.

The major cell death pathways, apoptosis, pyroptosis and necroptosis and their major components are shown. A feature shared by all these pathways is the requirement for caspases (initiator caspases depicted as grey circles, effector caspases as orange ovals and inflammatory caspases in purple). **a, b** BCL-2-regulated apoptosis involves caspase-9 activity; death-receptor-mediated apoptosis is dependent on caspase-8 function. **c** Necroptosis is inhibited by caspase-8 and is triggered when RipK1 and RipK3 activate MLKL. **d** Pyroptosis requires the activity of either caspase-1 (canonical inflammasome) or **e** caspase-11 (non-canonical inflammasome) to become activated.

1.3 Caspases as potential therapeutic targets in inflammation and diseases caused by defects in cell death

As mentioned above, caspases play important roles in various cellular processes. Some caspases can even be involved in more than one process, such as in the case of caspase-8 which plays an essential role in death receptor-induced apoptosis, in the inhibition of necroptosis and in the processing of the precursors of IL-1β and IL-18 during inflammation (Figure 1-3). The critical role of caspases in diverse cellular processes and their abundance across species spanning from the nematode *C. elegans* to humans, highlights the necessity to tightly regulate their enzymatic activity [131].

Abnormalities in caspase activation have been implicated in certain diseases [56]. Aberrant death of cells that should normally survive (e.g. long-lived neurons) associated with abnormally increased caspase activation has been implicated in degenerative disorders, such as neurodegenerative diseases. Conversely, given that certain caspases are implicated in immune defence and the production of inflammatory cytokines, defects in their activation can cause immune-deficiency [132]. An adequate immune response is crucial for the clearance of invading pathogens but after this threat has been overcome, immune responses must be terminated to prevent unwanted destruction of healthy tissues. Thus, insufficient caspase activation may result in a failure of clearing a pathogen, causing morbidity and possibly mortality in the host. Conversely, abnormally increased caspase activation may cause excess inflammation with associated pathologies. For example, inflammatory bowel disease, type 2 diabetes, atherosclerosis, Crohn's disease and Alzheimer's disease have all been linked to aberrations in the regulation of the inflammasome [118, 132, 133, 134, 135].

The search for caspase inhibitors began with the discovery of caspase-1 (initially called ICE for interleukin-1β converting enzyme) as the critical mediator of the release of bio-active IL-1β. IDUN, Pfizer and Merck have developed several small

molecule compounds that bind to the active sites of caspases and thereby inhibit their enzymatic activity, either in an irreversible or reversible manner [136, 137].

For example, the pan-caspase inhibitor Emricasan, originally identified by IDUN Pharmaceuticals, shows potent anti-apoptotic and anti-inflammatory properties and was initially used as a drug for treating liver disease [138]. Moreover, recent data suggests that its applications could potentially be extended in the future for cancer treatment in combination with other drugs (e.g. SMAC mimetics) [139].

With IL-1β being a key driver of inflammation, inhibitors of caspase-1 appear to be attractive compounds for the treatment of diseases that are associated with abnormally increased levels of IL-1β, such as type 2 diabetes or cryopyrin-associated periodic syndromes (CAPS). CAPS and other inflammatory diseases are often linked to mutations in the *Nlrp3* gene causing an overproduction of IL-1β [132, 135].

Generally, two ways are used today in inflammatory drug design: designing drugs that bind to the IL-1 receptor (e.g. Anakinra) thereby blocking the signal transduction or binding of the drug directly to IL-1 (e.g. Rilonacept and Canakinumab) thereby mediating its pro-inflammatory effects [140]. In 1993 Anakinra was released as the first IL-1 receptor agonist with the capacity to block both, IL-1α and IL-1β [141]. However, although Anakinra has proven successful in the treatment of gout and periodic fever syndrome patients, inhibitors of caspase-1 have yet to show efficacy in these or any other inflammatory diseases [142]. An explanation for this may be that Anakinra blocks both IL-1α and IL-1β signalling, whereas inhibitors of caspase-1 only impact Il-1β (and IL-18) signalling.

Two IL-1β neutralising drugs (Rilonacept and Canakinumab) were released shortly after Anakinra was accepted for treatment. The antibody Rilonacept acts as IL-1β inhibitor and was designed by Regeneron Pharmaceuticals and approved for the treatment of CAPS [140]. Canakinumab (by Novartis) is a human monoclonal antibody specifically targeting IL-1β, approved in 2009 for treatment of different forms of cryopyrin-associated periodic syndromes (CAPS) [140, 141, 142]. These (and other) drugs are also in clinical trials for treatment of other conditions such as diabetes and cardiovascular disease [143].

Interestingly, in some cancer models, particularly models of AML, inhibitors of caspase-8 were shown to kill malignant cells *in vitro* and even *in vivo* [139, 144]. The

explanation for this is that these tumour cells produce small amounts of TNF and when caspase-8 is blocked this unleashes MLKL dependent necroptosis in these cells.

However, there are a number of challenges that need to be considered for the deployment of caspase inhibitors for the treatment of disease, in particular because there exist so many caspases with overlapping functions and the fact that several caspases operate in several cellular processes.

The type of cell death to be inhibited needs to be identified as well as the exact time during the course of the disease when caspase inhibitors should be administered. Aberrant cell death and/or inflammation might only be present at specific stages of disease; thus, treatment with caspase inhibitors should be restricted to these stages. Of note, caspases are involved in a number of processes; therefore, one might expect a number of on-target adverse side effects, such as unwanted induction of necroptosis resulting from the inhibition of caspase-8 [136, 137, 145]. For the treatment of degenerative disorders, the aim is to block apoptosis without incurring the risk of inducing necroptosis instead, it might therefore be of interest to develop compounds that specifically inhibit several caspases but not caspase-8. Conversely, to develop cancer therapies that elicit necroptosis in tumour cells but do not inhibit apoptosis, it would be desirable to have inhibitors that only target caspase-8 but not other caspases.

1.4 Open questions addressed by this thesis

Since caspases play critical roles in several cell death processes and inflammation it is not surprising that a vast number of bacteria, viruses and fungi have evolved inhibitors of caspases or inhibitors of components of their upstream activators [146]. Since caspases play major roles in a broad range of cellular processes, there is substantial interest in understanding their mechanisms of action and their impact on the course of infection.

The functions of certain caspases, in particular caspase-12, are still poorly understood. Moreover, the overlapping roles of the inflammatory caspases (caspases-1, -11 and -12) in cell death and inflammation and the innate as well as adaptive immune systems have not yet been identified. Furthermore, there is unexplored potential of a wider functional overlap within the family of CARD containing caspases (i.e. also involving caspases-2 and -9) or all initiator caspases (i.e. also involving caspases-8 and in humans -10). With the prospects of the development of drugs that inhibit select caspases or groups of caspases, these questions need to be answered.

To address these questions through experiments *in vitro* as well as *in vivo* a mouse model lacking all three inflammation associated caspases, caspases-1, -11 and -12, must be generated and thoroughly characterised. I addressed the above listed questions using a novel triple knockout mouse strain lacking caspases-1, -11 and -12. I characterised this novel mouse strain and utilised it to generate mice lacking not only these inflammatory caspases but also additional caspases, such as caspases-2 and -9 or caspase-8 (the latter made possible by the additional loss of RipK3 to prevent embryonic lethality due to aberrant necroptosis). With these newly generated strains of mice I was able to study the functional overlap that exists within the caspases, with particular focus on their roles in different pathways to cell death, inflammation an immune defence against pathogens. The knowledge gained from these investigations may be useful for designing novel treatments of infections with pathogens, such as *Salmonella* Typhimurium, as well as diseases linked to caspase dysfunction, such as auto-inflammatory diseases or cancer.

Chapter 2: Materials & Methods

Generation of caspase-1/11/12/8 RipK3$^{-/-}$ mouse strain

The caspase-1/11/12$^{-/-}$ mice described in Chapter 2 were inter-crossed with caspase-8 RipK3 deficient mice supplied by Prof. John Silke. The caspase-8 RipK3$^{-/-}$ strain contains two mutations, a *delcre caspase-8* gene and a knockout mutation for Rip kinase 3 (RipK3) [147]. By crossing caspase-1/11/12$^{-/-}$ triple knockout mice with the caspase-8 RipK3$^{-/-}$ strain, we obtained mice deficient for caspases-1, -11, -12 and-8 as well as RipK3. Crossing heterozygous caspase-1/11/12/8 RipK3$^{-/+}$ mice, we generated caspase-1/11/12 RipK3$^{-/-}$ko mice, which served as controls lacking caspases-1, -11 and -12 as well as Rip kinase 3.

The caspase-2$^{-/-}$/9$^{-/+}$ mice used are described in [148], these mice were crossed to the caspase-1/11/12$^{-/-}$ strain and the generated heterozygous F1 offspring was subsequently inter-crossed to obtain caspase-1/11/12/2$^{-/-}$/9$^{-/+}$ offspring.

TRIF mice used are described in [149].

The caspase-1/11$^{-/-}$ mice deficient for caspase-1 and -11 are described in [150].

Genotyping of mice

Genotyping was performed by standard PCR technique with tail clippings from the individual mice taken at weaning age (3-4 weeks old). The tissue was digested in 200 µL DirectPCR lysis buffer (Viagen Biotech) with 0.4 mg/mL Proteinase K (Sigma-Aldrich). The tails were incubated shaking at 54 °C for a minimum of 8 h or overnight. The mix was incubated for 45 min at 86 °C to inactivate the Proteinase K. 1 µL extracted DNA was added to 10 µL GoTaq Green Master Mix (Promega) for the subsequent PCR reaction. PCR primers were added directly to the Master Mix. Primers (Integrated DNA Technologies) were added to the Green Mix to a final concentration of 0.5 µM. Primer sequences are depicted in the publication (Material and Methods).

Genotyping oligos shown in Table 2.1 and PCR protocols and resulting fragments in Table 2.2. Products were analysed on a 2% agarose gel containing 0.002% ethidium bromide (run for 40 minutes at 110V).

Gene of interest	**Oligo sequences**	**Expected band size**
Caspase-8 knock-in	FWD: ATAATTCCCCCAAATCCTCGCATC REV: GGCTCACTCCCAGGGCTTCCT	200 bp (wt) 300 bp (knock in-lox)
Caspase-8 knockout	FWD: TCCTGTACCATATCTGCCTGAACGCT REV: ATAATTCCCCCAAATCCTCGCATC	600 bp (wt) 200 bp (dec-recombinant gene) 800 bp (knock in-lox)
RipK3	RipK3-1: CGCTTTAGAAGCCTTCAGGTTGAC RipK3-2: GCCTGCCCATCAGCAACTC RipK3-3: CCAGAGGCCACTTGTGTAGCG	320 bp (wt) 485 bp (ko)
Caspase-1/11/12	FWD: CACACCTAAAAACAGAGTAAAAGGC REV1: GGGACTGTATGAAGAATGGATCC REV2: CAGCACCTTGAATTATGAGTTGG	413 bp (ko) 245 bp (wt)
Caspase-1	FWD: CTGCCCAGAGCACAAGACT REV: CATGCCTGAATAATGATCACC	197 bp (wt) No band for ko
Neo	Neo3: CATTGAACAAGATGGATTGCAC REV: GCATCAGCCATGATGGATAC	354 bp (neo cassette in ko)
Caspase-2	FWD: GCAGTGAACAGAAGGAGGTGCC REV: TCATCCAAGCATGTCGTGGAGG Neo: TTAAGAAGGGTGAGAACAGAG	150bp (wt) 250bp (ko)

Caspase-9	FWD: AGGCCAGCCACCTCCAGTTCC REV: CAGAGATGTGTAGAGAAGCCCACT Neo FWD: TCTCCTCTTCCTCATCTCCGGGCC Neo REV: GAACAGTTCGGCTGGCGCGAGCCC	250bp (wt) 500bp (ko)

Table 2-1: Oligo sequences and resulting PCR fragments for genotyping of knockout mouse strains.

Gene of interest	PCR Protocol
Caspase-8	Step 1: 95°C 3 min Step 2: 95 °C 1 min Step 3: 62 °C 1 min Step 4: 72 °C 90 sec; Step 5: go to step 2 for 35 cycles Step 6: 72 °C 3 min Step 5: 25 °C forever
RipK3, Caspase-2 and Caspase-9	Step 1: 94°C 4 min Step 2: 94 °C 40 sec Step 3: 55 °C 30 sec Step 4: 72 °C 1 min; Step 5: go to step 2 for 30 cycles Step 6: 72 °C 5 min Step 7: 25 °C forever
Caspase-1/11/12 and Caspase-1	Step 1: 95°C 5 min Step 2: 95 °C 30 sec Step 3: 60 °C 30 sec Step 4: 72 °C 1 min; Step 5: go to step 2 for 30 cycles Step 6: 72 °C 7 min Step 7: 25 °C forever

Table 2-2: PCR programs to genotype knockout mouse strains.

Mice and ethics

Experiments with mice were conducted according to the guidelines and with approval from the Walter and Eliza Hall Institute Animal Ethics Committee as well as the animal committee from the Peter Doherty Institute (Parkville, Victoria, Australia).

Bacterial strains

Salmonella enterica serovar Typhimurium (*S .*Typhimurium) strains; SL1344, BRD509ΔaroA and SL1344 Δ*fliC*Δ*fljB* were kindly obtained from frozen glycerol stocks provided by Dr. Paul Whitney, A/Prof. Sammy Bedoui and Prof. Richard Strugnell (Department of Microbiology and Immunology, The University of Melbourne). For *in vitro* gentamycin assays performed in Cambridge, U.K., the *S.* Typhimurium SL1344 strain was kindly supplied by Prof. Clare Bryant [6].

The wildtype SL1344 strain and SL1344 Δ*fliC*Δ*fljB* mutant strain were used only for *in vitro* infections. For *in vivo* assays the attenuated *Salmonella* Typhimurium strain BRD509ΔaroA was used exclusively.

***Salmonella* preparation for *in vitro* infections**

S. Typhimurium (either SL1344 strain or SL1344 Δ*fliC*Δ*fljB* strain*)* was cultured on Luria-Bertani Agar plates (LB agar, prepared in-house) at 37 °C overnight. A single colony was selected and cultured in 10 mL Luria-Bertani broth (LB broth, made in-house) at 37 °C for 17.5 h shaking (180mph). The bacteria were sub-passaged (500 µL) in 5 ml fresh pre-warmed LB broth and incubated for 2 h at 37 °C shaking at 180 mph to obtain log-phase bacteria. Bacteria were pelleted at 4300 RCF for 10 min at room temperature. Supernatant was removed, and the bacterial pellet was resuspended in 5 mL fresh antibiotic-free supplemented cell culture medium (DMEM, 10% FCS (Sigma-Aldrich, 12003C), 20% L929 (in-house made)) and then diluted to the desired concentration for *in vitro* infection.

Gentamycin protection assay

Primary Bone Marrow-Derived Macrophages (BMDM) were harvested from mouse tibia and femur and differentiated in Dulbecco's modified Eagle's medium (DMEM) containing 10% foetal calf serum (FCS Sigma-Aldrich, 12003C), 100 U/mL penicillin and 100 µg/mL streptomycin and supplemented with 20% L929 conditioned

medium (complete medium) for six to eight days. Differentiated macrophages were plated in triplicate at a concentration of $200x10^5$ cells/well onto tissue culture treated 96-well flat bottom plates in the afternoon proceeding infection. On the day of infection cells were infected with log-phase *S.* Typhimurium strain SL1344 (or mutant strains as indicated) at the indicated Multiplicity of Infection (MOI). Following 1 h of infection the supernatant was replaced with media containing a high dose of gentamycin (50 μg/mL, Sigma) and incubated for a further 1 h. Subsequently, the media was replaced with a low dose of gentamicin (10 μg/mL) for the 6hr and 24 h time-points, whilst the 2 h timepoint was analysed.

Serum cytokine levels

At each timepoint, the supernatant was removed from the cells and transferred into a fresh 96 well plate. Cytokine levels in supernatants of treated cells were determined using murine enzyme-linked immunosorbent assay system (IL-1β from R&D IL-18 from MBL International Corp.). The assay was carried out following the manufacturer's instructions. For wildtype genotypes, samples were diluted 1:5 in supplemented media.

Lactate dehydrogenase assay

At each timepoint, cells were washed twice with room temperature PBS and lysed in 40 μL cold 0.5% Triton X-100 in PBS and incubated on ice for 20 minutes. After incubation, cells were scraped off the plate (using a p10 pipette)and 10 μL of lysed cells were added to 105 μL 1.23% Triton X-100 (made in PBS and filtered sterile) onto a new 96 well plate (Gibco) and incubated for 1 hour at 37 °C. Following this incubation step, 10 μL of cell lysate was transferred into a new 96 well plate and diluted further into 40 μL PBS. Following the manufacturer's instructions (CytoTox 96® Non-Radioactive Cytotoxicity Assay (Promega)), 50 μL substrate mix was added to each well and the plate was incubated protected from light at room temperature for 30 mins. Finally, 50 μL stop solution was added to the lysate to inhibit further reaction to occur. Cell viability was determined by measuring absorbance at 490 nm (with reference at 620 nm) on the Clario Star (BMG, Labtech) as per instructions using a standard curve as reference.

To determine bacterial viability at 2, 6 and 24 h, 10 µL of the cell lysate (lysed in 40 µL cold 0.5% Triton X-100 in PBS, see Lactate dehydrogenase assay above) was further serially diluted into PBS up to 10^{-4} dilution. Dilutions were plated out on agar plates using drop plate method in triplicates for each dilution.

In vivo Salmonella infections

For *in vivo* infections, the attenuated strain BRD509ΔaroA was diluted from a pre-prepared infectious stock. Mice were intravenously (i.v.) infected with 200 colony forming units (CFU) of bacteria in 200 µl PBS.

To prepare an infectious stock, a single *S.* Typhimurium colony was prepared as above (*in vitro* infections) but following sub-passage the 5 ml broth was mixed at a ratio of 50:50 with 80% (v/v) sterile glycerol, aliquoted and stored at -80°C. The concentration of viable *S.* Typhimurium was estimated by culturing serial dilutions of multiple thawed infectious stock vials.

Sample preparation post-infection

At the experimental endpoint, mice were euthanised and the spleen, liver and gall bladder removed. The spleens and livers were transferred into a clean plastic bag and macerated before adding 5 mL of PBS. Bags were placed on the stomacher 80 (Biomaster, Lab Systems) for 10 min at room temperature on the high instrument settings "high". Gall bladders were mixed with 500 µL PBS and passed through a 70 µM sieve. The organs were serially diluted and 20 µL of each organ dilution was plated on Luria Agar plates supplemented with 50 µg/mL Streptomycin Sulphate. Plates were incubated at 37 °C overnight and organ colony counts determined.

Cytokine bead array assay

Organs were collected and prepared as indicated above. Bead array flex set assays from BD bioscience were used following manufacturer's instructions (catalogue numbers: MCP-1 558342; MIP-1α; 558449; MIP-1β, 558343; MIG 558341; TNF 558299; RANTES 558345; IL-12 p40 560151; IL-10 558300; IL-6 558301; KC 558340).

Samples were analysed by flow cytometry on a BD Fortessa analyser and data was run and analysed on FlowJo software.

Generation of immortalised bone marrow-derived macrophages (iBMDMs)

BMDMs were immortalised as described in [151]. On day 1, both tibiae and femora of mice were collected and placed into 70% EtOH for 30 seconds to kill off fibroblasts attached to the outsides of the bones. Both ends of each bone were cut and bones were subsequently flushed using a precision needle (BD PrecisionGlide, 26 G 0,45mm x 13 mm) with PBS containing 5% foetal calf serum (FCS) and bone marrow was strained through a minisart filter unit 0.45 µm (sartorius stedim, Biotech) into a 50 mL tube. To wash the bone marrow, tubes were topped up to a final volume of 40 mL with PBS containing 5% FCS before spin centrifugation (5 min 1500 rpm using a Heraeus Multifuge 3SR from Kendro laboratories or Rotofix 32A from Hettich). Supernatant was removed, and the bone marrow pellet was resuspended in 10 mL Dulbecco's modified Eagle's medium (DMEM) containing 10% foetal calf serum (FCS Sigma-Aldrich, 12003C) 100 U/mL penicillin and 100 µg/mL streptomycin (complete medium) and supplemented with 20% L929 conditioned medium (a source of M-CSF). The resuspended cells from one mouse were split into two 15 cm bacterial petri-dishes in 20-25 mL complete medium. On day 3, cells were collected by scraping them into the supernatant and spun down for 5 min at 1500 rpm. Supernatant was removed, and pellet was resuspended in 16 mL CreJ2 viral supernatant supplemented with 4 mL pure L929 (source of M-CSF, made in-house)[152]. After 48 h of infection, on day 5, the infection with CreJ2 virus was repeated. Medium was changed into complete medium (DMEM containing 10% foetal calf serum 100 U/mL penicillin and 100 µg/mL streptomycin) every 3-4 days. Upon reaching confluency, cells were split into DMEM 10% FCS 15% L929. Splitting the cells was repeated while reducing L929 supplementation slowly (10%, 7%, 5%, 2.5%, 1,25%, 0.75%) until L929 was no longer added.

Cells containing the J2 recombinant retrovirus, derived from a replication-defective 3611-Moloney sarcoma virus (MSV) carrying the v-raf/v-myc oncogenes) [151, 152] were grown on a 15 cm petri dish in 20 mL DMEM 10& FCS medium until confluent. Supernatant of virus was used for infection, 2-3 days after reaching confluency.

T cell Blast stimulation

Per mouse strain $14x10^6$ splenocytes were extracted and washed once in FMA (DMEM+ 10% FCS, 40 mM sodium bicarbonate, 1 mM HEPES, 100 U/ mL penicillin/ streptomycin, 0.0135 folic acid, 0.24 mM L-aspargine monohydrate, 0.55 mM L-arginine monohydrochloride, 50 μM β-mercaptoethanol and 100 μM aspargine). After centrifugation, the cell pellet was resuspended in 7 mL FMA medium supplemented with 2 μg/ mL ConA and in-house made IL-2 from supernatant of X63/0 cells transduced with an IL-2 expression vector used at a concentration established by titration experiments [153].

At day 3 the cytokines were removed from the cells by adding the cell suspension onto 1ml FCS. Cells were spun down at 1500 rpm for 5 minutes at room temperature and 1500 rpm (using a Heraeus Multifuge 3SR from Kendro laboratories or Rotofix 32A from Hettich) and supernatant was discarded. Subsequently the cells were washed twice using FMA medium. Next, cells were resuspended into FMA medium supplemented with IL-2. On day 4 cells were washed again in FCS once followed by 2 FMA washes and plated out at a concentration of $2\text{-}3x10^4$ cells per well in 100 μL FMA (supplemented with IL-2 and without, as control) on a 96 well plate. At the indicated timepoints, cells were washed once in PBS and resuspended in Annexin V binding buffer (2.5 mM $CaCl_2$, 0.1 m NaCl, 0.01 M HEPES in H_2O) with 0.5 -1 μg/mL propidium iodide (made in-house) in combination with Annexin V-FITC (produced in-house or Thermo Fisher catalog number: A13199 used as directed). Cell survival was measured in a BD FACS Calibur flow cytometer and analysed using FlowJo software, Build number 10.4.2. All cell survival data are presented as normalised to untreated control cells unless specified differently.

Thymocyte death assay

Single cell suspensions of thymi isolated from Ly 5.1 mice at 8-14 weeks post-reconstitution. Cells were prepared in FMA medium medium (DMEM+ 10% FCS, 40 mM sodium bicarbonate, 1 mM HEPES, 100 U/ mL penicillin/ streptomycin, 0.0135 folic acid, 0.24 mM L-aspargine monohydrate, 0.55 mM L-arginine monohydrochloride, 50 μM β-mercaptoethanol and 100 μM aspargine). $5x\ 10^4$ thymocytes per well were seeded out in in 96-well plates in FMA medium. Cells were left untreated or treated with ionomycin (0.5 μg/ mL or 1 μg/ mL) diluted in FMA.

At indicated timepoints, cells were washed once in PBS and resuspended in Annexin V binding buffer (2.5 mM $CaCl_2$, 0.1 m NaCl, 0.01 M HEPES in H_2O). 0.5 -1 µg/mL propidium iodide in combination with Annexin V-FITC (produced in-house or Thermo Fisher catalog number: A13199 used as directed). Cell survival was measured on a BD FACS Calibur flow cytometer and analysed using FlowJo software. All cell survival data are presented in a manner normalised to untreated control cells unless specified differently.

Foetal liver reconstitutions

Foetal livers for bone marrow reconstitutions were harvested from wt or caspase-1/11/12/2/9$^{-/-}$ embryos at embryonic stage E14.5 and washed in PBS once. Foetal liver cells were subsequently frozen in FCS supplemented with 8-10% DMSO at -80 °C until the day of reconstitution. On reconstitution, 2 foetal livers were defrosted and washed in PBS once, followed by filtration through a 70 µM filter. Cells of 2 foetal livers were pooled and resuspended in 1200 µL PBS. 2 foetal livers were used to reconstitute a total of 5 recipient mice with 200 µL per mouse. Recipient Ly5.1 mice (6- 10 weeks of age) were lethally irradiated (2 doses of 550 rad) and then received either 200 µL wildtype or 200 µL caspase-1/11/12/2/9$^{-/-}$ foetal liver cells in PBS suspension, which is approximately a total of 3 x 10^6 cells per recipient mouse. Mice were sacrificed and analysed 8-14 weeks post-reconstitution and donor cells were identified by labelling with anti-CD 45.2 marker clone 104 (purchased from Biolegend, conjugated to brilliant violet or Alexa Fluor® 700).

Embryo analysis

Embryos were harvested at indicated stages and analysed using a Zeiss Stemi 2000-C microscope. Images were taken at 10x or 20x magnification.

The following Materials and Methods section has been published as the following paper in the journal Cell Death & Differentiation, 2018 Aug 28,
DOI 10.1038/s41418-018-0188-2

R Salvamoser, K Brinkmann, LA O'Reilly, L Whitehead, A Strasser, MJ Herold (2018). Characterisation of mice lacking the inflammatory caspases-1/11/12 reveals no contribution of caspase-12 to cell death and sepsis [154].

Generation of caspase-1/11/12 triple ko mice

The *caspase-1/11/12*$^{-/-}$ mice were generated by Taconic Bioscience GmbH. The genomic region encompassing *caspases-1, -11 and -12* was deleted using the targeting strategy in C57BL/6 ES cells depicted in Figure 1a. The targeting vector was generated using BAC clones from the C57BL/6J RPCIB-731 BAC library and was transfected into the Taconic C57BL/6N Tac ES cell line. The targeting construct contained a puromycin resistance cassette used for positive selection of recombinant clones as well as a thymidine kinase for negative selection. The positive selection cassette was subsequently excised using Flp-FRT mediated recombination.

The heterozygous *caspase-1/11/12*$^{+/-}$ offspring were inter-crossed to obtain *caspase-1/11/12*$^{-/-}$ mice. Genotyping (by PCR) confirmed the absence of the *caspase-1/11/12* locus. Primer sets used for genotyping: 23:5'cacacctaaaaacagagtaaaaggc, 24: 5'gggactgtatgaagaatggatcc, 25: 5'cagcaccttgaattatgagttgg. PCR program: 95 °C for 5 min followed by 95 °C (for 30 sec), primer annealing at 60 °C (30 sec) then 72 °C (1 min). All three steps were repeated for a total of 30 cycles and this was followed by a final single elongation step at 72 °C.

Endotoxic shock model

Experiments with mice were conducted according to the guidelines and with approval from the Walter and Eliza Hall Institute (Parkville, Victoria, Australia) Animal Ethics Committee. Mice were injected intraperitoneally (i.p.) with 18 or 54 mg/kg body weight ultrapure LPS (*E. coli* O111:B4, InvivoGen, catalog code: tlrl-eblps). Some treated mice were sacrificed after 4 h for heart bleeds and cytokine analysis. Mice for survival studies were taken when showing physical signs of ill

health and/or a drop in body temperature below 33°C. A scoring sheet was followed to assess the overall physical condition of the mice. This included features, such as posture, respiratory rate, responsiveness and eye closure. The body temperature and physical condition of each mouse were checked hourly and every 15 min within the first hour until sacrifice. Only males were used for these LPS shock experiments and all animals were between 6-12 weeks of age. The mice used in these experiments were derived from independent colonies, namely the C57BL/6 (wt control), *caspase-1/11* double knockout and *caspase-1/11/12* triple knockout lines.

In vivo treatment with tunicamycin

C57BL/6 (wt control) and caspase-1/11/12 triple knockout mice were injected with 1 mg/kg body weight tunicamycin (Sigma-Aldrich, product code T776) dissolved in DMSO as per the manufacturer's instructions and diluted in PBS buffer. Mice were injected i.p. and sacrificed 24 or 72 h post-injection. The mice were monitored regularly for signs of discomfort during this period. At sacrifice, kidneys and livers were harvested for histological analysis and TUNEL staining. ALT levels in the sera were measured as described previously [89].

TUNEL staining

After harvesting, kidneys (and livers) were incubated in formalin for 12 h at room temperature followed by treatment with 70% EtOH. Preparation of tissue sections and staining with haematoxylin and eosin (H&E) were carried out in-house by the histology department. Dewaxed paraffin sections were incubated in 20 µg/mL proteinase K (Roche, product code 03115879001) for 15 min followed by three 2 min washes in PBS. Endogenous peroxidase activity was blocked by treatment with 3% H_2O_2 in methanol for 5 min at room temperature. Following three 2 min washes in PBS, each section was incubated in TUNEL reaction mix consisting of bio dUTP (0.3 nmol/µL) (Roche, product code 11093070910) + $CoCl_2$ (25 mM) +TdT buffer+ TdT (25 U/µL) (Promega, product code M828C) + H_2O to a total volume of 50 µL per section for 1 h at 37 °C in a moist chamber. This was followed by further washes with PBS (3x 2 min). The slides were then incubated with the ABC reagent (Vectastain Elite ABC Kit, Vector labs, product code PK-6100) for 30 min at room temperature (as per the manufacturer's instructions). After further washes, the sections were incubated in DAB peroxidase substrate mix for 5 min (Vector labs; SK-4100). Finally, slides were washed with H_2O and counterstained with haematoxylin and mounted by the in-house histology department. All slides were scored visually by microscopy. Additionally, two organ sections for each genotype and treatment were scanned and computationally analysed. The images were scanned using a 3DHISTEC slide scanner and quantification of the $TUNEL^+$ cells was performed using FIJI [155] with a custom written scoring macro. For Figure 5, the image contrast and brightness were adjusted using Adobe Photoshop CS6 version 13.0.4.

Measurement of cytokine levels in the serum of mice

Blood from mice was taken at death or 4 h after treatment with LPS by cardiac puncture. The levels of cytokines were determined using ELISA (IL-1β from R&D; IL-18 from MBL International Corp.). The levels of all other cytokines and chemokines in the sera from mice were quantified by using the Bio-Rad Bio-Plex Pro mouse cytokine 23-plex assay (product code M60-009RDPD).

Flow cytometric analysis

Mice were euthanised and organs harvested into sterile BSS supplemented with 5% foetal calf serum (FCS, Sigma-Aldrich, 12003C). For the detection of cell surface markers the following rat or hamster monoclonal antibodies that had been conjugated to FITC, APC, R-PE or biotin (made in-house or purchased from eBioscience) were used: TER119 (TER119), MAC-1 (M1/70), NK1.1 (PK136), B220 (14.8 or RA3-6B2), CD3 (145-2C11), CD4 (GK1.5, H129 or YTA3.2.1), CD8 (53-6.7 or YTS169), TCRβ (H57-597), CD44 (IM781), CD25 (PC61), IgD (11-26C), IgM (5.1), CD62L (MEL-14), CD5 (53-7.3) and GR-1 (RB6-8C5). Streptavidin conjugates to PE-Cy7 or APC (BioLegend) were used for the detection of biotin-conjugated antibodies. Cells were washed in BSS supplemented with 2% FCS) and analysed using an LSR-II flow cytometer (BD Biosciences). Dead cells (PI^+) were excluded from analysis by staining with propidium iodide (PI, 5 μg/mL; Sigma-Aldrich). Intracellular staining for FoxP3 (clone FJK-16s) was performed using the eBioscience FoxP3/transcription factor staining buffer set. All data were analysed using FlowJo 9.9.4 software.

Cell death assays

Three independent mouse dermal fibroblasts (MDF) cell lines were generated from caspase-1/11/12 triple knockout and wt mice each. The fibroblasts were isolated from the dermis of mice and subsequently immortalised by transfection with an expression vector encoding the SV40 large T antigen.

Primary bone marrow derived macrophages (BMDMs) were generated (see below) and plated on non-coated 96-well plates over night with 1 x 10^4 cells seeded into each well containing 100 μL Dulbecco's modified Eagle's medium (DMEM) containing 10% foetal calf serum (FCS, Sigma-Aldrich, product code 12003C), 100 U/mL penicillin, 100 μg/mL streptomycin (complete medium) and supplemented with 20% L929 cell conditioned medium (a source of M-CSF). For immortalised MDFs, 1-2 x10^4 cells per well were plated out on regular 96-well coated tissue culture plates in complete medium the night before treatment. Immortalised bone marrow-derived macrophages were plated out at a density of 1-2 x10^4 cells per well in 100 μL Dulbecco's modified Eagle's medium containing 10%FCS, 100 U/mL penicillin, 100 μg/mL streptomycin. All cell types were treated with the drugs as

indicated. The treatments used in these assays included TNF (100 ng/mL, made in-house), SMAC mimetic (CompA from Tetralogic, 500 nM), the caspase inhibitor QVD-Oph (10 μM, MP Biomedicals, OPH109), thapsigargin (Sigma, product code T9033), taxol (paclitaxel from Sigma-Aldrich, product code T7402), tunicamycin (Sigma, product code T7765) and etoposide (Sigma, product code T7402). At the indicated timepoints, cells were harvested and stained with 1-5 μg/mL propidium iodide alone or in combination with Annexin V-FITC (produced in-house). Cell survival was measured in a BD FACS Calibur flow cytometer. All cell survival data are presented in a manner normalised to untreated control cells unless data for untreated cells are shown separately. Untreated cells were cultured in complete medium.

In vitro assays with BMDMs

Primary BMDMs were generated from single cell suspensions of bone marrow that had been flushed with PBS containing 2% foetal calf serum (FCS) from mouse tibiae and femora and cultured in Dulbecco's modified Eagle's medium (DMEM) containing 10% foetal calf serum (FCS Sigma-Aldrich, 12003C) 100 U/mL penicillin and 100 μg/mL streptomycin (complete medium) and supplemented with 20% L929 conditioned medium (a source of M-CSF) for 6 days before plating out on treated tissue culture plates. Approximately $1x10^6$ cells were plated per well on coated 12-well tissue culture plates in 1 mL of complete medium plus M-CSF. On day 7 the cells were stimulated with 20 ng/mL ultrapure LPS (LPS from *E. coli* O111:B4, InvivoGen, catalog code: tlrl-eblps) for 24 h before harvesting the supernatants and cell pellets separately. For qRT-PCR analysis of the expression of *caspases-1, -11* and *-12*, BMDMs were treated with 20 ng/mL or 500 ng/mL LPS for 3 h. The cell pellet was subsequently washed twice with ice cold PBS and lysed in 1 mL TRIzol (Thermo Fisher Scientific product code 1559-6018).

Western blot analysis

Cell pellets were lysed in Onyx buffer (20 mM Tris/HCL pH 7.4, 135 mM NaCl, 1.5 mM $MgCl_2$, 1 mM EGTA, 1% Triton X-100, 10% Glycerol in H_20) with protease inhibitor cocktail (Roche, 4693159001) added fresh and samples of varying concentration (between 10-30 μg, depending on protein abundance) were loaded onto NuPAGE Novex 10% Bis-Tris protein gels (Thermo Fisher Scientific) for size

fractioning and run in MES buffer. Transfers were carried out on the iBlot 2 dry blotting system (Invitrogen, IB21001) onto nitrocellulose membranes (Invitrogen, IB23001 or IB23001). Membranes were blocked in 5% skim milk powder in PBS with 0.1% Tween-20 and then probed with monoclonal antibodies against caspase-1 (clone 1H11; made in-house; see below, and available from Enzo LifeSciences), caspase-11 (4E11; made in house; see below available from Adipogene and Enzo LifeSciences) or HSP70 (clone N6, a gift from Dr Robin Andersson, Peter MacCallum Cancer Centre, Melbourne, Australia), the last one used as a loading control. Bound primary antibodies were detected by goat anti-rat IgG or goat anti-mouse IgG antibodies conjugated to HRP (Southern Biotech). The ECL reaction was used for detection and blots were developed using the ChemiDoc Touch System (Bio-Rad Laboratories). Protein concentrations were determined by Bradford assay using Protein Assay Dye Reagent Concentrate as per manufacturer's instructions (product code 5000006).

Generation of rat monoclonal antibodies against caspase-1 and caspase-11

Monoclonal antibodies against caspase-1 and caspase-11 were produced as we have described previously [156, 157]. Briefly, Wistar rats were initially immunised by subcutaneous injection (s.c.) with the p20 fragment of mouse caspase-1, a KLH conjugated mouse caspase-1 peptide (aa 206-220) or the p20 fragment of mouse caspase-11 dissolved in complete Freund's adjuvant (Difco, Detroit, MI). Two subsequent boosts with each of the immunogens resuspended in incomplete Freund's adjuvant (Difco) were given 3 and 6 weeks later. A final boost with the immunogen dissolved in phosphate-buffered saline (PBS) was given i.v. and i.p. 4 weeks later. Three days later, spleen cells from each of the immunised rats were fused with the SP2/0 myeloma cell line as previously described [157]. Hybridomas producing antibodies against either caspase-1 or caspase-11 and their isotypes were identified by a screening strategy that we have previously described. Briefly, 293T cells were transiently transfected with an EE-tagged inactive cysteine mutant of either mouse caspase-1 (to screen for antibodies against casapse-1) or caspase-11 (to screen for antibodies against casapse-11), fixed in 1% paraformaldehyde/PBS, permeabilised with 0.3% saponin (Sigma) and stained with hybridoma supernatants. Bound antibodies were revealed with fluorescein

isothiocyanate (FITC)-conjugated goat anti-rat Ig antibodies (Southern Biotechnology) and analysed by flow cytometry. A single peak of low immunofluorescence indicated that a particular antibody did not recognise caspase-1 or caspase-11. A single peak of high intensity indicated binding to molecules other than caspase-1 or caspase-11. A double peak histogram of low and high intensity staining, due to the presence of both non-transfected and transfected cells, identified hybridomas producing antibodies specific to either caspase-1 or caspase-11. Antibodies against the EE epitope tag (BabCO) were used as a positive control and hybridomas producing antibodies against KLH were eliminated. Hybridomas producing antibodies of the desired specificity were cloned twice and adapted for growth in low serum medium. The caspase-1 antibody producing hybridoma clone 1H11 and the caspase-11 antibody producing hybridoma clone 4E11 were selected for further use. For production of large amounts of antibodies, hybridomas were cultured for several weeks in the miniPERM classic 12.5-kd production and nutrient modules (Heraeus). Antibodies were purified on protein G-sepharose columns (Pharmacia) according to the manufacturer's instructions.

In vitro stimulation with LPS and ELISA to detect IL-18

For *in vitro* stimulation of caspase-1, primary BMDMs were primed with 20 ng/mL ultrapure LPS (LPS from *E. coli* O111:B4, InvivoGen, catalog code: tlrl-eblps) for 3 h and subsequently activated using 5 mM ATP (Sigma, product number A 2383) for 1 h after which cells and supernatants were harvested individually. For caspase-11 activation, cells were primed with 500 ng/mL ultrapure LPS for 3 h before activation with 2 μg/mL ultrapure LPS that was transfected into the cells using lipofectamine (LPS : lipofectamine was used at a ratio of 1:1.3). Priming and activation were performed in reduced serum opti-MEM medium (Gibco). After 6 h, this medium was replaced with complete medium supplemented with 20% L929 cell conditioned medium (a source of M-CSF) and after an additional 16 h incubation the supernatants as well as cell pellets were harvested. The levels of cytokines and chemokines in the cell supernatants were determined by ELISA (IL-1β and Rantes/CCL5 from R&D, lL-18 from MBL International Corp.).

qRT-PCR analysis

For measuring the levels of mRNA expression, total RNA was isolated from organs or cultured cells and cDNA was synthesised by using the SuperScript III first-strand synthesis system (ThermoFisher). qRT-PCR was performed in triplicates using TaqMan assay from ThermoFisher Scientific, with primers for mouse *caspase-1* (Mm00438023_m1), *caspase-11* (Mm00432304_m1), *caspase-12* (Mm00438038_m1), β-actin (Mm02619580_g1) and hmbs (Mm01143545_m1) (loading control). qRT-PCR was run using Viia7 real-time PCR and an ABI7900 machine. β-actin was chosen as an internal control gene and ΔCt calculation was performed as fallows: ΔCt = (Ct gene of interest – Ct internal control). $2^{-\Delta\Delta Ct}$ values were calculated as described in [158] using the equation: $2^{-\Delta\Delta Ct}$ = Δ Ct (treated sample)- Δ Ct (untreated sample).

To set a threshold qRT-PCR cycle number for each gene of interest (considered as background noise), we tested Ct values for *caspase-1*, *caspase-11* and *caspase-12* in cells from caspase-1/11/12 triple knockout mice (data not shown). For *caspase-1* expression, the maximum cycle threshold was set at 35 cycles, anything over 37 cycles in the case of *caspase-11* and higher Ct than 39 for *caspase-12* were considered as no RNA detected.

Statistical analysis

Mouse survival curves were generated and analysed with GraphPad Prism (GraphPad Software Inc, La Jolla, CA, USA). Mouse survival cohorts were compared using the log-rank Mantel–Cox test. *P*-values of <0.05 were considered significant. *In vitro* cell survival data were plotted and analysed with GraphPad Prism using one-way or 2way ANOVA statistical test. For ELISA data on cytokine levels in sera from mice, graphs were plotted using Prism software and examined by using the ordinary one-way ANOVA test. ELISA data on the levels of cytokines in supernatants from cultured cells were evaluated by using Prism applying a 2-way ANOVA tests. Data are presented as standard error of the mean (±S.E.M.).

Chapter 3: Characterisation of mice lacking the inflammatory caspases-1/11/12 reveals no contribution of caspase-12 to cell death and sepsis

R Salvamoser, K Brinkmann, LA O'Reilly, L Whitehead, A Strasser, MJ Herold

Accepted and published
Cell Death & Differentiation
2018 Aug 28
DOI 10.1038/s41418-018-0188-2

Cell Death & Differentiation
https://doi.org/10.1038/s41418-018-0188-2

Cell Death & Differentiation

ARTICLE

Characterisation of mice lacking the inflammatory caspases-1/11/12 reveals no contribution of caspase-12 to cell death and sepsis

Ranja Salvamoser[1,2] · Kerstin Brinkmann[1,2] · Lorraine A. O'Reilly[1,2] · Lachlan Whitehead[1,2] · Andreas Strasser[1,2] · Marco J. Herold[1,2]

Received: 18 March 2018 / Revised: 2 July 2018 / Accepted: 27 July 2018

Abstract

Caspases exert critical functions in diverse cell death pathways, including apoptosis and pyroptosis, but some caspases also have roles in the processing of cytokines into their functional forms during inflammation. The roles of many caspases have been unravelled by the generation of knockout mice, but still very little is known about the overlapping functions of caspases as only a few studies report on double or triple caspase knockout mice. For example, the functions of caspase-12 in cell death and inflammation, on its own or overlapping with the functions of caspase-1 and caspase-11, are only poorly understood. Therefore, we generated a novel mutant mouse strain lacking all three inflammatory caspases, caspases-1, -11 and -12. Analysis under steady state conditions showed no obvious differences between *caspase-1/11/12*$^{-/-}$ and wildtype (WT) mice. Since caspases-1 and -11 are involved in endotoxic shock, we analysed the response of *caspase-1/11/12*$^{-/-}$ mice to high-dose LPS injection. Interestingly, we could not detect any differences in responses between *caspase-1/11/12*$^{-/-}$ mice vs. caspase-1/11 double knockout mice. Furthermore, cell lines generated from *caspase-1/11/12*$^{-/-}$ mice showed no differences in their apoptotic or necroptotic responses to a diverse set of cytotoxic drugs in vitro when compared to WT cells. Importantly, these drugs also included ER stress-inducing agents, such as thapsigargin and tunicamycin, a form of cell death for which a critical pro-apoptotic function of caspase-12 has previously been reported. Additionally, we found no differences between *caspase-1/11/12*$^{-/-}$ and WT mice in their in vivo responses to the ER stress-inducing agent, tunicamycin. Collectively, these findings reveal that caspase-12 does not have readily recognisable overlapping roles with caspases-1 and -11 in the inflammatory response induced by LPS and in necroptosis and apoptosis induced by diverse cytotoxic agents, including the ones that elicit ER stress.

Introduction

Inflammatory caspases play a crucial role in the innate immune response and are therefore an important part of defence against pathogenic attack [1]. The murine inflammatory caspase locus on chromosome 9 encodes for caspases-1, -11 and -12 [1]. Humans have four inflammatory caspases (encoded by genes located on chromosome 11), namely caspases-1, -4, -5 and -12 [1]. Caspases-4 and -5 in humans are thought to be the orthologues of mouse caspase-11 and probably arose from the duplication of an ancestral gene [1]. The inflammatory caspases have N-terminal CARD (caspase activation and recruitment domains) pro-domains, and because they can proteolytically activate the effector caspases (i.e. caspases -3, -6 and -7) they are classified as initiator caspases [1–3]. This places them alongside the CARD-containing caspase-9, which plays a role in the intrinsic apoptotic pathway [4, 5] and the DED-containing caspase-8, which is essential for death receptor-induced apoptosis [6] and the prevention of necroptosis [7, 8]. The CARD and DED pro-domains function as protein–protein interaction motifs serving

Edited by G. Melino

Electronic supplementary material The online version of this article (https://doi.org/10.1038/s41418-018-0188-2) contains supplementary material, which is available to authorised users.

✉ Marco J. Herold
herold@wehi.edu.au

[1] The Walter and Eliza Hall Institute of Medical Research, Parkville, VIC, Australia

[2] Department of Medical Biology, University of Melbourne, Parkville, VIC, Australia

as activation platforms to convert inactive zymogens into fully active initiator caspases [1, 9]. This results in the assembly of multimeric protein complexes, such as the apoptosome (APAF-1, cytochrome c plus pro-caspase-9) or inflammasome (NLRP1, NLRC4, or ASC plus pro-caspase-1) [10, 11].

CARD-containing caspases, such as caspases-1 and −11, promote inflammation by driving the secretions of functional IL-1β and IL-18 [1]. Upon infection or injury, caspases are required to destroy and rapidly clear the cells. These processes must be tightly regulated because too much or too little cell death or inflammation can lead to failure of clearing an infection, cause auto-inflammatory diseases, or cancer [12, 13].

Caspase-1, formerly known as ICE (Interleukin-1 Converting Enzyme) was discovered through its ability to generate the biologically active form of the pro-inflammatory cytokine IL-1β by cleavage [14, 15]. Caspase-1 becomes activated via two signals: an initial 'priming' stimulus provided by the membrane-bound receptors and an 'activation' signal produced by cytosolic pattern recognition receptors (PRRs) [16]. Stimulation of membrane receptors by pathogen-associated molecular patterns (PAMPs), such as TLR4 being activated by bacterial LPS or host-derived danger-associated molecular patterns (DAMPs), triggers signalling cascades that promote the transcription of the genes encoding pro-interleukin-1β (pro-IL-1β), intracellular PRRs (i.e. NOD-like receptors, NLRs) and other mediators of inflammation [10]. Upon sensing cytosolic DAMPs or PAMPs, the newly expressed NLRs prime the assembly of a multi-protein scaffold, termed as inflammasome [17–19]. This structure recruits and thereby facilitates the activation of caspase-1. This causes proteolytic activation of the cytokines pro-IL-1β and pro-IL-18, and induction of pyroptosis. This lytic form of cell death is driven by caspase-1 or caspase-11mediated proteolytic activation of gasdermin D, which permeabilises the plasma membrane [2, 9, 17, 20].

Caspase-11 was shown to function as a cytosolic sensor for Gram-negative bacteria, such as directly binding the LPS from *Escherichia coli*, and like caspase-1, it is involved in the induction of pyroptosis [21–23]. Furthermore, caspase-11 has been shown to initiate the canonical NLRP3 inflammasome to support the caspase-1driven release of IL-1β and IL-18 and it also promotes the secretion of the pro-inflammatory factors IL-1α and high-mobility group box 1 protein (HMGB1) [22, 24]. Exactly how caspase-11 triggers inflammasome activation is still unclear and, as mentioned above, in humans caspases-4 and -5 are thought to be the orthologues of murine caspase-11 and perform these functions [22].

Only limited insight is available on the other member of this family, caspase-12. Apart from having two caspase-11like genes, another difference between mice and humans is that due to an early stop codon (TGA), all humans of Asian and Caucasian descent can only express a truncated version of caspase-12 that contains the CARD, but lacks the domains critical for proteolytic activity [25, 26]. The expression of full-length caspase-12 is confined to 20–25% of people of African descent. A role for caspase-12 in inflammation in mice (and possibly other species) appears likely, given its gene is clustered closely with the genes for caspases-1 and −11 within the inflammatory caspase locus [25]. Caspase-12 is only expressed in certain cell types and can be upregulated in response to certain inflammatory stimuli [27]. Caspase-12 has been implicated in apoptosis triggered by ER stress in one study [28], but this was not substantiated by follow-up investigations [27, 29].

To examine the overall roles of all inflammatory caspases, we generated mice deficient for caspase-1/11/12. Analysis of these animals reveals that additional loss of caspase-12 does not further diminish the septic shock response beyond the attenuation afforded by the combined loss of caspases-1 and -11. Moreover, we found no evidence for an overall role for these three inflammatory caspases in the response of cells to diverse inducers of apoptosis or necroptosis in vitro or to inducers of ER stress in vitro and in vivo.

Results

Generation and validation of caspase-1/11/12 triple deficient mice

To determine the overall role of inflammatory caspases-1, -11 and -12 in inflammation and cell death, we generated mice deficient for these three CARD-containing caspases. Therefore, the entire locus spanning the coding regions of caspases-1, −11 and −12 was constitutively deleted in C57BL/6 ES cells (Fig. 1a). The genomic region encompassing caspase-1 including 1.7 kb of genomic sequence upstream of *caspase-1* exon 1 (promoter region), *caspase-11* and *caspase-12* (total of 76.3 kb) was replaced with a FRT-flanked puromycin resistance (PuroR) cassette that was subsequently removed using site-directed Flp-FRT-mediated recombination. This resulted in a constitutive caspase-1/11/12 knockout (ko) allele. Intercrossing *caspase-1/11/12*$^{+/-}$ mice generated *caspase-1/11/12*$^{-/-}$ offspring at the expected mendalian frequency. The *caspase-1/11/12*$^{-/-}$ mice displayed no overt abnormalities, appeared healthy up to at least 18 months of age and were fertile (data not shown).

The loss of the three caspase genes was verified by PCR, amplifying a 413 bp band for the mutant allele and a 245 bp band for the WT allele (Fig. 1b). To further validate the

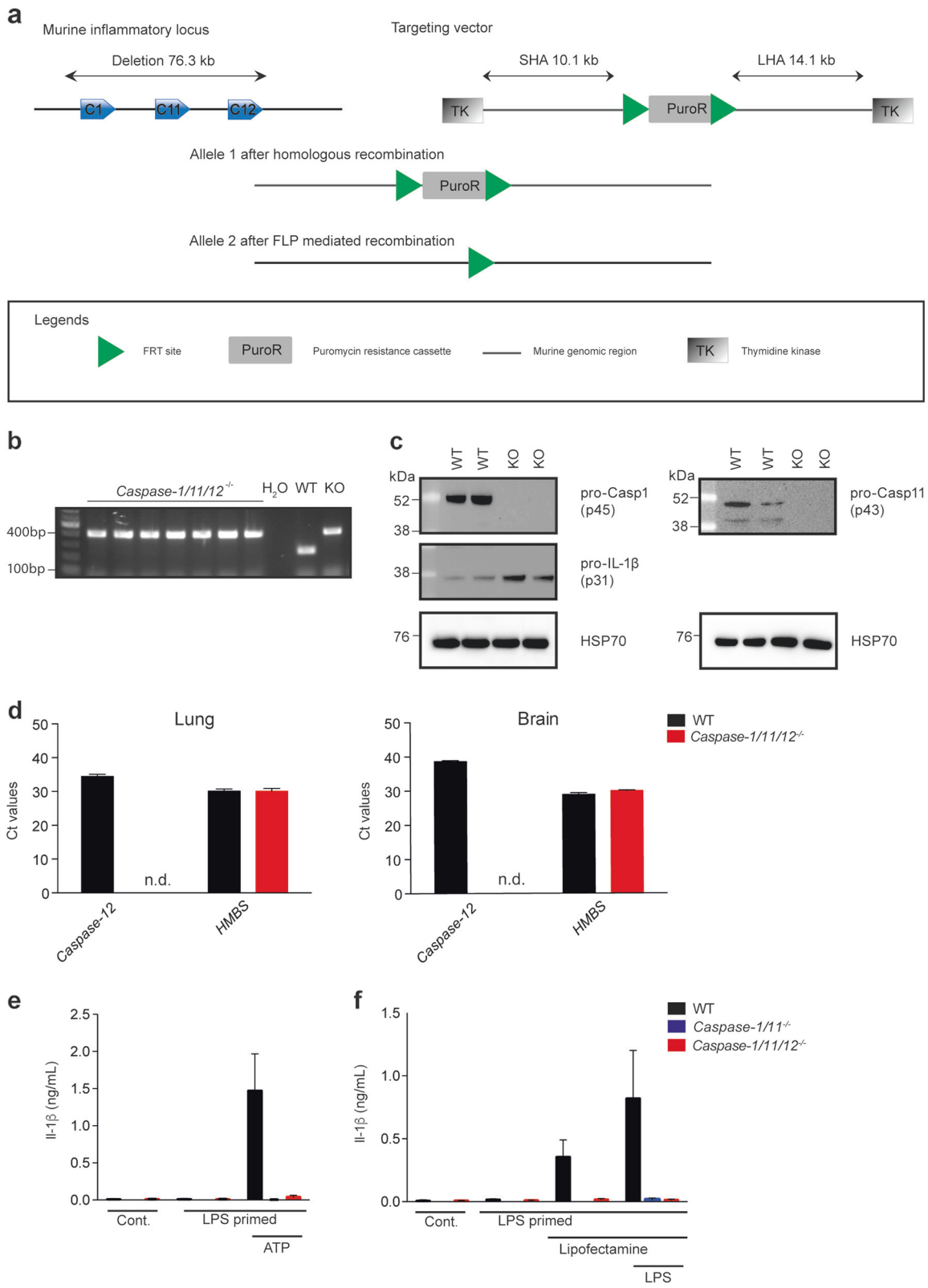

knockout mice, we stimulated primary bone marrow-derived macrophages (BMDMs) derived from these animals with LPS and analysed the expression of caspases-1 and -11 by western blotting. This revealed steady state expression of caspase-1 and LPS-induced upregulation of caspase-11 in BMDMs from WT mice, while as predicted, both caspases-1 and -11 were absent in the cells from caspase-1/11/12 triple knockout mice (Fig. 1c). Due to the lack

◀ **Fig. 1** Generation and validation of caspase-1/11-12 triple knockout mice. **a** Targeting strategy to generate mice constitutively deficient (KO) for caspases-1, -11 and -12. **b** Genotyping of *caspase-1/11/12*$^{-/-}$ mice. DNA from WT mice or H_2O served as controls. Band sizes, WT: 245 bp, KO: 413 bp. **c** Western blot analysis to detect caspases-1 and -11 in BMDMs of the indicated genotypes after 24 h of stimulation with 20 ng/mL LPS. Left panel: blot probed for caspase-1; right panel: blot probed for caspase-11. Both membranes were also probed for HSP70 (loading control) and the left membrane was additionally probed for pro-IL-1ß. The western blot shown is representative of two independent experiments. **d** Raw Ct values from qRT-PCR analysis of mRNA expression for *caspase-12* and *HMBS* (loading control) in extracts from the lung (left panel) and brain (right panel) from caspase-1/11/12 triple knockout and WT control mice. n.d. indicates no RNA was detected. $n = 3$. Graphs show the mean ± S.E.M. of triplicate tests. **e**, **f** IL-1ß release from LPS-primed BMDMs of the indicated genotypes that had been stimulated with **e** 5 mM ATP or **f** 2 µg/mL LPS, that had been transfected into cells using lipofectamine. (Cont., medium alone). All graphs show mean ± S.E.M. of $n \geq 4$. Adjusted p values in Supplementary Table 1 a and b

of suitable caspase-12 antibodies, we verified the loss of *caspase-12* expression by qRT-PCR (Fig. 1d). As previously reported [27], we detected *caspase-12* mRNA in the lungs and brain from unchallenged WT mice but, as expected, this mRNA was absent from the corresponding tissues from the *caspase-1/11/12*$^{-/-}$ mice (Fig. 1d).

Next, we conducted a functional assay for caspases-1 and -11. Both of these caspases are known to be critical for the production of IL-1β during pyroptosis [22]. BMDMs were primed with LPS, and caspases-1 or -11 were activated by the further addition of ATP or transfection of cells with LPS, respectively (Fig. 1e, f). Substantial levels of IL-1β were detected in the supernatants of stimulated BMDMs from wt mice, but no IL-1β was produced by BMDMs from the caspase-1/11/12 knockout mice (Fig. 1e, f). BMDMs from caspase-1/11 double knockout mice served as a control and, as predicted, these cells also did not produce IL-1β (Fig. 1e, f). Collectively, these findings demonstrate that we have successfully generated a novel strain of mice deficient for all three inflammatory caspases-1/11/12.

Caspase-12 mRNA expression is upregulated to a similar extent in wildtype and caspases-1/11 deficient cells upon treatment with LPS in vitro

It is possible that the deletion of caspases-1 and -11 may interfere with *caspase-12* gene expression. To investigate this possibility and determine the expression of caspases-1, -11 and -12, we treated primary BMDMs with 20 ng/mL or 500 ng/mL LPS and analysed the expression of these genes using qRT-PCR.

Upon LPS stimulation, the expression of *caspase-11* increased ~20-fold in BMDMs from WT mice, but was not detected in BMDMs from the *caspase-1/11*$^{-/-}$ mice (Figure S1). Stimulation with LPS increased the levels of *caspase-1* mRNA in wt BMDMs approximately threefold. The *caspase-1* gene in the *caspase-1/11*$^{-/-}$ mice lacks parts of exons 6 and 7 and therefore no functional caspase-1 protein can be produced. However, a shortened *caspase-1* transcript that can be recognised by the PCR primers can be generated in cells from these animals, which explains why a qRT-PCR signal was obtained in the BMDMs from *caspase-1/11*$^{-/-}$ mice (Figure S1).

The levels of *caspase-12* mRNA were not significantly different between untreated BMDMs from WT vs. those from the *caspase-1/11*$^{-/-}$ mice. Upon LPS stimulation, the levels of *caspase-12* mRNA rose to a similar extent in BMDMs of either genotype (Figure S1). This reveals that loss of caspases-1/11 does not affect the levels of *caspase-12* mRNA expression.

Caspase-1/11/12$^{-/-}$ mice do not exhibit noticable defects in the haematopoietic system

To study the roles of caspases-1, -11 and -12 in the haematopoietic system, we performed flow cytometric analysis to compare the myeloid and lymphoid cell subset composition between the caspase-1/11/12 knockout and WT mice. In the thymus no differences were found in the frequencies and numbers of double-negative ($CD4^-CD8^-$; including all DN1-4 subsets), double-positive ($CD4^+CD8^+$) or single-positive ($CD4^+$ or $CD8^+$) T cells (Fig. 2a and S2a). Moreover, the caspase-1/11/12 knockout mice had normal numbers of $CD4^+$ as well as $CD8^+$ mature T cells in their spleens, with normal distributions of naïve ($CD62L^{hi}CD44^-$), activated ($CD62L^{lo}CD44^+$) and memory ($CD62^{hi}CD44^+$) subsets found in both the $CD4^+$ and $CD8^+$ T cell lineages (Fig. 2b and S2b). Finally, the caspase-1/11/12 knockout mice had similar numbers of $CD4^+FOXP3^+$ T regulatory cells (T_{reg}) as WT controls (Fig. 2c and S2c).

We also found no abnormalities in the B-lymphocyte compartment of the caspase-1/11/12 knockout mice. They contained normal frequencies and numbers of pro-B/pre-B ($B220^+IgM^-$), immature B ($B220^+IgM^{hi}IgD^{lo}$) and mature B cells ($B220 + IgM^{lo}IgD^{hi}$) in the bone marrow and normal frequencies, and numbers of follicular ($B220^+IgD^+IgM^{lo}$), marginal zone and B-1 B cells in the spleen and lymph nodes (Fig. 2d, e and S2d, e).

Next, we examined the impact of the combined loss of caspases-1, -11 and -12 in myeloid cells. At steady state, the numbers of neutrophils ($GR\text{-}1^+MAC\text{-}1^+$) and monocytes ($GR\text{-}1^{lo}MAC\text{-}1^+$) were found to be normal in the bone marrows and spleens of the caspase-1/11/12 knockout mice (Fig. 2f and S2f). Collectively, these results demonstrate that the combined loss of caspases-1, -11 and -12 does not cause detectable abnormalities in the haematopoietic system of mice under steady state.

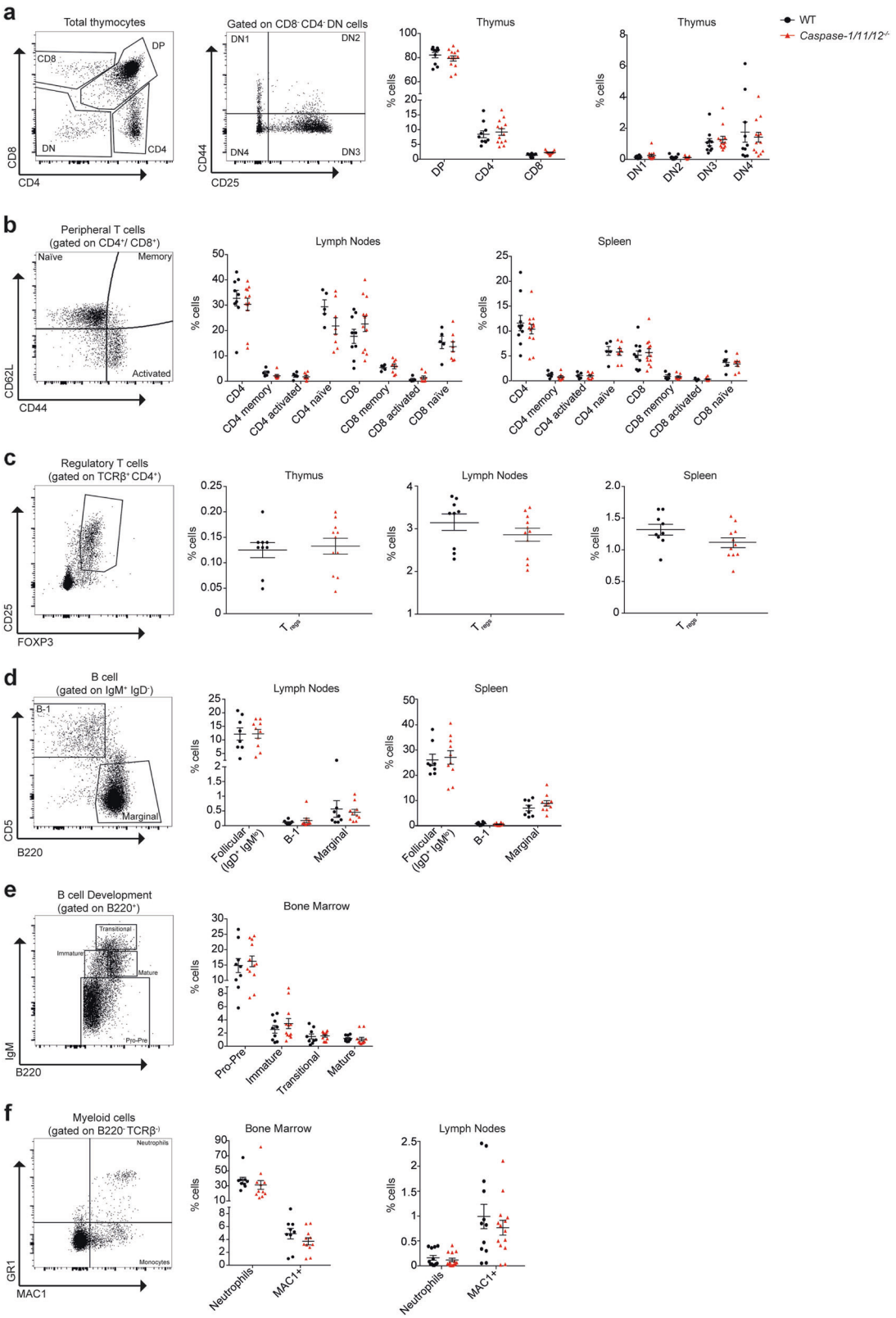
a
Total thymocytes
DP
CD8
DN
CD4
Gated on CD8⁻CD4⁻DN cells
DN1
DN2
DN4
DN3
CD44
CD25
Thymus
% cells
DP
CD4
CD8
Thymus
DN1
DN2
DN3
DN4
WT
Caspase-1/11/12⁻/⁻
b
Peripheral T cells
(gated on CD4⁺/ CD8⁺)
Naïve
Memory
Activated
CD62L
CD44
Lymph Nodes
Spleen
% cells
CD4
CD4 memory
CD4 activated
CD4 naïve
CD8
CD8 memory
CD8 activated
CD8 naïve
c
Regulatory T cells
(gated on TCRβ⁺ CD4⁺)
CD25
FOXP3
Thymus
Lymph Nodes
Spleen
% cells
T regs
d
B cell
(gated on IgM⁺ IgD⁻)
B-1
Marginal
CD5
B220
Lymph Nodes
Spleen
% cells
Follicular
(IgD⁺ IgM^lo)
B-1
Marginal
e
B cell Development
(gated on B220⁺)
Transitional
Immature
Mature
Pro-Pre
IgM
B220
Bone Marrow
% cells
Pro-Pre
Immature
Transitional
Mature
f
Myeloid cells
(gated on B220⁻ TCRβ⁻)
Neutrophils
Monocytes
GR1
MAC1
Bone Marrow
Lymph Nodes
% cells
Neutrophils
MAC1+

◀ **Fig. 2** Normal haematopoietic cell subset composition in the bone marrow (both tibia and femur), lymph nodes (axial, brachial and inguinal), thymus and spleen of caspase-1/11/12 triple knockout mice. **a** (Left) Representative flow cytometry plots to examine T cell development in the thymus. Cell populations during development defined as $CD8^+$, $CD4^+$ and DP for $CD4^+CD8^+$ double-positive T cells. Additional analysis on double-negative ($CD8^-CD4^-$) progenitor cells, denoted DN, using antibodies against CD25 and CD44. Gating strategy on DN progenitor cells depicted in second flow cytometry plot from the left to further subdivide into DN1–4 stages as follows: DN1 ($CD44^+CD25^-$), DN2 ($CD44^+CD25^+$), DN3 ($CD44^-CD25^+$) and DN4 ($CD44^-CD25^-$). **a** (Right) Percentages for each of these T cell populations in the thymus of caspase-1/11/12 knockout and WT control mice. **b** (Left) Representative gating strategy for $CD4^+$ T-cell activation. Naïve T cells that have not yet encountered an antigen do not express CD44 on the cell surface (top left quadrant). Upon activation by an antigen, T cells upregulate the CD44 expression (right panels). T cells with upregulated CD62L expression are considered memory T cells, whereas the so-called activated $CD4^+$ T cells circulating in the periphery express low levels of CD62L. **b** (Right) Quantification of percentages of naïve, memory and activated $CD4^+$ T cells in the spleen and lymph nodes from caspase-1/11/12 triple knockout and WT control mice. **c** (Left) Representative flow cytometry plots of T-cell populations in the lymphoid organs. Gating on regulatory T cells (T_{regs}) ($CD4^+CD25^+FOXP3^+$). **c** (Right) T_{reg} cell percentages in the thymus, lymph nodes and spleen. **d** (Left) Representative plots of B cell populations defined as B-1 ($IgM^+CD5^+B220^-$) or marginal zone ($IgM^+B220^+CD5^-$) B cells. **d** (Right) Percentages in lymph nodes and spleen are shown for each of these B-cell populations. **e** (Left) B-cell development using flow cytometric analysis. Representative plots showing pro-B/pre-B ($B220^+IgM^-$), immature B ($B220^+IgM^{lo}$), transitional B ($B220^+IgM^{hi}$) and mature B cells ($B220^{hi}IgM^{lo}$) in the bone marrow. **e** (Right) Quantitative analysis of these B cell populations. **f** (Left) Representation of myeloid cell populations analysed by flow cytometry. Top right represents neutrophils ($GR\text{-}1^+MAC\text{-}1^+$) and bottom right the monocyte population ($GR\text{-}1^-MAC\text{-}1^+$). **f** (Right) Percentages of these cells found in the bone marrow and lymph nodes. Graphs show means ± S.E.M. Cell numbers are presented in Supplementary Figure 2. $n \geq 5$. Symbols represent individual mice. Results tested with two-way ANOVA or unpaired two-tailed Student's *t* test

The additional loss of caspase-12 does not provide further protection against LPS-induced septic shock beyond the protection afforded by combined loss of caspase-1 and caspase-11

It has previously been shown that mice lacking caspase-11 or both caspases-1 and -11 are resistant to LPS-induced septic shock [22, 30]. Since caspase-12 is a CARD-containing caspase encoded by a gene that is co-located in the inflammatory caspase locus together with the genes encoding caspases-1 and -11, we hypothesised that it might play a role overlapping with the functions of these two caspases in the septic shock response. To test this idea, we injected WT, caspase-1/11 knockout and caspase-1/11/12 knockout mice with intermediate or high doses of LPS (18 or 54 mg/kg body weight, respectively). As previously reported [22], the caspase-1/11 knockout mice survived the septic shock longer than the control WT animals (Fig. 3a, b). Of note, the caspase-1/11/12 knockout mice did not show further extended survival compared with the caspase-1/11 double knockout animals (Fig. 3a, b).

Caspases-1 and -11 exert important functions in the maturation and secretion of several cytokines. It has been postulated that caspase-12, as a CARD-containing caspase being located in the inflammatory caspase locus, may also play a role in cytokine production. To test this hypothesis, we measured the cytokine levels 4 h post injection of high-dose LPS in the blood of mice (Fig. 3b and S3d, e). IL-18 levels were highly elevated in WT mice upon LPS treatment and this was abrogated in the caspase-1/11 double knockout mice. Thus, no further reduction in the levels of IL-18 was possible in the LPS-treated caspase-1/11/12 knockout mice. Generally, for all cytokines tested, the levels were similar between the caspase-1/11/12 triple knockout and the caspase-1/11 double knockout mice, both before and after the treatment with LPS.

At both concentrations of LPS used, there was a trend towards a reduction in IFN-γ in the WT mice compared with the caspase-1/11/12 knockout and caspase-1/11 knockout animals (Figure S3c and Figure S3d). This may be explained by the observation that IFN-γ can be proteolysed by caspase-1 [31]. Furthermore, multiplex analysis suggested an abnormal increase in the levels of chemokine Rantes/CCL5 in the caspase-1/11/12 knockout mice after LPS treatment, but this could not be confirmed in a single cytokine ELISA (Figure S3e). Collectively, these findings demonstrate that caspase-12 does not play a major role in septic shock alongside caspases-1 and -11.

The combined deletion of caspases-1, -11 and -12 does not confer cells with protection against cytotoxic drugs in vitro

Caspase-12 has been implicated in cell death elicited by diverse cytotoxic agents [27, 28, 32, 33]. For example, loss of caspase-12 was shown to protect mouse embryonic fibroblasts (MEFs) from killing induced by several ER stress-inducing agents [28]. However, this finding was challenged in subsequent studies using B16 [27] and several myeloma-derived cell lines [29]. To examine the overall roles of all three inflammatory caspases in cell death, we generated mouse dermal fibroblasts (MDFs) from caspase-1/11/12 knockout and WT mice, and exposed them to a variety of cytoytoxic agents, including the ER stressors thapsigargin and tunicamycin, the microtubule inhibitor taxol and the DNA-damage-inducing drug etoposide. Furthermore, we generated primary BMDMs from caspase-1/11/12 knockout as well as WT mice and treated them with the combinations of TNF plus a SMAC mimetic (CompA) (T + S) or TNF, SMAC mimetic plus caspase inhibitor QVD-OPH (T + S + Q), to cause apoptosis or necroptosis, respectively [34]. In

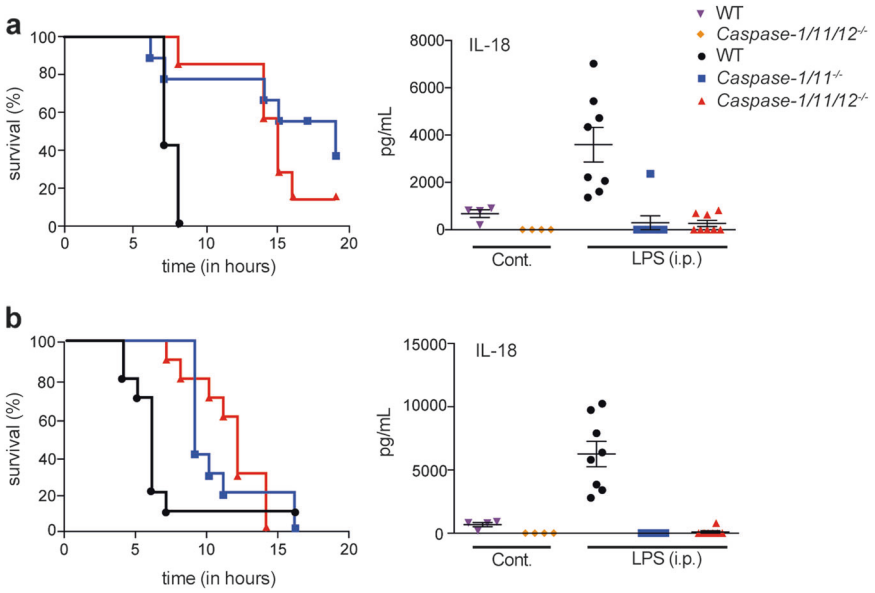

Fig. 3 Loss of caspase-12 does not provide additional protection against LPS-induced lethal septic shock above the protection afforded by combined loss of caspases-1 and -11. **a** Survival of mice of the indicated genotypes after i.p. injection with 18 mg/kg LPS (left panel). Serum levels of IL-18 at 4 h after i.p. injection of 18 mg/kg LPS (Cont. represents no treatment). **b** Similar presentation of data as in **a**, but mice were injected i.p. with 54 mg/kg LPS. Symbols represent individual mice. Data are presented as mean ± S.E.M. Adjusted *p* values are supplied in Supplementary Table 2. Results of the levels of cytokines were analysed by one-way ANOVA

general, the combined loss of caspases-1/11/12 afforded no significant protection against any of the cytotoxic agents tested in either of the two cell types examined (Fig. 4). These findings reveal that caspases-1, -11 and -12 do not exert significant roles in the intrinsic or death receptor apoptotic pathways or in necroptotic cell death.

Caspase-1/11/12 triple deficient mice show a normal ER stress response in vivo

Caspase-12 has been implicated in ER stress-induced cell killing in vivo [28]. To examine the overall roles of the inflammatory caspases in ER stress responses in vivo, we injected *caspase-1/11/12*$^{-/-}$ mice and WT controls with sublethal doses of tunicamycin. Histological analysis revealed similar damage to the kidneys at 72 h post treatment (Fig. 5a). Untreated caspase-1/11/12 triple knockout mice exhibited normal architecture of their kidneys (Fig. 5a). At 72 h post injection of tunicamycin, the overall architecture was damaged, especially in the outer medullary areas, and there were no differences in severity of damage between the caspase-1/11/12 triple knockout and WT mice (Fig. 5a). TUNEL staining revealed increased numbers of apoptotic cells predominantly in the outer medullary areas (Fig. 5a, b). Computational analysis of TUNEL^{+} cells revealed that there were no consistent differences between the caspase-1/11/12 knockout vs. control WT mice at 72 h post injection of tunicamycin (Fig. 5b and S4a). Moreover, WT animals treated with vehicle (DMSO) presented negligible numbers of TUNEL^{+} cells in their kidneys (Figure S4a). Untreated WT and caspase-1/11/12 knockout mice had normal serum levels of ALT (marker of liver damage) (Supplementary Figure 4b), demonstrating that the loss of caspases-1, -11 and -12 had no deleterious impact on these organs. After treatment with tunicamycin for 24 h, caspase-1/11/12 knockout and WT mice showed comparable but minor increases in the serum levels of ALT (Supplementary Figure 4b).

Finally, we examined the expression of the *caspase-1, -11* and *-12* genes in the organs examined for ER stress-induced damage, i.e. the kidneys and liver. In the liver and kidneys, unstressed mice express the *caspase-1, -11* and *-12* genes at low levels (Supplementary Table 5; relative expression compared to actin, depicted as $2^{-\Delta Ct}$ values in Supplementary Figure S5).

Collectively, these results demonstrate that the inflammatory caspases overall, and hence caspase-12, have no discernible role in tunicamycin-induced cell killing as well as renal or liver damage in vivo.

Discussion

Here, we describe the characterisation of a novel mouse strain lacking the three murine inflammatory caspases-1, -11 and -12. Loss of these three caspases had no impact on the general health of the mice. Moreover, extensive flow cytometric analysis revealed that the caspase-1/11/12 knockout mice had a normal haematopoietic system at steady state.

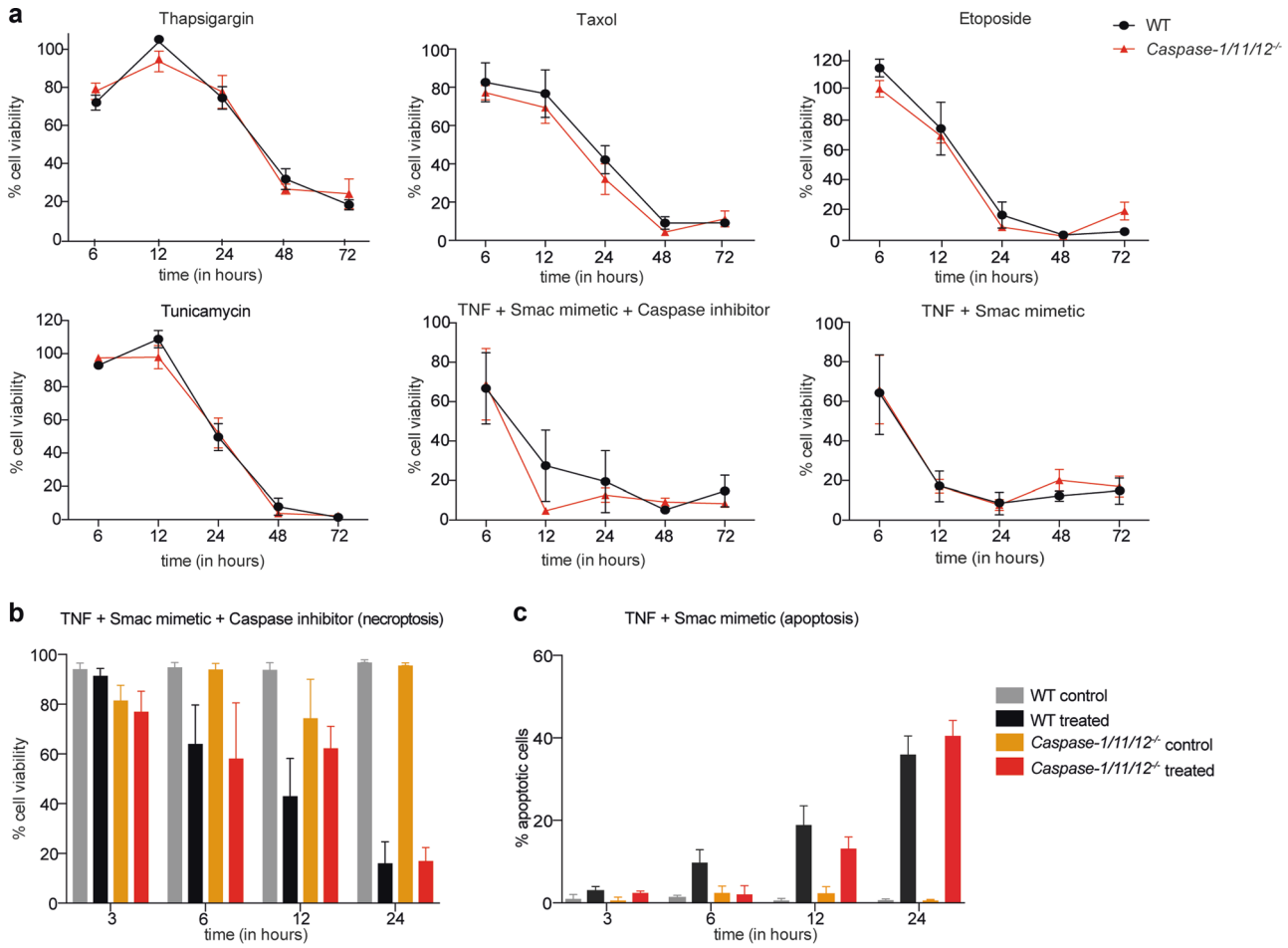

Fig. 4 Combined loss of caspases-1/11/12 does not confer protection against treatment with a broad range of cytotoxic insults to cells in vitro. **a** Mouse dermal fibroblasts (MDF) from caspase-1/11/12 triple knockout or WT control mice were treated with thapsigargin (123 nM), taxol (10 μM), etoposide (300 μM), tunicamycin (1 μM), TNF (100 ng/mL) + SMAC mimetic (500 nM) and TNF (100 ng/mL) + SMAC mimetic (500 nM) + caspase inhibitor Q-VD-Oph (10 μM), and cell survival was measured at the indicated time points by flow cytometry. Graphs shown are for one representative experiment with $n = 3$ cell lines per genotype. Data are normalised to untreated control cells. Cell viability was measured by PI and Annexin V staining, followed by flow cytometric analysis. Data are presented as mean ± S.E.M. and were analysed using two-way ANOVA. **b, c** Primary BMDMs from caspase-1/11/12 triple knockout and WT control mice were treated with **b** TNF + SMAC mimetic + caspase inhibitor QVD-OPH (T + S + Q) to induce necroptosis or **c** TNF + SMAC mimetic (T + S) to induce apoptosis. Cell viability was measured at the indicated time points by Annexin V or Annexin V plus PI staining in the case of T + S + Q treatment, followed by flow cytometric analysis. All data were analysed using one-way ANOVA test. $n \geq 3$. Data are presented as mean ± S.E.M.

It is well known that caspases-1 and -11 have critical roles in pyroptotic cell death, the production of IL-1β and IL-18 and in sepsis [18, 22, 30]. We and others have hypothesised that caspase-12, closely related and encoded in the same locus as caspases-1 and -11, may have overlapping functions with caspases-1 and -11. Therefore, we investigated whether the additional loss of caspase-12 might further increase the resistance to LPS-induced septic shock that is afforded by the combined loss of caspases-1 and -11. However, the caspase-1/11/12 knockout mice were no more resistant to LPSinduced septic shock than the caspase-1/11 double knockout animals. The overall condition and body temperature were monitored until the LPStreated mice reached the ethical endpoint. Upon LPS injection, signs of morbidity and poor health appeared later and with reduced severity (at least at early time points) in the caspase-1/11 knockout and the caspase-1/11/12 knockout mice compared with the LPStreated WT animals. Since no significant differences were observed between the caspase-1/11/12 knockout vs. the caspase-1/11 knockout mice, this suggests that caspase-12 does not play a significant role in this septic shock model.

Caspase-12 has also been implicated in ER stress-induced apoptosis [25, 28, 32, 35]. Moreover, caspases-1 and -11 have recently been implicated in the death of certain cancer cells by chemotherapeutic drugs [36]. However, we found that combined loss of caspases-1, -11 and -12 did not protect several types of haematopoietic cells and fibroblasts in vitro against a diverse range of cytotoxic drugs. It has

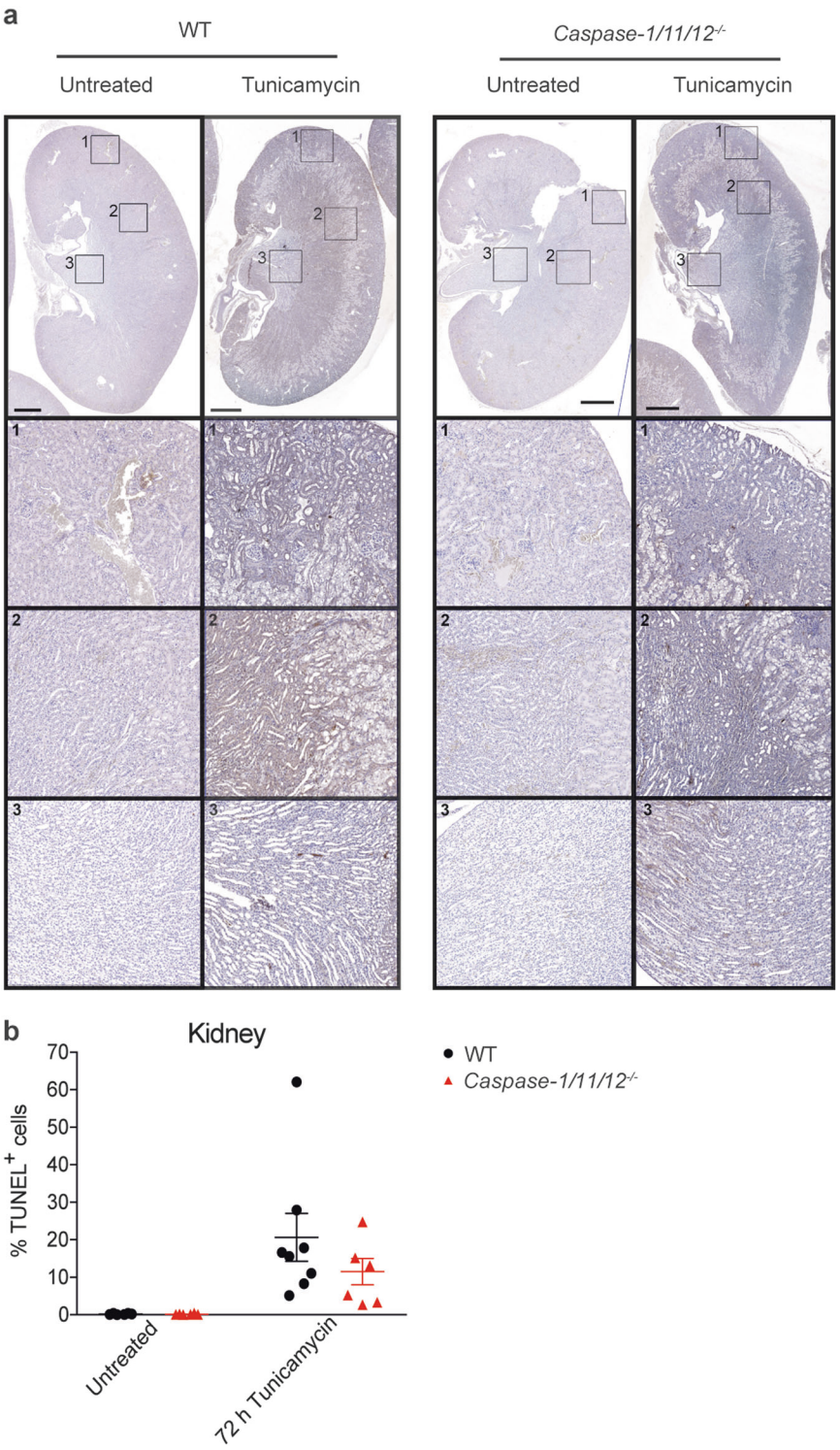

Fig. 5 Combined loss of caspases-1, -11 and -12 does not protect mice against ER stress-induced renal damage. **a** Immunohistochemical staining of kidneys from tunicamycin-treated (1 mg/kg body weight, harvested after 72 h) and -untreated mice to detect TUNEL^{+} (dead) cells of WT mice are shown in the left panels, and for caspase-1/11/12 triple knockout mice in the right right panels. One representative image shown per genotype and treatment. $n \geq 3$. Sections: cortex (1), outer medulla (2) and inner medulla (3). Scale bar represents 1 mm, total magnification of kidney ×20. **b** Bar graphs showing quantification of results from **a** $n \geq 3$ mice per genotype, two kidney sections per mouse were scored computationally

also been reported that caspase-12 deficiency renders mice resistant to tunicamycin-induced renal damage in vivo that is associated with induction of apoptosis in this tissue [28]. However, we did not detect any differences in renal damage and the frequency of apoptotic cells in the kidneys between caspase-1/11/12 knockout and WT mice. These findings may indicate that inflammatory caspases are only critical for cytotoxic drug-induced cell killing in selected cell types. Moreover, it remains possible that we have not yet tested a cell death inducer for which caspases-1/11/12 collectively play critical roles. Activation of the murine inflammatory caspases-1 and -11 requires a two-step process, namely a

priming signal and a secondary stimulus, called the activation step [11, 22, 37, 38]. While caspase-1 can be activated by a broad range of stimuli, caspase-11 is only induced in cells and therefore capable of being activated upon sensing Gram-negative bacteria [22, 39]. It is possible that caspase-12 activation may similarly need specific priming and activation signals, that have not been identified yet. In BMDMs as well as in the kidney and liver, the absence of caspase-1/11 had no impact on the levels of *caspase-12* mRNA.

The substantial LPSinduced increase in the levels of *caspase-12* mRNA suggests a role of caspase-12 in response to bacterial infection and sepsis. Potential regulatory effects of caspase-12 on caspases-1 and -11 (serving as possible effectors) cannot be revealed in our mice since they lack all three inflammatory caspases.

Moreover, similar to caspase-1, the caspase-12 zymogen may have to bind to an adaptor protein to undergo the conformational changes required for activation. An adaptor for caspase-12 has not yet been identified and it is possible that the expression of such an activator of caspase-12 may also need a specific signal. Furthermore, it is possible that caspase-12 acts as a regulator upstream of caspases-1 and -11. Due to an early stop codon in one of the human caspase-12 genes, only a short, truncated version of this protein can be generated in people of Asian and Caucasian descent as well as in most Africans. This non-proteolytic form of human caspase-12 is structurally similar to the so-called CARD-only proteins (COPs), including ICEBERG and COP/pseudo-ICE. These proteins that contain a CARD, but lack the domains for enzymatic activity have previously been shown to have regulatory functions that impact cytokine secretion, NF-κB signalling and certain other signalling pathways [40, 41]. It is therefore possible that caspase-12, particularly the truncated form expressed in most humans, might fulfil a regulatory function or serve as a non-catalytic scaffolding platform in some signalling pathways, similar to the COPs. To rule out the possibility of upstream regulation, a single caspase-12deficient mouse strain would be useful for future studies. Our newly generated caspase-1/11/12 triple knockout mice will serve as a valuable tool in such investigations and we will make them available to the scientific community.

In conclusion, we have generated a strain of caspase-1/11/12 triple knockout mice. The analysis of these animals failed to identify a critical role of caspase-12, overlapping with the functions of caspases-1 and -11, in septic shock induced by LPS or the response of cells to a broad range of cytotoxic insults. Our caspase-1/11/12 triple knockout mice are expected to help identify important functions that are safeguarded by extensive functional overlap between many caspases, such as the ones operating in the fight against pathogens.

Materials and methods

Generation of caspase-1/11/12 triple knockout mice

The *caspase-1/11/12*$^{-/-}$ mice were generated by Taconic Bioscience GmbH. The genomic region encompassing *caspases-1, -11* and *-12* was deleted using the targeting strategy in C57BL/6 ES cells depicted in Fig. 1a. The targeting vector was generated using BAC clones from the C57BL/6J RPCIB-731 BAC library and was transfected into the Taconic C57BL/6N Tac ES cell line. The targeting construct contained a puromycin resistance cassette used for positive selection of recombinant clones as well as a thymidine kinase for negative selection. The positive selection cassette was subsequently excised using Flp-FRT-mediated recombination.

The heterozygous *caspase-1/11/12*$^{+/-}$ offspring were intercrossed to obtain *caspase-1/11/12*$^{-/-}$ mice. Genotyping (by PCR) confirmed the absence of the *caspase-1/11/12* locus. Primer sets used for genotyping: 23:5′cacacctaaaaacagagtaaaaggc, 24: 5′gggactgtatgaagaatggatcc, 25:5′cagcaccttgaattatgagttgg. PCR programme: 95 °C for 5 min followed by 95 °C (for 30 s), primer annealing at 60 °C (30 s) then 72 °C (1 min). All three steps were repeated for a total of 30 cycles and this was followed by a final single elongatation step at 72 °C.

Endotoxic shock model

Experiments with mice were conducted according to the guidelines and with approval from the Walter and Eliza Hall Institute (Parkville, Victoria, Australia) Animal Ethics Committee. The caspase-1/11 mice used in these (and other following) experiments were derived from a caspase-1/11 double knockout colony published previously [42, 43] and were not littermates from the caspase-1/11/12 triple knockout mice. Mice were injected intraperitoneally (i.p.) with 18 or 54 mg/kg body weight ultrapure LPS (*E. coli* O111:B4, InvivoGen, catalogue code: tlrl-eblps). Some treated mice were sacrificed after 4 h for heart bleeds and cytokine analysis. Mice for survival studies were taken when showing physical signs of ill health and/or a drop in body temperature below 33 °C. A scoring sheet was followed to assess the overall physical condition of the mice. This included features, such as posture, respiratory rate, dehydration, responsiveness and eye closure. The body temperature and physical condition of each mouse were checked hourly and every 15 min within the first hour until sacrifice. Only males were used for these LPS shock experiments, and all animals were between 6 and 12 weeks of age. The mice used in these experiments were derived from independent colonies, namely the C57BL/6 (WT control), *caspase-1/11* double knockout and *caspase-1/11/12* triple knockout lines.

In vivo treatment with tunicamycin

C57BL/6 (WT control) and caspase-1/11/12 triple knockout mice were injected with 1 mg/kg body weight tunicamycin (Sigma-Aldrich, product code T776) dissolved in DMSO as per the manufacturer's instructions and diluted in PBS buffer. Mice were injected i.p. and sacrificed 24 or 72 h post injection. The mice were monitored regularly for signs of discomfort during this period. At sacrifice, kidneys and livers were harvested for histological analysis and TUNEL staining. ALT levels in the sera were measured as described previously [44].

TUNEL staining

After harvesting, the kidneys (and livers) were incubated in formalin for 12 h at room temperature, followed by treatment with 70% EtOH. Preparation of tissue sections and staining with haematoxylin and eosin (H&E) were carried out in-house by the histology department. Dewaxed paraffin sections were incubated in 20 µg/mL proteinase K (Roche, product code 03115879001) for 15 min, followed by three 2-min washes in PBS. Endogenous peroxidase activity was blocked by treatment with 3% H_2O_2 in methanol for 5 min at room temperature. Following three 2-min washes in PBS, each section was incubated in the TUNEL reaction mix consisting of bio dUTP (0.3 nmol/µL) (Roche, product code 11093070910) + $CoCl_2$ (25 mM) + TdT buffer + TdT (25 U/µL) (Promega, product code M828C) + H_2O to a total volume of 50 µL per section for 1 h at 37 °C in a moist chamber. This was followed by further washes with PBS (3 × 2 min). The slides were then incubated with the ABC reagent (Vectastain Elite ABC Kit, Vector labs, product code PK-6100) for 30 min at room temperature (as per the manufacturer's instructions). After further washes, the sections were incubated in DAB peroxidase substrate mix for 5 min (Vector labs; SK-4100). Finally, slides were washed with H_2O, counterstained with haematoxylin and mounted by the in-house histology department. All slides were scored visually by microscopy. Additionally, two organ sections for each genotype and treatment were scanned and computationally analysed. The images were scanned using a 3DHISTEC slide scanner, and quantification of the $TUNEL^+$ cells was performed using FIJI [45] with a custom written scoring macro. For Fig. 5, the image contrast and brightness were adjusted using Adobe Photoshop CS6 version 13.0.4.

Measurement of cytokine levels in the serum of the mice

Blood from mice was taken at death or 4 h after treatment with LPS by cardiac puncture. The levels of cytokines were determined using ELISA (IL-1β from R&D; IL-18 from MBL International Corp.). The levels of all other cytokines and chemokines in the sera from the mice were quantified by using the Bio-Rad Bio-Plex Pro mouse cytokine 23-plex assay (product code M60-009RDPD).

Flow cytometric analysis

Mice were euthanised and organs were harvested into sterile BSS supplemented with 5% foetal calf serum (FCS, Sigma-Aldrich, 12003C). For the detection of cell surface markers, the following rat or hamster monoclonal antibodies that had been conjugated to FITC, APC, R-PE or biotin (made in-house or purchased from eBioscience) were used: TER119 (TER119), MAC-1 (M1/70), NK1.1 (PK136), B220 (14.8 or RA3-6B2), CD3 (145-2C11), CD4 (GK1.5, H129 or YTA3.2.1), CD8 (53-6.7 or YTS169), TCRβ (H57-597), CD44 (IM781), CD25 (PC61), IgD (11-26C), IgM (5.1), CD62L (MEL-14), CD5 (53-7.3) and GR-1 (RB6-8C5). Streptavidin conjugates to PE-Cy7 or APC (BioLegend) were used for the detection of biotin-conjugated antibodies. Cells were washed in BSS supplemented with 2% FCS and analysed using a LSR-II flow cytometer (BD Biosciences). Dead cells (PI^+) were excluded from analysis by staining with propidium iodide (PI, 5 µg/mL; Sigma-Aldrich). Intracellular staining for FoxP3 (clone FJK-16s) was performed using the eBioscience FoxP3/transcription factor staining buffer set. All data were analysed using FlowJo 9.9.4 software.

Cell death assays

Three independent MDF cell lines were generated from caspase-1/11/12 triple knockout and WT mice each. The fibroblasts were isolated from the dermis of mice and subsequently immortalised by transfection with an expression vector encoding the SV40 large T antigen. Primary BMDMs were generated (see below) and plated on non-coated 96-well plates over night with 1×10^4 cells seeded into each well containing 100 µL Dulbecco's modified Eagle's medium (DMEM) containing 10% FCS (Sigma-Aldrich, product code 12003C), 100 U/mL penicillin, 100 µg/mL streptomycin (complete medium) and supplemented with 20% L929 cell conditioned medium (a source of M-CSF). For immortalised MDFs, $1–2 \times 10^4$ cells per well were plated out on regular 96-well coated tissue culture plates in complete medium the night before the treatment. All cell types were treated with the drugs as indicated. The treatments used in these assays included TNF (100 ng/mL, made in-house), SMAC mimetic (CompA from Tetralogic, 500 nM), the caspase inhibitor QVD-Oph (10 µM, MP Biomedicals, OPH109), thapsigargin (Sigma, product code T9033), taxol (paclitaxel from Sigma-Aldrich, product code T7402), tunicamycin (Sigma, product code T7765) and etoposide (Sigma, product code T7402). At the

indicated time points, cells were harvested and stained with 1–5 µg/mL propidium iodide alone or in combination with Annexin V-FITC (produced in-house). Cell survival was measured in a BD FACS Calibur flow cytometer. All cell survival data are presented in a manner normalised to untreated control cells unless data for untreated cells are shown separately. Untreated cells were cultured in complete medium.

In vitro assays with BMDMs

Primary BMDMs were generated from single-cell suspensions of bone marrow that had been flushed with PBS containing 2% FCS from mouse tibiae and femora and cultured in Dulbecco's modified Eagle's medium (DMEM) containing 10% FCS (Sigma-Aldrich, 12003C), 100 U/mL penicillin and 100 µg/mL streptomycin (complete medium) and supplemented with 20% L929 conditioned medium (a source of M-CSF) for 6 days before plating out on treated tissue culture plates. Approximately 1×10^6 cells were plated per well on coated 12-well tissue culture plates in 1 mL of complete medium plus M-CSF. On day 7, the cells were stimulated with 20 ng/mL ultrapure LPS (LPS from *E. coli* O111:B4, InvivoGen, catalogue code: tlrl-eblps) for 24 h before harvesting the supernatants and cell pellets separately. For qRT-PCR analysis of the expression of *caspases-1, -11* and *-12*, BMDMs were treated with 20 ng/mL or 500 ng/mL LPS for 3 h. The cell pellet was subsequently washed twice with ice-cold PBS and lysed in 1 mL TRIzol (Thermo Fisher Scientific product code 1559-6018).

Western blot analysis

Cell pellets were lysed in Onyx buffer (20 mM Tris/HCL pH 7.4, 135 mM NaCl, 1.5 mM $MgCl_2$, 1 mM EGTA, 1% Triton X-100, 10% glycerol in H_2O) with protease inhibitor cocktail (Roche, 4693159001) added fresh, and samples of varying concentration (between 10 and 30 µg, depending on protein abundance) were loaded onto NuPAGE Novex 10% Bis–Tris protein gels (Thermo Fisher Scientific) for size fractioning and run in MES buffer. Transfers were carried out on the iBlot 2 dry blotting system (Invitrogen, IB21001) onto nitrocellulose membranes (Invitrogen, IB23001 or IB23001). Membranes were blocked in 5% skim milk powder in PBS with 0.1% Tween-20 and then probed with monoclonal antibodies against caspase-1 (clone 1H11; made in-house; see below, and available from Enzo Life-Sciences), caspase-11 (4E11; made in house; see below available from Adipogene and Enzo LifeSciences) or HSP70 (clone N6, a gift from Dr. Robin Andersson, Peter MacCallum Cancer Centre, Melbourne, Australia); the last one used as a loading control. Bound primary antibodies were detected by goat anti-rat IgG or goat anti-mouse IgG antibodies conjugated to HRP (Southern Biotech). The ECL reaction was used for detection, and blots were developed using the ChemiDoc Touch System (Bio-Rad Laboratories). Protein concentrations were determined by Bradford assay using Protein Assay Dye Reagent Concentrate as per the manufacturer's instructions (product code 5000006).

Generation of rat monoclonal antibodies against caspase-1 and caspase-11

Monoclonal antibodies against caspase-1 and caspase-11 were produced as we have described previously [46, 47]. Briefly, Wistar rats were initially immunised by subcutaneous injection (s.c.) with the p20 fragment of mouse caspase-1, a KLH conjugated mouse caspase-1 peptide (aa 206–220) or the p20 fragment of mouse caspase-11 dissolved in complete Freund's adjuvant (Difco, Detroit, MI). Two subsequent boosts with each of the immunogens resuspended in incomplete Freund's adjuvant (Difco) were given 3 and 6 weeks later. A final boost with the immunogen dissolved in phosphate-buffered saline (PBS) was given i.v. and i.p. 4 weeks later. Three days later, spleen cells from each of the immunised rats were fused with the SP2/0 myeloma cell line as previously described [47]. Hybridomas producing antibodies against either caspase-1 or caspase-11 and their isotypes were identified by a screening strategy that we have previously described. Briefly, 293T cells were transiently transfected with an EE-tagged inactive cysteine mutant of either mouse caspase-1 (to screen for antibodies against casapse-1) or caspase-11 (to screen for antibodies against casapse-11), fixed in 1% paraformaldehyde/PBS, permeabilised with 0.3% saponin (Sigma) and stained with hybridoma supernatants. Bound antibodies were revealed with fluorescein isothiocyanate (FITC)-conjugated goat anti-rat Ig antibodies (Southern Biotechnology) and analysed by flow cytometry. A single peak of low immunofluorescence indicated that a particular antibody did not recognise caspase-1 or caspase-11. A single peak of high intensity indicated binding to molecules other than caspase-1 or caspase-11. A double peak histogram of low and high intensity staining, due to the presence of both non-transfected and transfected cells, identified hybridomas producing antibodies specific to either caspase-1 or caspase-11. Antibodies against the EE epitope tag (BabCO) were used as a positive control and hybridomas producing antibodies against KLH were eliminated. Hybridomas producing antibodies of the desired specificity were cloned twice and adapted for growth in low serum medium. The caspase-1 antibody producing hydridoma clone 1H11 and the caspase-11 antibody producing hybridoma clone 4E11 were selected for further use. For production of large amounts of antibodies, hybridomas were

cultured for several weeks in the miniPERM classic 12.5-kd production and nutrient modules (Heraeus). Antibodies were purified on protein G-sepharose columns (Pharmacia) according to the manufacturer's instructions.

In vitro stimulation with LPS and ELISA to detect IL-18

For in vitro stimulation of caspase-1, primary BMDMs were primed with 20 ng/mL ultrapure LPS (LPS from *E. coli* O111: B4, InvivoGen, catalogue code: tlrl-eblps) for 3 h and subsequently activated using 5 mM ATP (Sigma, product number A 2383) for 1 h, after which the cells and supernatants were harvested individually. For caspase-11 activation, the cells were primed with 500 ng/mL ultrapure LPS for 3 h before activation with 2 μg/mL ultrapure LPS that was transfected into the cells using lipofectamine (LPS: lipofectamine was used at a ratio of 1:1.3). Priming and activation were performed in reduced serum opti-MEM media (Gibco). After 6 h, this medium was replaced with complete medium supplemented with 20% L929 cell conditioned medium (a source of M-CSF), and after an additional 16 h incubation the supernatants as well as cell pellets were harvested. The levels of cytokines and chemokines in the cell supernatants were determined by ELISA (IL-1β and Rantes/CCL5 from R&D, lL-18 from MBL International Corp.).

qRT-PCR analysis

For measuring the levels of mRNA expression, total RNA was isolated from the organs or cultured cells and cDNA was synthesised by using the SuperScript III first-strand synthesis system (ThermoFisher). qRT-PCR was performed in triplicates using TaqMan assay from ThermoFisher Scientific with primers for mouse *caspase-1* (Mm00438023_m1), *caspase-11* (Mm00432304_m1), *caspase-12* (Mm00438038_m1), β-actin (Mm02619580_g1) and hmbs (Mm01143545_m1) (loading control). qRT-PCR was run using Viia7 real-time PCR and an ABI7900 machine. β-actin was chosen as a internal control gene and ΔCt calculation was performed as fallows: ΔCt = (Ct gene of interest−Ct internal control). $2^{-\Delta\Delta Ct}$ values were calculated as described in ref. [48] using the equation: $2^{-\Delta\Delta Ct} = \Delta Ct$ (treated sample)−ΔCt (untreated sample). The relative difference of gene expression was calculated using *β-actin* as a reference for comparison. To set a threshold qRT-PCR cycle number for each gene of interest (considered as background noise), we tested Ct values for *caspase-1*, *caspase-11* and *caspase-12* in cells from caspase-1/11/12 triple knockout mice (data not shown). For *caspase-1* expression, the maximum cycle threshold was set at 35 cycles, anything over 37 cycles in the case of *caspase-11* and higher Ct than 39 for *caspase-12* were considered as no RNA detected.

Statistical analysis

Mouse survival curves were generated and analysed with GraphPad Prism (GraphPad Software Inc., La Jolla, CA, USA). Mouse survival cohorts were compared using the log-rank Mantel–Cox test. *P* values of <0.05 were considered significant. In vitro cell survival data were plotted and analysed with GraphPad Prism using one-way or two-way ANOVA statistical test. For ELISA data on cytokine levels in the sera from the mice, graphs were plotted using Prism software and examined by using the ordinary one-way ANOVA test. ELISA data on the levels of cytokines in the supernatants from cultured cells were evaluated by using Prism, applying a two-way ANOVA tests. Data are presented as standard error of the mean (±S.E.M.).

Acknowledgements We thank T Ballinger, S Russo, G Siciliano, C Stivala. and S Stoev for their help with experiments with mice; S Monard and his team for their help with flow cytometry. Our work is supported by the Australian National Health and Medical Research Council (Project Grant 1145728 to MJH and 1143105 to MJH and AS; Programme Grant 1016701 to AS and Fellowship 1020363 to AS), the Leukaemia and Lymphoma Society of America (LLS SCOR 7001-13 to AS and MJH), the Cancer Council of Victoria (1052309 to AS and Venture Grant MJH and AS) and by operational infrastructure grants through the Australian Government Independent Research Institute Infrastructure Support Scheme (9000220) and the Victorian State Government Operational Infrastructure Support Program.

Compliance with ethical standards

Conflict of interest The authors declare that they have no conflict of interest.

References

1. Martinon F, Tschopp J. Inflammatory caspases: linking an intracellular innate immune system to autoinflammatory diseases. Cell. 2004;117:561–74.
2. Man SM, Kanneganti TD. Gasdermin D: the long-awaited executioner of pyroptosis. Cell Res. 2015;25:1183–4.
3. Ramirez MLG, Salvesen GS. A primer on caspase mechanisms. Semin Cell Dev Biol. 2018 Jan 12. pii: S1084-9521(17)30108-8. https://doi.org/10.1016/j.semcdb.2018.01.002.
4. Czabotar PE, Lessene G, Strasser A, Adams JM. Control of apoptosis by the BCL-2 protein family: implications for physiology and therapy. Nat Rev Mol Cell Biol. 2014;15:49–63.
5. Youle RJ, Strasser A. The BCL-2 protein family: opposing activities that mediate cell death. Nat Rev Mol Cell Biol. 2008;9:47–59.
6. Strasser A, Jost PJ, Nagata S. The many roles of FAS receptor signaling in the immune system. Immunity. 2009;30:180–92.
7. Feltham R, Vince JE, Lawlor KE. Caspase-8: not so silently deadly. Clin Transl Immunol. 2017;6:e124.
8. Sagulenko V, Lawlor KE, Vince JE. New insights into the regulation of innate immunity by caspase-8. Arthritis Res Ther. 2016;18:4.

9. Pop C, Salvesen GS. Human caspases: activation, specificity, and regulation. J Biol Chem. 2009;284:21777–81.
10. Latz E, Xiao TS, Stutz A. Activation and regulation of the inflammasomes. Nat Rev Immunol. 2013;13:397–411.
11. Man SM, Kanneganti TD. Regulation of inflammasome activation. Immunol Rev. 2015;265:6–21.
12. Shaw PJ, McDermott MF, Kanneganti TD. Inflammasomes and autoimmunity. Trends Mol Med. 2011;17:57–64.
13. Hanahan D, Weinberg RA. The hallmarks of cancer. Cell. 2000;100:57–70.
14. Black RA, Kronheim SR, Merriam JE, March CJ, Hopp TP. A pre-aspartate-specific protease from human leukocytes that cleaves pro-interleukin-1 beta. J Biol Chem. 1989;264:5323–6.
15. Kostura MJ, Tocci MJ, Limjuco G, Chin J, Cameron P, Hillman AG, et al. Identification of a monocyte specific pre-interleukin 1 beta convertase activity. Proc Natl Acad Sci USA. 1989;86:5227–31.
16. Suresh R, Mosser DM. Pattern recognition receptors in innate immunity, host defense, and immunopathology. Adv Physiol Educ. 2013;37:284–91.
17. Lamkanfi M, Dixit VM. Mechanisms and functions of inflammasomes. Cell. 2014;157:1013–22.
18. Lamkanfi M. Emerging inflammasome effector mechanisms. Nat Rev Immunol. 2011;11:213–20.
19. de Zoete MR, Palm NW, Zhu S, Flavell RA. Inflammasomes. Cold Spring Harb Perspect Biol. 2014;6:a016287.
20. Vince JE, Silke J. The intersection of cell death and inflammasome activation. Cell Mol Life Sci. 2016;73:2349–67.
21. Hagar JA, Powell DA, Aachoui Y, Ernst RK, Miao EA. Cytoplasmic LPS activates caspase-11: implications in TLR4-independent endotoxic shock. Science. 2013;341:1250–3.
22. Kayagaki N, Warming S, Lamkanfi M, Vande Walle L, Louie S, Dong J, et al. Non-canonical inflammasome activation targets caspase-11. Nature. 2011;479:117–21.
23. Kayagaki N, Wong MT, Stowe IB, Ramani SR, Gonzalez LC, Akashi-Takamura S, et al. Noncanonical inflammasome activation by intracellular LPS independent of TLR4. Science. 2013;341:1246–9.
24. Ramirez MLG, Poreba M, Snipas SJ, Groborz K, Drag M, Salvesen GS. Extensive peptide and natural protein substrate screens reveal that mouse caspase-11 has much narrower substrate specificity than caspase-1. J Biol Chem. 2018;293:7058–67.
25. Lamkanfi M, Kalai M, Vandenabeele P. Caspase-12: an overview. Cell Death Differ. 2004;11:365–8.
26. Hermel E, Klapstein KD. A possible mechanism for maintenance of the deleterious allele of human CASPASE-12. Med Hypotheses. 2011;77:803–6.
27. Kalai M, Lamkanfi M, Denecker G, Boogmans M, Lippens S, Meeus A, et al. Regulation of the expression and processing of caspase-12. J Cell Biol. 2003;162:457–67.
28. Nakagawa T, Zhu H, Morishima N, Li E, Xu J, Yankner BA, et al. Caspase-12 mediates endoplasmic-reticulum-specific apoptosis and cytotoxicity by amyloid-beta. Nature. 2000;403:98–103.
29. Obeng EA, Boise LH. Caspase-12 and caspase-4 are not required for caspase-dependent endoplasmic reticulum stress-induced apoptosis. J Biol Chem. 2005;280:29578–87.
30. Wang S, Miura M, Jung YK, Zhu H, Li E, Yuan J. Murine caspase-11, an ICE-interacting protease, is essential for the activation of ICE. Cell. 1998;92:501–9.
31. Ghayur T, Banerjee S, Hugunin M, Butler D, Herzog L, Carter A, et al. Caspase-1 processes IFN-gamma-inducing factor and regulates LPS-induced IFN-gamma production. Nature. 1997;386:619–23.
32. Nakagawa T, Yuan J. Cross-talk between two cysteine protease families. Activation of caspase-12 by calpain in apoptosis. J Cell Biol. 2000;150:887–94.
33. Rao RV, Hermel E, Castro-Obregon S, del Rio G, Ellerby LM, Ellerby HM, et al. Coupling endoplasmic reticulum stress to the cell death program. Mechanism of caspase activation. J Biol Chem. 2001;276:33869–74.
34. Murphy JM, Czabotar PE, Hildebrand JM, Lucet IS, Zhang JG, Alvarez-Diaz S, et al. The pseudokinase MLKL mediates necroptosis via a molecular switch mechanism. Immunity. 2013;39:443–53.
35. Jimbo A, Fujita E, Kouroku Y, Ohnishi J, Inohara N, Kuida K, et al. ER stress induces caspase-8 activation, stimulating cytochrome c release and caspase-9 activation. Exp Cell Res. 2003;283:156–66.
36. Wang Y, Gao W, Shi X, Ding J, Liu W, He H, et al. Chemotherapy drugs induce pyroptosis through caspase-3 cleavage of a gasdermin. Nature. 2017;547:99–103.
37. Mariathasan S. ASC, Ipaf and Cryopyrin/Nalp3: bona fide intracellular adapters of the caspase-1 inflammasome. Microbes Infect. 2007;9:664–71.
38. Mariathasan S, Weiss DS, Newton K, McBride J, O'Rourke K, Roose-Girma M, et al. Cryopyrin activates the inflammasome in response to toxins and ATP. Nature. 2006;440:228–32.
39. Wang S, Miura M, Jung Y, Zhu H, Gagliardini V, Shi L, et al. Identification and characterization of Ich-3, a member of the interleukin-1beta converting enzyme (ICE)/Ced-3 family and an upstream regulator of ICE. J Biol Chem. 1996;271:20580–7.
40. Druilhe A, Srinivasula SM, Razmara M, Ahmad M, Alnemri ES. Regulation of IL-1beta generation by Pseudo-ICE and ICEBERG, two dominant negative caspase recruitment domain proteins. Cell Death Differ. 2001;8:649–57.
41. Humke EW, Shriver SK, Starovasnik MA, Fairbrother WJ, Dixit VM. ICEBERG: a novel inhibitor of interleukin-1beta generation. Cell. 2000;103:99–111.
42. Li P, Allen H, Banerjee S, Franklin S, Herzog L, Johnston C, et al. Mice deficient in IL-1 beta-converting enzyme are defective in production of mature IL-1 beta and resistant to endotoxic shock. Cell. 1995;80:401–11.
43. Schott WH, Haskell BD, Tse HM, Milton MJ, Piganelli JD, Choisy-Rossi CM, et al. Caspase-1 is not required for type 1 diabetes in the NOD mouse. Diabetes. 2004;53:99–104.
44. Jost PJ, Grabow S, Gray D, McKenzie MD, Nachbur U, Huang DC, et al. XIAP discriminates between type I and type II FAS-induced apoptosis. Nature. 2009;460:1035–9.
45. Schindelin J, Arganda-Carreras I, Frise E, Kaynig V, Longair M, Pietzsch T, et al. Fiji: an open-source platform for biological-image analysis. Nat Methods. 2012;9:676–82.
46. O'Reilly LA, Cullen L, Visvader J, Lindeman GJ, Print C, Bath ML, et al. The proapoptotic BH3-only protein bim is expressed in hematopoietic, epithelial, neuronal, and germ cells. Am J Pathol. 2000;157:449–61.
47. O'Reilly LA, Cullen L, Moriishi K, O'Connor L, Huang DCS, Strasser A. Rapid hybridoma screening method for the identification of monoclonal antibodies to low abundance cytoplasmic proteins. Biotechniques. 1998;25:824–30.
48. Schmittgen TD, Livak KJ. Analyzing real-time PCR data by the comparative C(T) method. Nat Protoc. 2008;3:1101–8.

3.2 Supplementary Figures

S1

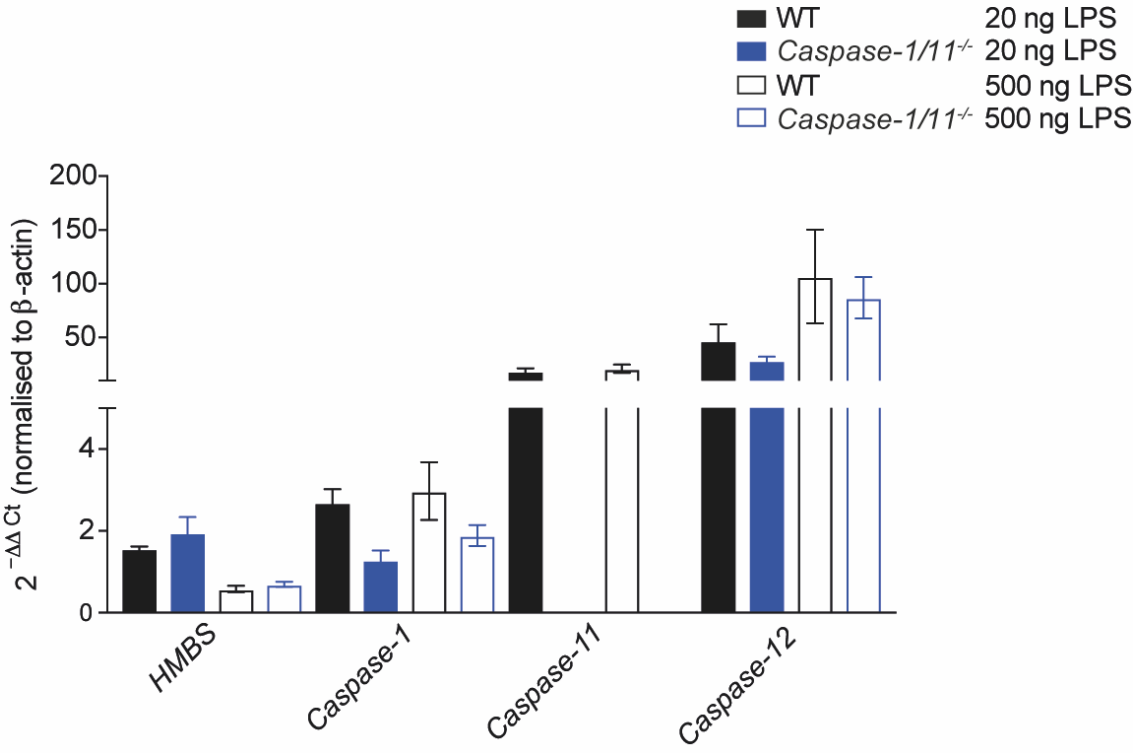

Supplementary Figure 1

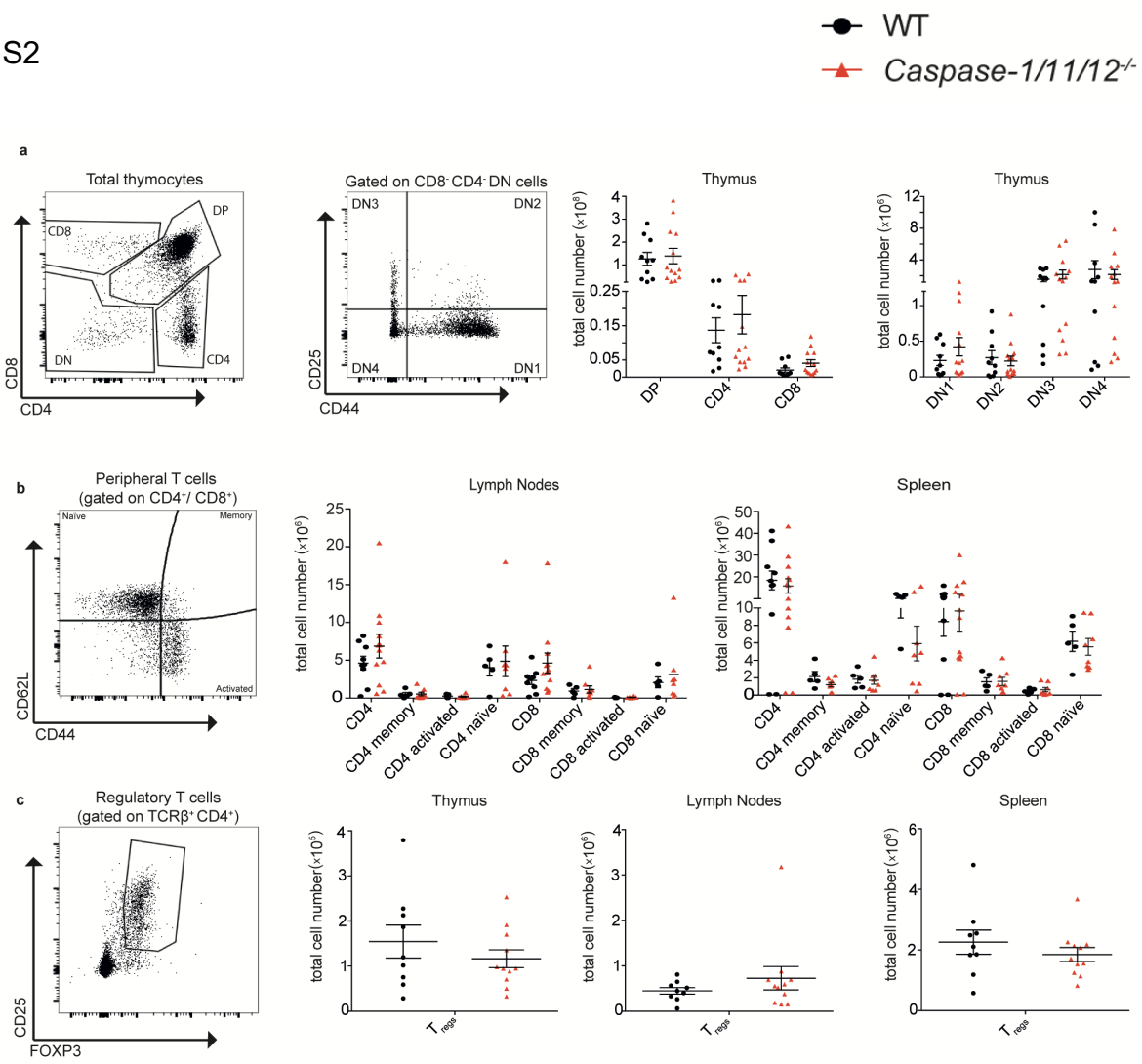

Supplementary Figure 2

S2 (continued)

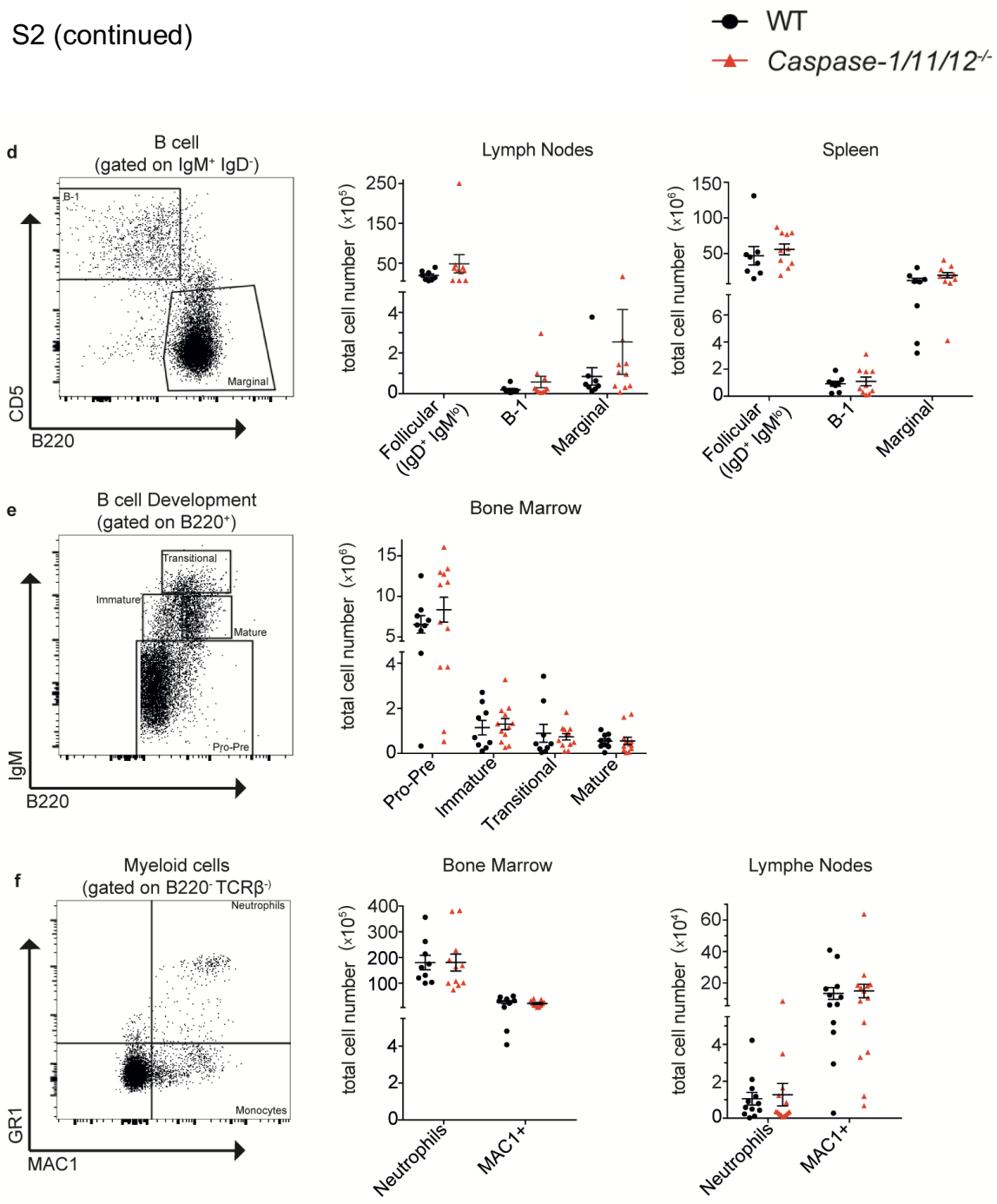

Continued from previous page.

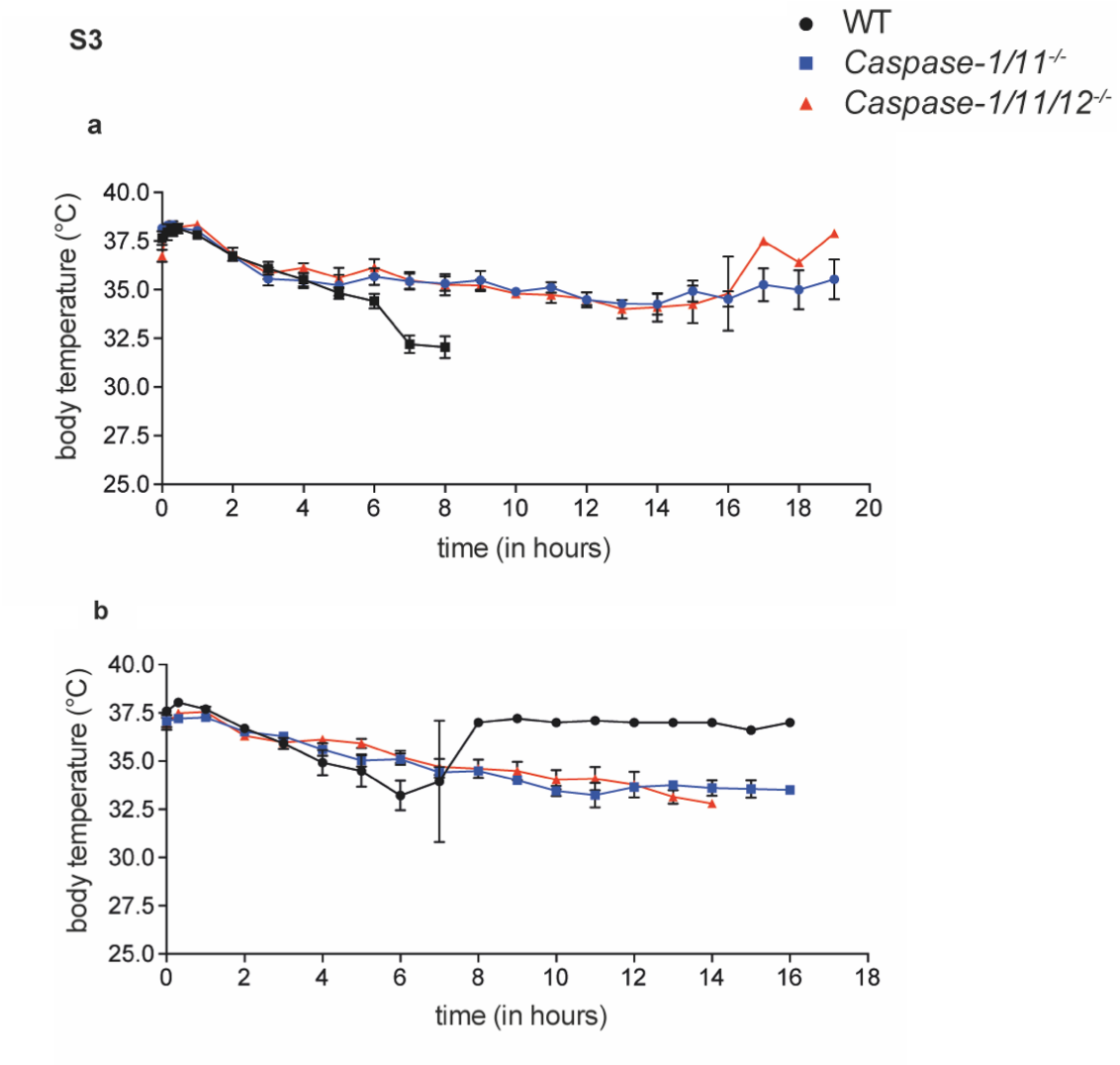

Supplementary Figure 3

S3c

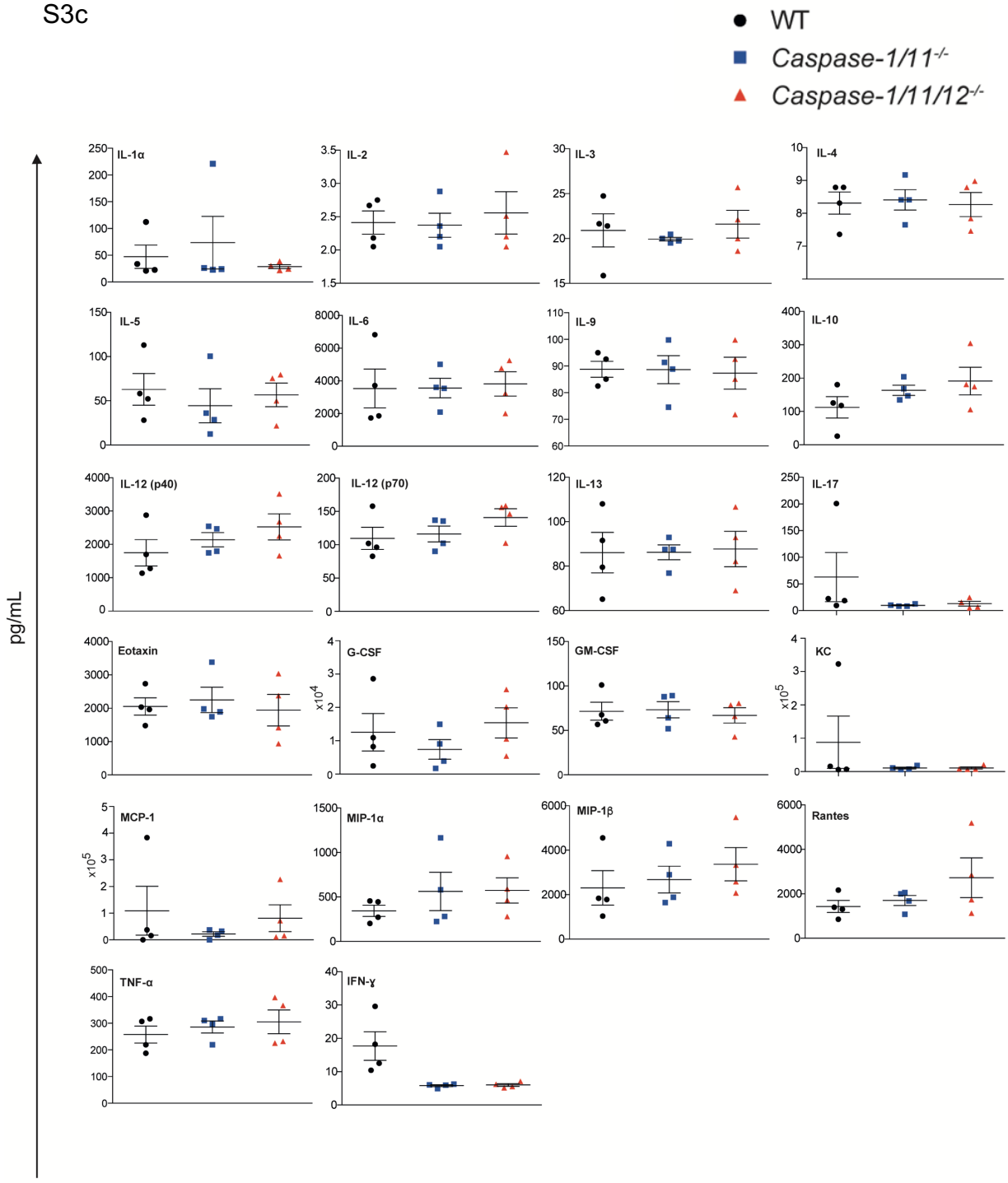

Supplementary Figure 3 continued.

S3

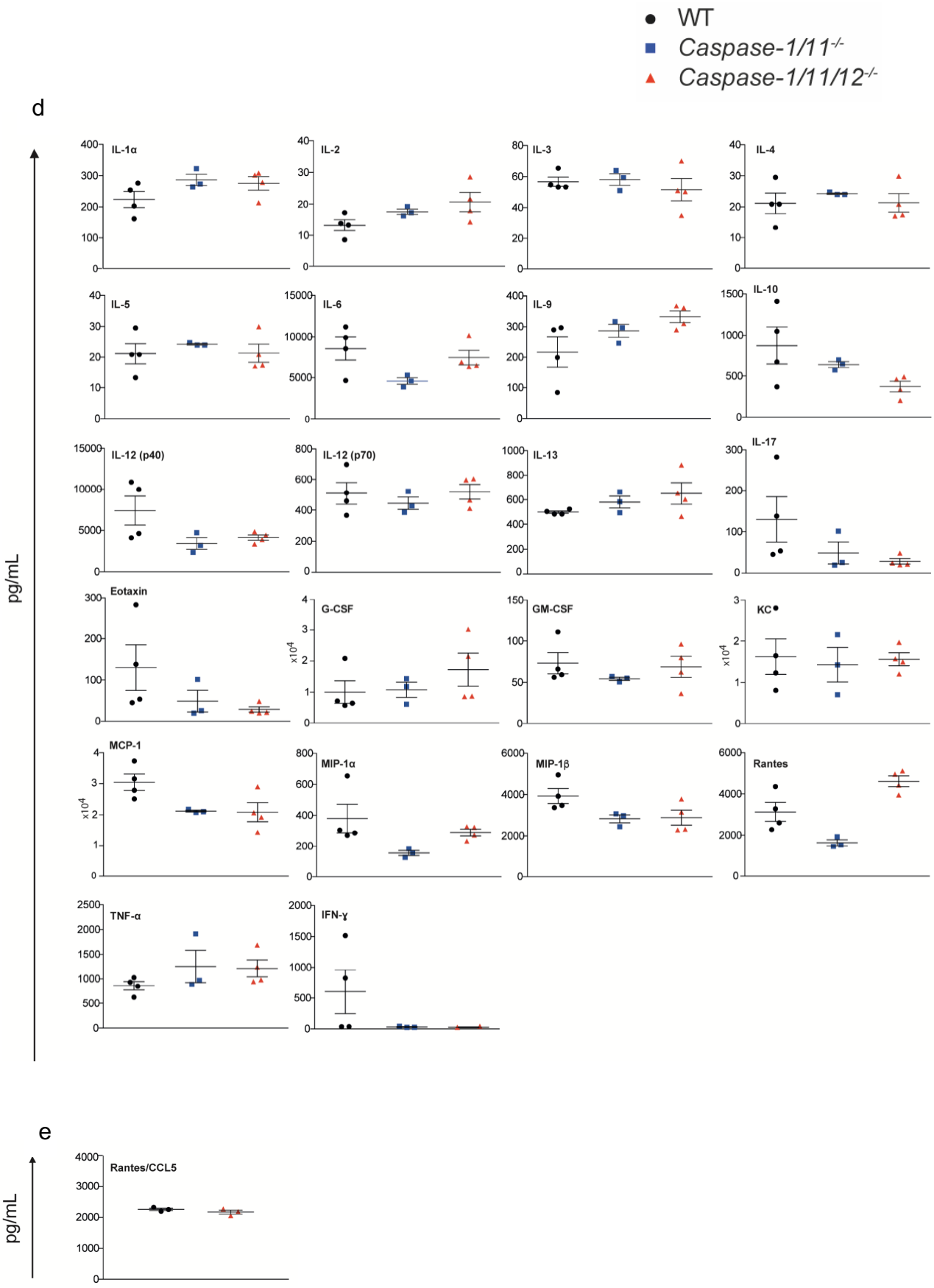

Supplementary Figure 3 continued.

S4

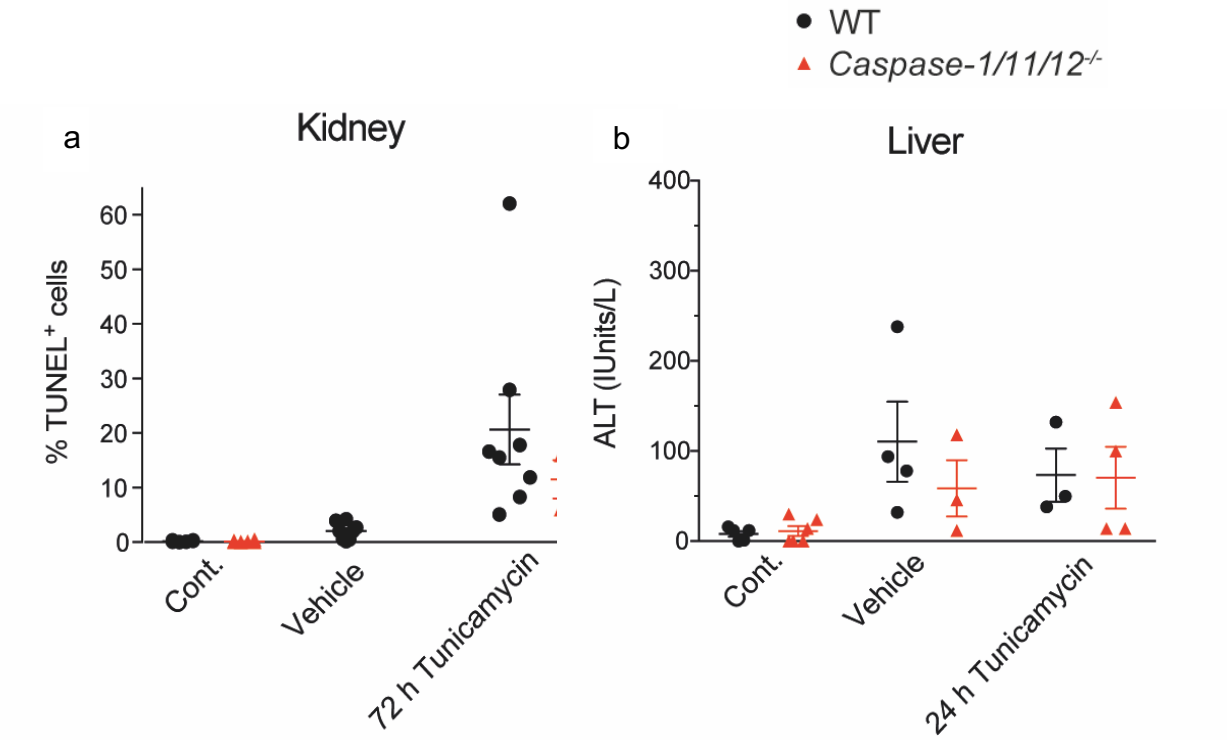

Supplementary Figure 4

S5

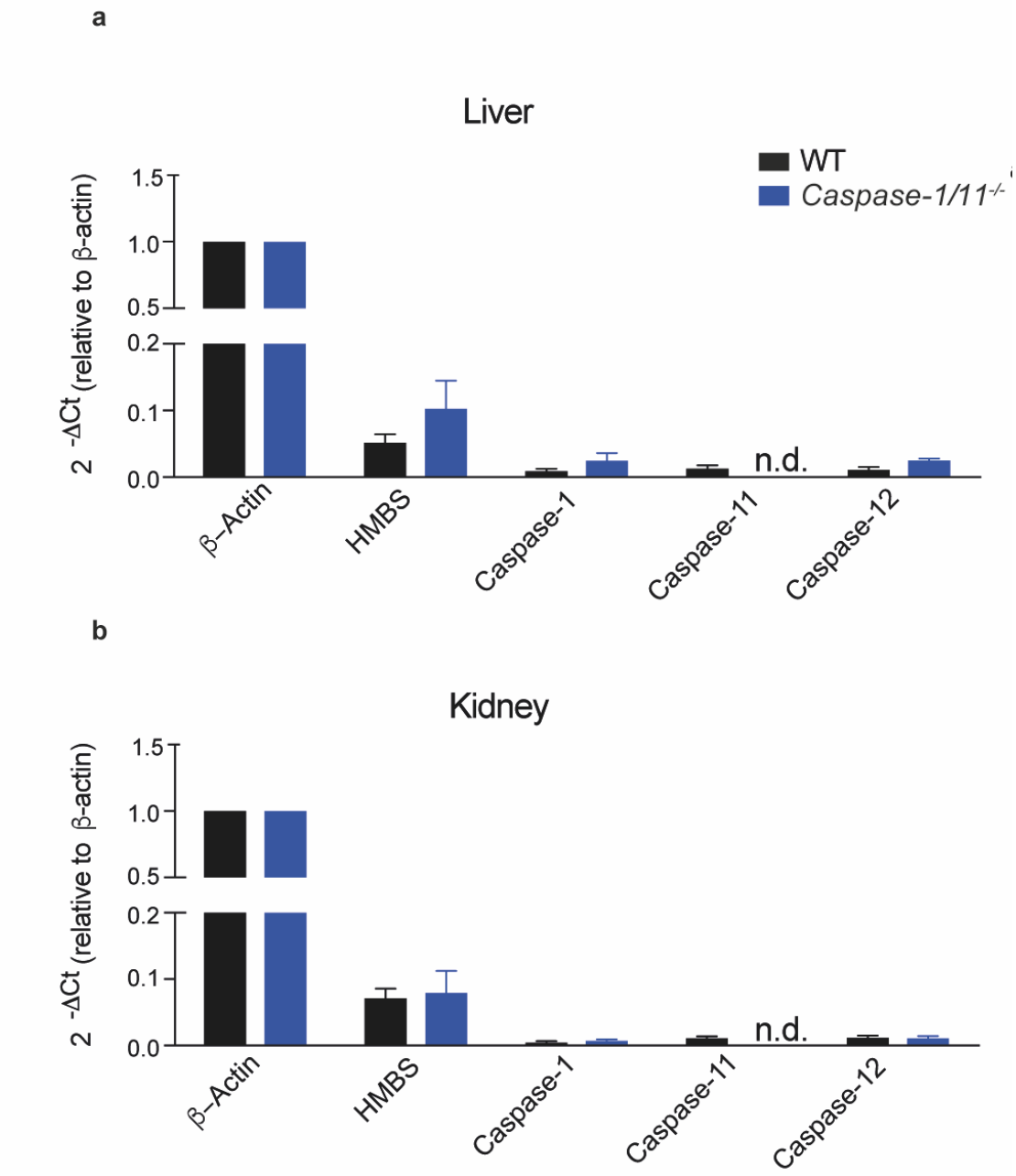

Supplementary Figure 5

Table 1 a: Caspase-1 assay IL-1β secretion		
		adjusted p values
WT vs. C1/11-/-	Activated	0.0001
WT vs. C1/11/12 -/-	Activated	0.0002

Table 1 b: Caspase-11 assay IL-1β secretion		
		adjusted p values
WT vs. C1/11-/-	Activated	0.001
WT vs. C1/11/12 -/-	Activated	0.001

Table 2 a: Survival statistics of mice post injection of 18 mg/kg	
	adjusted p values
WT vs. C1/11 -/-	p=0.009
WT vs. C1/11/12 -/-	p=0.001
C1/11 -/- vs. C1/11/12 -/-	p=0.1

Table 2 b: IL-18 secretion upon injection of 18 mg/kg	
	adjusted p values
Cont. WT vs. WT	0.002
Cont. C1/11/12 -/- vs. WT	0.0002
WT vs. C1/11 -/-	<0.0001
WT vs. C1/11/12 -/-	<0.0001

Table 2 b: Survival statistics of mice post injection of 54 mg/kg	
	adjusted p values
WT vs. C1/11 -/-	p=0.02
WT vs. C1/11/12 -/-	p=0.02

Table 2 c: IL-18 secretion upon injection of 54 mg/kg	
	adjusted p values
Cont. WT vs. WT	<0.0001
Cont. C1/11/12 -/- vs. WT	<0.0001
WT vs. C1/11 -/-	<0.0001
WT vs. C1/11/12 -/-	<0.0001

Table 3: Mean Ct values after indicated LPS treatment in BMDMs						
	β-actin		***HMBS***		***Caspase-1***	
	WT	Caspase-1/11-/-	WT	Caspase-1/11-/-	WT	Caspase-1/11-/-
Untreated	16	16.2	23.85	24.4	22.3	22.5
20 ng LPS	16.4	16.2	24.87	25.37	21.1	22.3
500 ng LPS	16.4	17.1	25.21	26	21.1	22.4

Table 3: Mean Ct values after indicated LPS treatment in BMDMs				
	Caspase-11		***Caspase-12***	
	WT	Caspase-1/11-/-	WT	Caspase-1/11-/-
Untreated	24.8	36.8	33.3	32.8
20 ng LPS	21	32.2	28.4	28
500 ng LPS	20.9	34.9	27.3	27.3

Table 4 a: INF-ɣ secretion, 18 mg/kg LPS I.P	
	adjusted p values
WT vs. C1/11 -/-	0.0206
WT vs. C1/11/12 -/-	0.0226

Table 4 b: Rantes/ CCL5 secretion, 54 mg/kg LPS I.P	
	adjusted p values
WT vs. C1/11 -/-	0.0428
WT vs. C1/11/12 -/-	0.0318
C1/11 -/- vs. C1/11/12 -/-	0.0009

Table 5: Mean Ct expression values of *caspase-1, -11,-12 and β-actin* in liver and kidney						
	β-actin		***HMBS***		***Caspase-12***	
	WT	Caspase-1/11-/-	WT	Caspase-1/11-/-	WT	Caspase-1/11-/-
Liver	24.45	25.33	28.79	28.82	31.26	30.66
Kidney	23.19	22.75	27.05	26.72	29.6	29.27

Table 5: Mean Ct expression values of *caspase-1, -11,-12 and β-actin* in liver and kidney						
	Caspase-1		***Caspase-11***		***Caspase-12***	
	WT	Caspase-1/11-/-	WT	Caspase-1/11-/-	WT	Caspase-1/11-/-
Liver	31.6	30.93	30.9	n.d.	31.26	30.66
Kidney	31.44	29.98	29.96	n.d.	29.6	29.27

The following data was not included in the manuscript:

3.3 Additional results and discussion

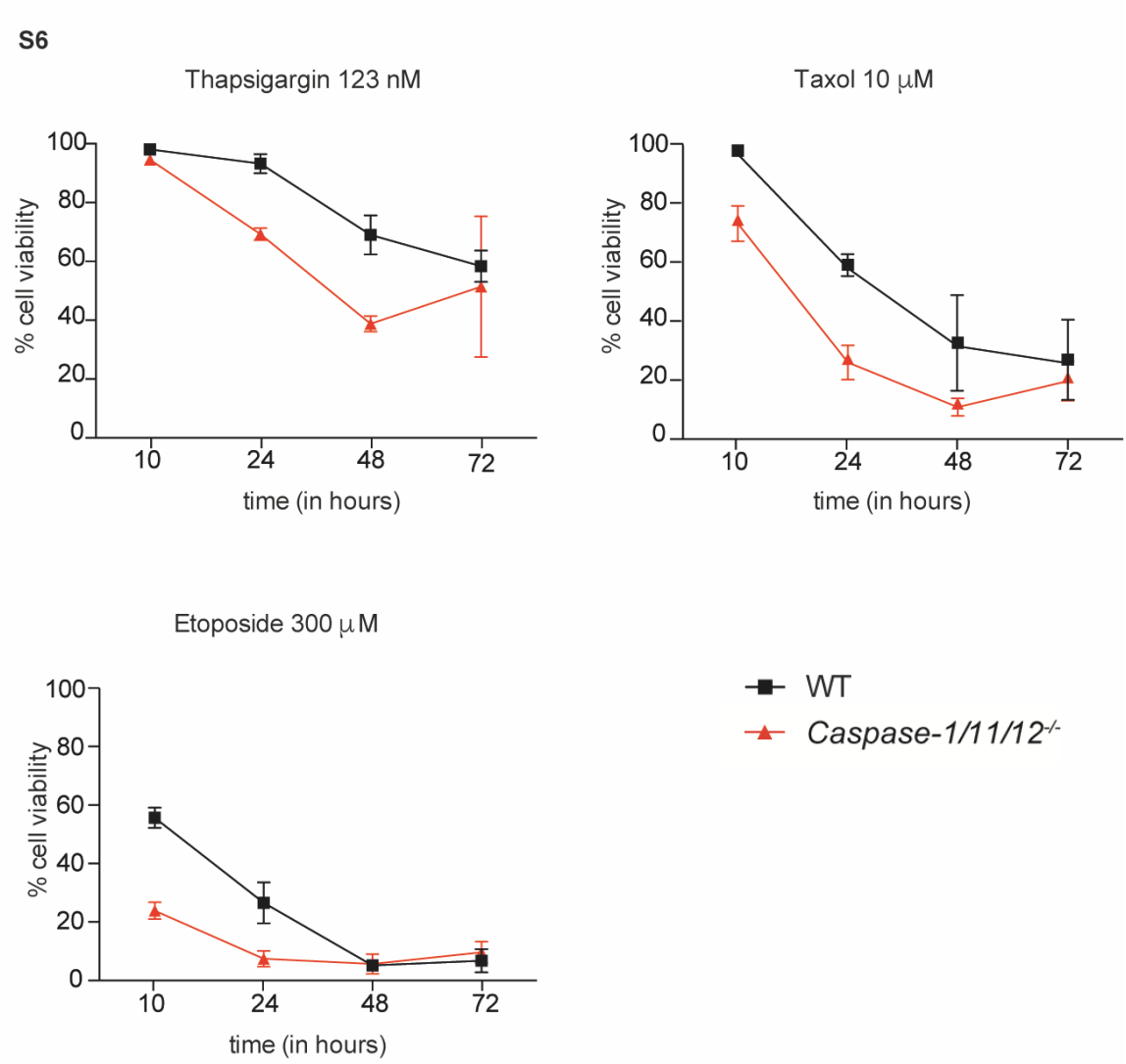

Figure 3-1: Caspase-1/11/12$^{-/-}$ iBMDMs show no survival advantage over wildtype cells when treated with different cytotoxic drugs.

Death assays on immortalised bone marrow-derived macrophages (iBMDMs) from wildtype and caspase-1/11/12$^{-/-}$ mice treated with indicated drugs (thapsigargin at 123 nM, taxol at 10 μM and etoposide at 300 μM).

Graphs show mean ± SEM, analysed using 2way ANOVA. P values in Table 6. N=3 independent experiments.

3.3.2 Additional Results

Lastly, we tested whether the deletion of caspases-1, -11 and -12 convey a survival advantage, for immortalised BMDMs (iBMDMs) in response to various cytotoxic drugs. Cells were treated with the indicated drug concentrations over the course of three days, but no significant differences could be observed between the wildtype and caspase-1/11/12 deficient iBMDMs (Figure 3-1).

3.3.3 Additional discussion

In our additional experiments we analysed the effects of deleting all inflammatory caspases on cell death induced by different cytotoxic drugs in iBMDMs . Although there was a trend of the wildtype cells to be more resistant to the different drugs, it was not significant. However, this trend can possibly be explained by the immortalisation process and hence selection of clones with higher survival capacity. Since we only tested one immortalised cell line per genotype, more wt and caspase-1/11/12 triple knockout cell lines need to be immortalised to obtain a conclusive result.

Thapsigargin 123nM	Significant?	Adjusted p value
WT vs. C1/11/12 $^{-/-}$	0.0236	*

Taxol 10 µM	Significant?	Adjusted p value
WT vs. C1/11/12 $^{-/-}$	0.0039	**

Etoposide 300 µM	Significant?	Adjusted p value
WT vs. C1/11/12 $^{-/-}$	0.0005	***

Table 3-1 Adjusted p values for cell death assays depicted in Figure 3-1.

Chapter 4: Unexpected overlapping roles of multiple caspases and programmed cell death pathways in the response to *Salmonella* infection

4.1 Introduction

Salmonella species are a leading bacterial cause of foodborne acquired acute gastroenteritis and typhoid fever causing a substantial burden on global human health [159]. *Salmonella enterica* is a Gram-negative facultative intracellular bacterium and is the major cause of salmonellosis in humans worldwide [160]. The clinical manifestations following *Salmonella* infection vary depending on the serovar. Typhoid fever caused by *Salmonella* serovar Typhi is regarded as a severely life-threatening infection [161]. In typhoidal infections, the bacteria adhere to the mucosal cells of the intestine and penetrate the mucosal epithelium, gaining access to lymphoid tissues such as the lymph nodes, spleen and liver [162]. The bacteria are able to evade the host immune response by remaining within a modified phagosome, known as the *Salmonella*-containing vacuole (SCV), which provides a suitable environment for bacterial survival and replication [163]. Non-typhoidal serovars (NTS), most commonly *Salmonella* Typhimurium, presents as a localised infection of the host's gut epithelia with the innate immune system limiting access to deeper tissues [162]. However, NTS may also cause invasive NTS (iNTS) infections, that occurs mainly in immunocompromised people, such as those with acquired immunodeficiency syndrome (AIDS) [164]. The facultative intracellular nature of *Salmonella* means that only a few antibiotics can be used to control infections. Combined with the ever-increasing number of multi-drug-resistant strains arising this is leading to a diminished efficacy of drug treatments [161, 165]. This can have especially detrimental outcomes in places with a higher bacterial burden (i.e.

hospitals) and countries with lower hygiene standards (i.e. developing countries) [159, 166]. Consequently, a better understanding of *Salmonella* virulence and infection mechanisms is crucial to identify better suited targets for improved drug design.
Infection with *Salmonella* induces inflammasome assembly and pyroptosis via the activation of caspases [167]. *Salmonella* Typhimurium triggers pyroptosis by activating caspases-1 and -11, in part via the Nlrp3 and Nlrc4 inflammasomes [168]. It is well understood that the inflammatory caspases-1 and -11 are crucial during host invasion and inflammation [111, 121]. A growing number of reports are implicating additional roles for caspase-8 (and possibly additional caspases) in the inflammatory response and immune defence against bacteria [6, 169]. Caspase-8 has been shown to be recruited to an ASC-caspase-1 inflammasome during *Salmonella* infection [6]. This finding suggests a degree of functional overlap within the caspase family, indicating that caspase-8 which functions as an essential initiator in death receptor-induced apoptosis and a brake on necroptosis, can also play a role overlapping with inflammatory caspases. Defects in individual programmed cell death pathways (e.g. apoptosis, necroptosis, pyroptosis) often cause surprisingly minor defects upon infection with an intracellular pathogen *in vitro* as well as in *in vivo* [170]. This can possibly be explained by substantial redundancy between different cell death pathways in the cellular response to pathogens, which allows the host to compensate for the loss or deregulation of an individual cell death pathway through the activation of another [170, 171].

To investigate the functional overlap between the different cell death pathways, i.e. the overall contributions of caspase-1, -11, -12 and -8 during bacterial infection, we generated mice deficient for three established forms of programmed cell death, namely death receptor-induced apoptosis (loss of caspase-8), pyroptosis (loss of caspases-1/11/(12)) and necroptosis (loss of RipK3).

Receptor-interacting serine/threonine-protein kinase 3, RipK3, is a regulator of cell death and inflammation [171]. It is best known for its activity during necroptotic cell death [172]. More recently, RipK3 has been implicated during inflammasome activation following host invasion and cytokine production [7, 53, 173]. However, the exact role of RipK3 and caspase-8 during inflammation are still poorly understood.

Salmonella virulence and TLR signalling

TLRs are crucial for pathogen recognition and induction of immune responses. Each TLR has a distinct specificity for microbial molecules, such as bacterial flagellin recognised by TLR5, bacterial lipoproteins recognised by TLR2, LPS bound by TLR4 and single-stranded RNA bound by TLR7 [174, 175]. Recognition of pathogen components by TLRs results in cytokine production and initiation of the immune response [49]. TLR2, TLR4 and TLR5 are key receptors for mediating *Salmonella* virulence [174, 176, 177]. However, the exact mechanisms of *Salmonella* virulence are not fully understood; particularly which bacterial components are important for infection or the activation of the immune response. One bacterial component, the flagella are important for the coordinated movement and invasiveness of *Salmonella* and other intracellular pathogens, but also play a role in activating the innate immune response [175]. The *Salmonella* Typhimurium genome contains two flagellin genes, namely *fli*C and *flj*B which encode the flagella filament structural proteins FliC and FljB that are interlaced in an alternating manner [178]. We used a flagella deficient strain, SL1344 Δ*fliC*Δ*fljB* that lacks both, FliC and FljB flagellin subunits, allowing to study the growth of *Salmonella in vitro* in the absence of this TLR ligand- TLR interaction.

TRIF- a master regulator?

Upon the binding of ligand (pathogen associated molecular patterns, PAMPs) to a membrane-associated TLR, TIR domain-containing adaptor-inducing IFN-β protein (TRIF) recruitment to the receptor is mediated via its TIR domain. This adaptor molecule engages with the TLR receptor to trigger IFN production and NF-κB signalling [179, 180]. TRIF engagement has been shown to be involved in TLR-induced apoptosis via FADD-caspase-8 engagement [181, 182, 183]. TRIF was also shown to play a role in inflammation through its involvement in the TLR4-TRIF-caspase-8-FADD dependent inflammasome formation in human monocytes which has been suggested to drive IL-1β secretion [184]. In response to microbial molecules the activation of TLR3 and TLR4 TRIF can trigger necroptosis via RipK3 and mixed lineage kinase domain like pseudokinase (MLKL) [7, 185]. Furthermore, it has been shown that TRIF can drive Nlrp3-mediated pyroptosis in response to Gram-negative bacteria [186]. Collectively, these findings raise an interesting question as to whether

the adaptor protein TRIF can act as a master regulator, switching between programmed cell death pathways during pathogenic infections. To investigate this notion, we included mice deficient for TRIF in our analysis.

4.2 Results

4.2.1 Combined deletion of caspases-1, -11, -12, -8 and the necroptotic mediator RipK3 renders cells highly resistant to cell death induction by intracellular pathogens *in vitro*

It has been proposed that different cell death pathways are induced upon the infection with intracellular pathogens [110, 175, 187]. In order to test the relative contribution of each individual pathway, we generated single and compound mutant mice lacking the ability to undergo pyroptosis (caspase-1/11/12 deletion), death receptor-mediated apoptosis (caspase-8 deletion) and necroptosis (RipK3 deletion). We generated primary BMDMs from these mice and infected them with various concentrations (multiplicity of infections, MOI) of the *Salmonella* Typhimurium strain SL1344 *in vitro.* As controls we used BMDMs from caspase-1/11/12$^{-/-}$, caspase-8 RipK3$^{-/-}$ and wildtype mice. After 2, 6 and 24 h, the supernatant of the infected cells was collected and assessed for IL-1β production by ELISA (Figure 4-1b). In parallel we lysed the infected cells and determined viability by measuring lactate dehydrogenase (LDH) levels. Moreover, the supernatants obtained from the lysed cells were plated onto Luria agar plates containing 100 μg/mL streptomycin to determine the number of viable intracellular *S.* Typhimurium SL1344 strain*.* The loss of the pyroptotic caspases-1 and -11 resulted in a delay in cell death (Figure 4-1a) compared to wildtype and caspase-8 RipK3 double deficient BMDMs. Interestingly, the combined deletion of caspase-8, RipK3 plus caspases-1, -11 and -12 resulted in a significant survival advantage in BMDMs upon the infection with *S.* Typhimurium SL1344 strain (Figure 4-1a). This was evident even after 24 h and upon infection with very high MOIs (500/ cell) (Figure 4-1a, bottom panel). The wildtype cells had mostly succumbed as early as 2 h after infection at an MOI of 50 or 500 with *S.* Typhimurium SL1344 strain. Cells lacking the inflammatory caspases-1, -11 and -12, showed a slight delay in their cell death response upon infection with *S.* Typhimurium SL1344 strain at an MOI of 50 or 500, indicating that pyroptosis contributes to but is not absolutely essential for the

bacteria to kill the host cells (Figure 4-1a, middle and bottom panel). In contrast, the caspase-1/11/12/8 RipK3 quintuple knockout BMDMs were almost completely resistant to cell death induced by the infection with *S.* Typhimurium SL1344 strain. At 6 h post-infection, 80-100% of quintuple knockout BMDMs were still alive even at an MOI as high as 500 (Figure 4- 1a, bottom panel).

Next, we analysed the levels of cytokines released into the supernatant following bacterial infection of the BMDMs derived from the various knockout and control wildtype mice (Figure 4-1b). As expected, and in agreement with previously published data showing that caspases-1 and -11 are essential for the secretion of IL-1β and IL-18 upon Gram-negative bacterial infection [121], IL -1β in the supernatant of cells lacking caspase-1 and -11 was significantly reduced, especially at timepoints 6 and 24 h and at MOI 10 and 50 (Figure 4-1b, top panels). Furthermore, the deletion of caspases-8 and RipK3 significantly reduced cytokine secretion upon *S.* Typhimurium SL1344 strain infection, but IL -1β could still be detected at later timepoints and at higher MOIs, which is in accordance with published literature (Figure 4.-1b) [6, 188].

Additionally, the deletion of caspase-8 and RipK3 showed lower IL-1β production at 24 hours compared to the levels detected in the caspase-1/11/12 triple knockout cells (Figure 4.-1b). Surprisingly, infection of caspase-1/11/12/8 RipK3 quintuple BMDM cells with *S.* Typhimurium SL1344 strain completely ablated IL-1ß production in these quintuple BMDM cells at any bacterial concentration (MOI 10, MOI 50 or MOI 500) or at any timepoint (2, 6, 24 h) (Figure 4-1b).

In order to determine the number of *Salmonella* in the infected BMDMs derived from mice of the various genotypes, cell lysates were plated onto agar plates and 1-3 days later the number of grown bacterial colonies were counted. At all MOIs and timepoints the wildtype as well as the caspase-8 RipK3 double deficient BMDMs harboured fewer intracellular *S.* Typhimurium bacteria (from SL1344 strain) compared to the caspase-1/11/12 triple knockout and the caspase-1/11/12/8 RipK3 quintuple knockout BMDMs (Figure 4-1c). The lowest overall bacterial counts were observed in the wildtype and caspase-8 RipK3 BMDMs. Generally, the caspase-1/11/12 and caspase-1/11/12/8 RipK3 knockout BMDMs contained

between 10 to 100-fold higher numbers of bacteria compared to the wildtype and caspase-8 RipK3 double knockout BMDMs (Figure 4-1c).

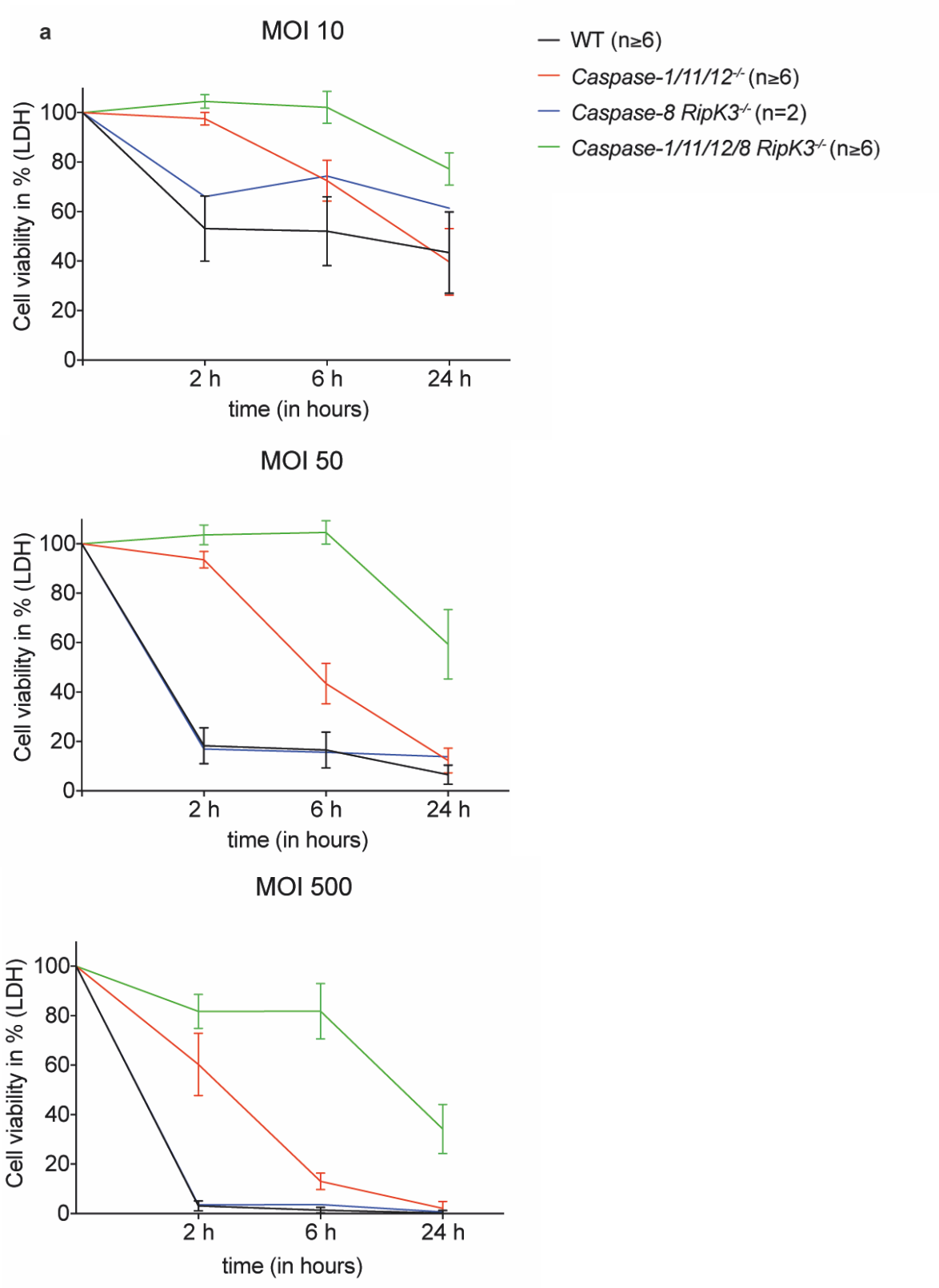

Figure 4-1: Combined loss of caspases-1, -11, -12, -8 and RipK3 impairs cytokine secretion and cell death in BMDMs following *Salmonella* Typhimurium infection *in vitro.*

a Infection of BMDMs from indicated genotypes with 10, 50 and 500 MOI of *S.* Typhimurium SL1344 *in vitro.* Caspase-1/11/12/8 RipK3$^{-/-}$ show higher viability compared to BMDMs of the other genotypes. **b** The levels of IL-1β were measured by ELISA in the supernatants of the BMDMs of the indicated genotypes after 2, 6 and 24 h after infection with *S.* Typhimurium SL1344. **c** Intracellular numbers of *S*. Typhimurium (SL1344 strain) were determined from lysed infected BMDMs of the indicated genotypes following plating on selective Luria agar. Time represents the length of incubation after addition of *S.* Typhimurium SL1344 to the cells. Adjusted p values in Table 6. *p<0.05, **p<0.01, ***p<0.001, ****p<0.0001, Graph shows mean ± SEM, triplicate wells, 2way ANOVA. Graphs show N≥2 sets of independent experiments.

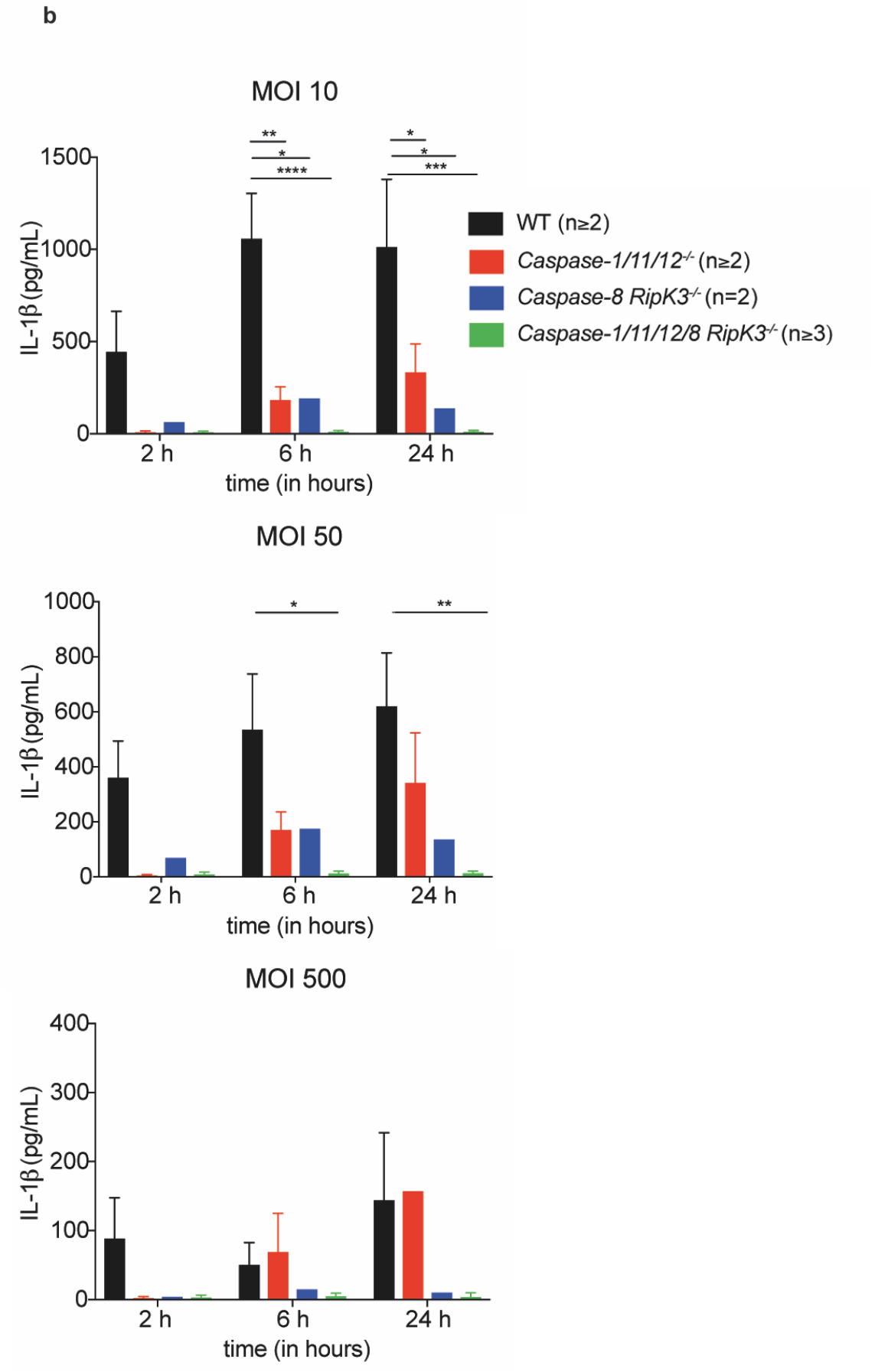

Figure 4-1 continued:

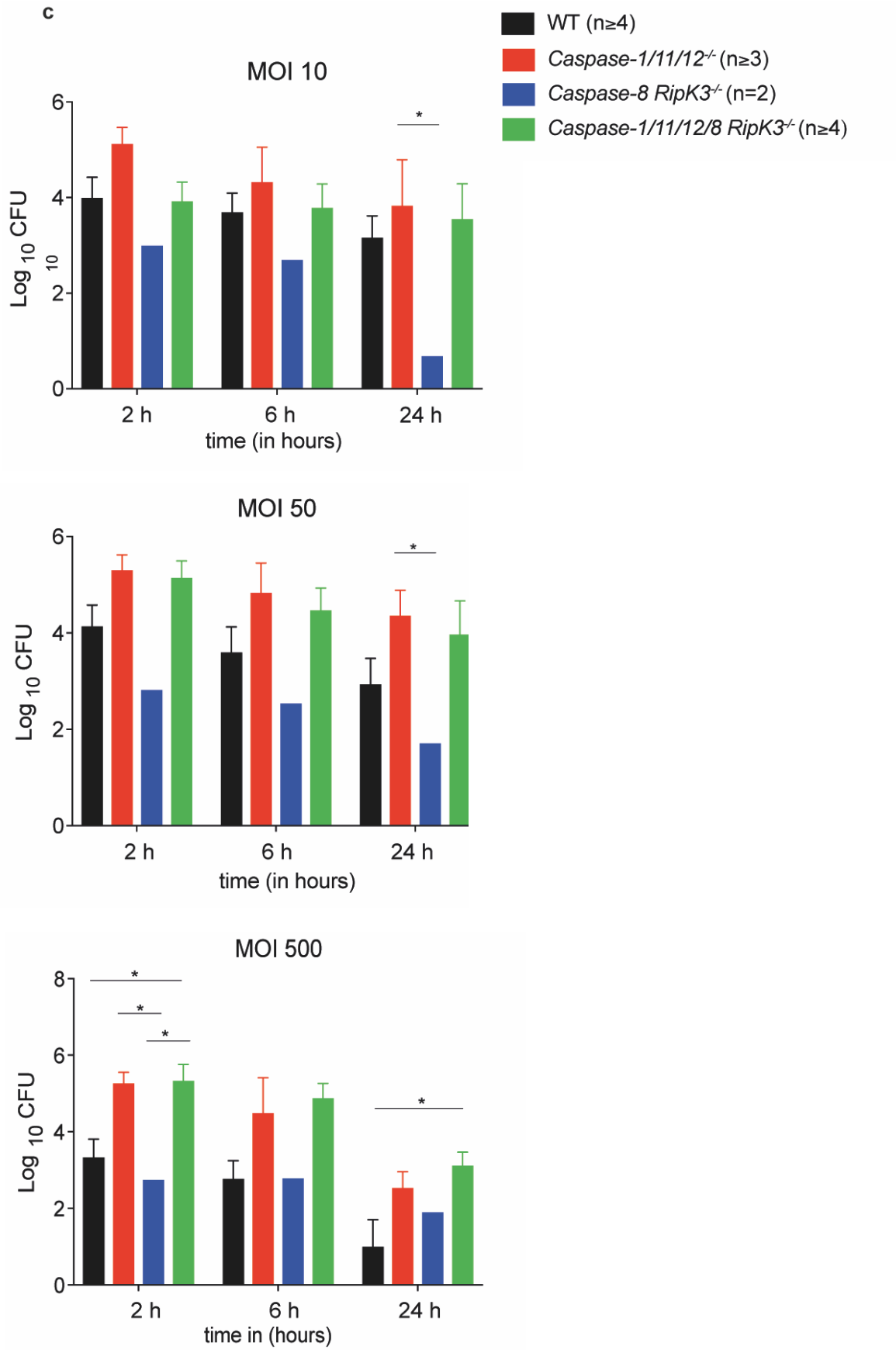

Figure 4-1 continued:

4.2.2 The combined loss of caspases-1, -11, -12, -8 and the necroptotic mediator RipK3 severely impairs *Salmonella* Typhimurium clearance in mice

We next aimed to address whether the increased expansion of *S.* Typhimurium caused by the absence of caspases-1, -11, -12, -8 and RipK3 observed with BMDMs *in vitro* (described in 4.2.1) would translate into impaired clearance of bacteria within the whole mouse. Specifically, we were interested to determine, whether there was a defect in the clearance of the pathogen in mice deficient for pyroptosis, death receptor-induced apoptosis and necroptosis. Following intravenous (i.v.) infection of the various knockout mice with the *S.* Typhimurium vaccine strain BRD509ΔaroA, the mice were monitored daily for signs of distress and weight loss (Figure 4-3). The attenuated *S.* Typhimurium vaccine strain BRD509ΔaroA was used for all *in vivo* infections.

S. Typhimurium Δ*aro* mutant vaccine strains are useful in the studies of *Salmonella* infection *in vivo,* as they cause an immune response without affecting the survival of wildtype mice.

Overall, all mice appeared healthy and no weight loss was observed (Figure 4-3). However, around 19-21 days post-infection the caspase-1/11/12/8 RipK3 deficient mice began to show signs of sickness with a few mice meeting the ethical end-point (day 21). The caspase-1/11/12/8 RipK3 deficient mice infected with the vaccine strain were not able to clear the bacteria efficiently as evidenced by a 1000- and 10,000-fold higher bacterial load in the spleen and liver or gall bladder, respectively, compared to the wildtype controls (Figure 4-2). It is known that the loss of caspases-1 and -11 leads to an increased susceptibility to *S.* Typhimurium infection [189] which we were able to reproduce in our experiments. We found a 10-fold increase in bacterial burden in the livers and gall bladder of caspase-1/11 double deficient mice compared to wildtype controls. Interestingly, the additional deletion of caspase-12 in the caspase-1/11/12 ko mice resulted in a significant (approximately 100-fold) increase of bacterial load in the gall bladder of these mice when compared to the caspase-1/11 double deficient mice (Figure 4-2).

Furthermore, the additional absence of caspase-8 RipK3 in the caspase-1/11/12 triple ko mice increased the bacterial burden in all organs compared to the wildtype, caspase-1/11 double deficient and the caspase-1/11/12 triple deficient mice (Figure 4-2). Collectively, these findings demonstrate that the caspase-1/11/12/8 RipK3 ko mice have a striking defect in their ability to control the spread of a vaccine strain (BRD509ΔaroA) of *S.* Typhimurium into various organs.

Lastly, cytokine levels in the liver and spleen of *S.* Typhimurium strain BRD509ΔaroA infected mice were examined using cytokine bead arrays and flow cytometry (Figure 4-4). Levels of IFN-γ, IL-6, MIG, MCP-1, MIP-1α, MIP-1β, RANTES, TNF and IL-12 p40 of wt and caspase-1/11/12/8 RipK3$^{-/-}$ were compared in liver and spleen. In both organs (liver and spleen), both, MIP-1α and MIP-1β levels were increased in the caspase-1/11/12/8 RipK3 knockout mice after infection with *S.* Typhimurium BRD509ΔaroA, however this was not significant. All cytokines analysed showed elevated levels in the spleens of caspase-1/11/12/8 RipK3 knockout mice with MIG and IL-12 p40 levels being significantly increased compared to infected wildtype mice.

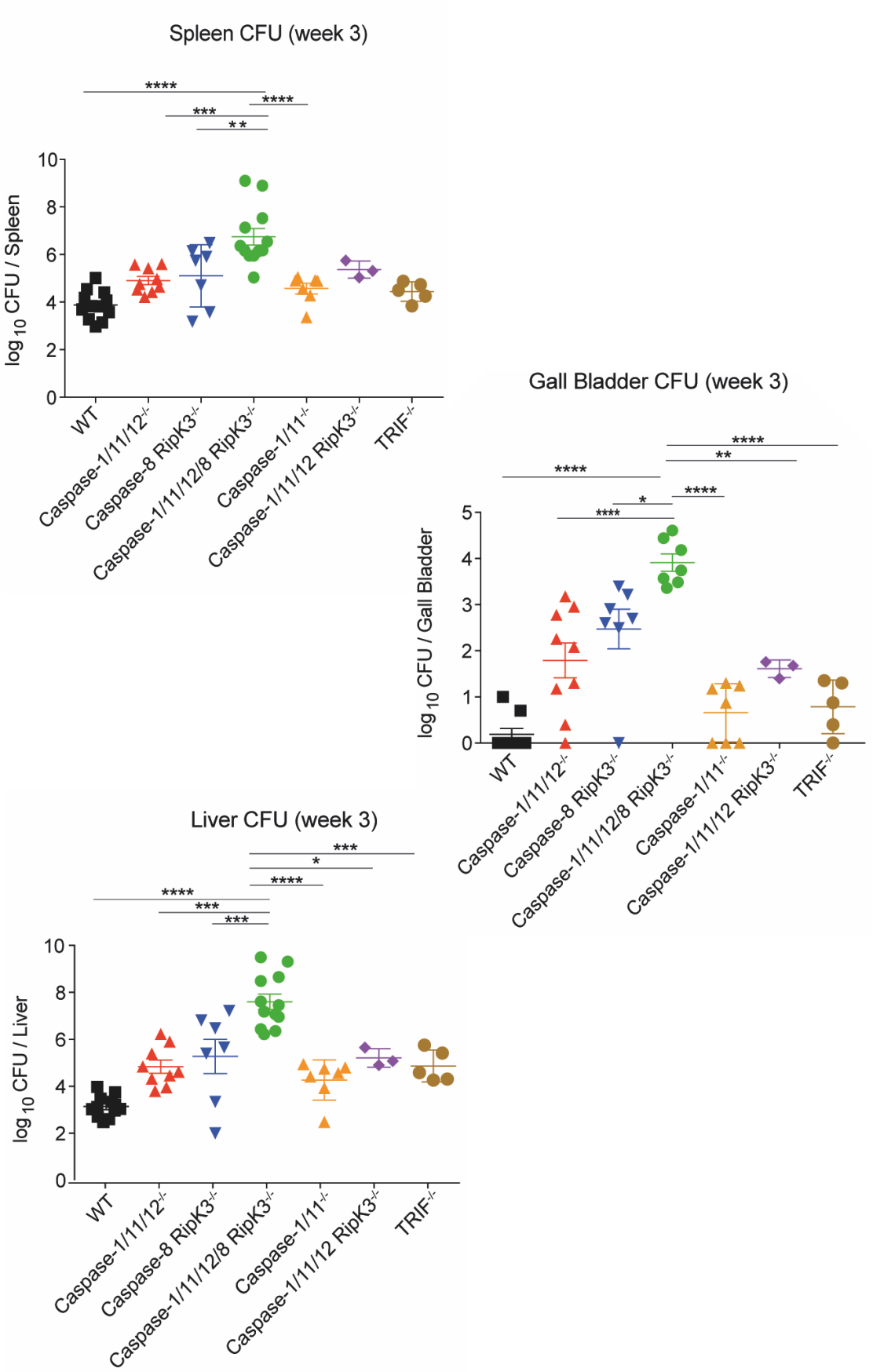

Figure 4-2: The caspase-1/11/12/8 RipK3$^{-/-}$ mice are severely defective in their ability to clear *Salmonella* Typhimurium infection.

Bacterial counts in the spleen, liver and gall bladder of mice of indicated genotypes following infection with *S.* Typhimurium vaccine strain BRD509ΔaroA, 200 CFU i.v. The indicated organs were harvested 3 weeks post-infection. Graph shows mean ± SEM, 2way ANOVA. Significances shown for the strains of interest: caspase-1/11/12/8 RipK3$^{-/-}$. All other adjusted p values in Table 9. *p<0.05, **p<0.01, ***p<0.001, ****p<0.0001. n≥3, symbols represent individual mice.

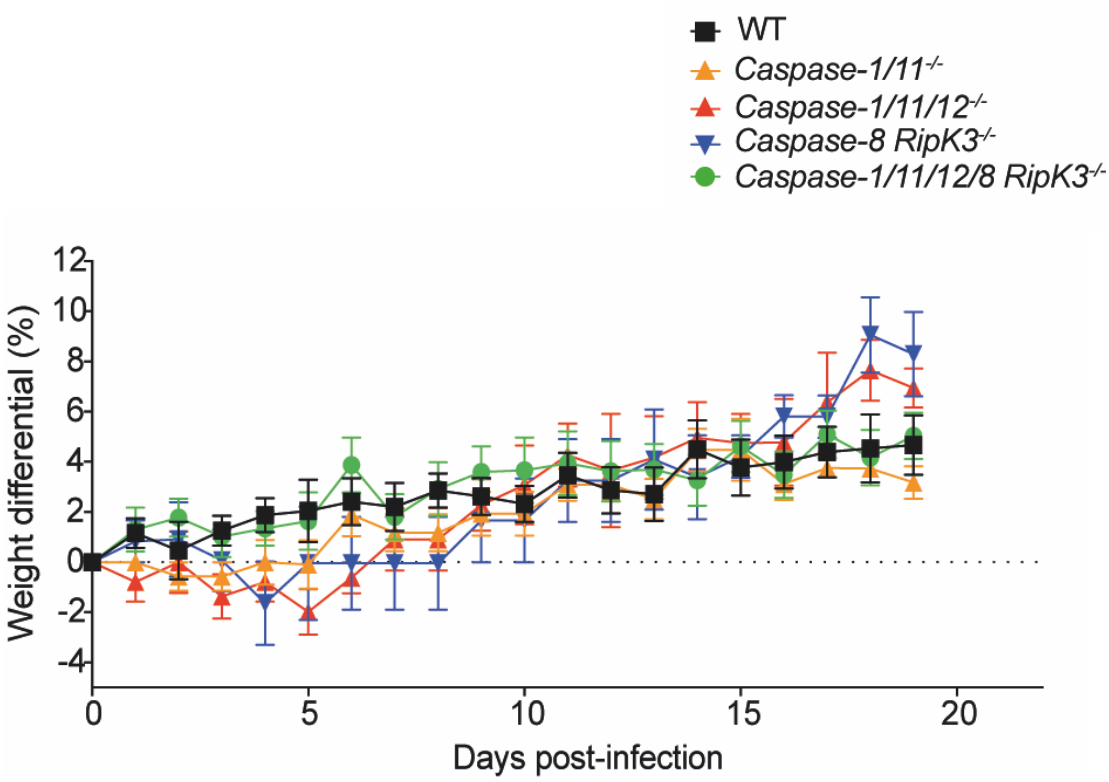

Figure 4-3: Infection of mice with *Salmonella* Typhimurium vaccine strain BRD509ΔaroA does not cause weight loss.

Weights of the mice of the indicated genotypes were taken daily after i.v. infection with *S.* Typhimurium strain BRD509ΔaroA, at 200 CFU i.v. n≥6.

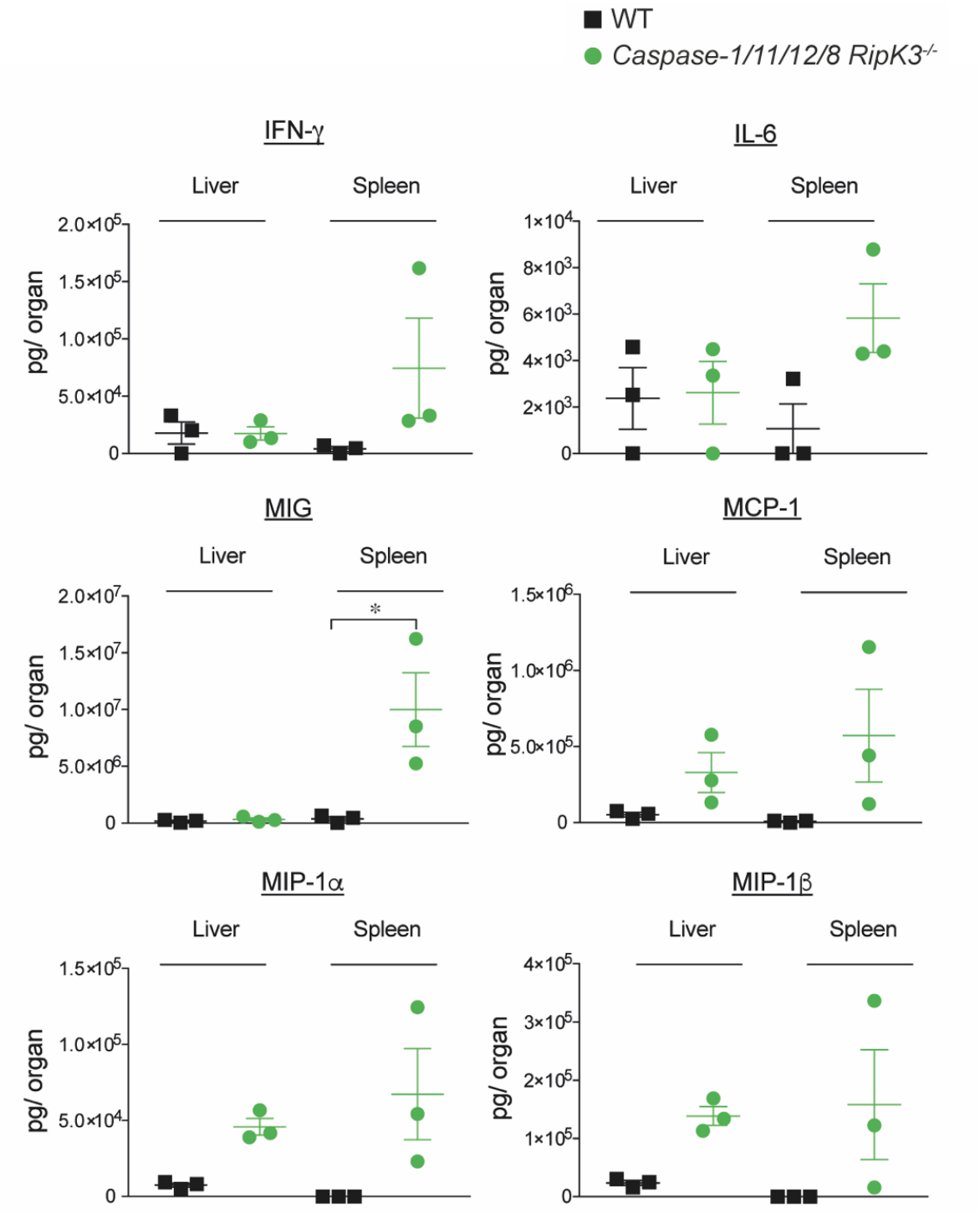

Figure 4-4: Increased cytokine levels in mice deficient for caspase-1/11/12/8 and RipK3 upon *Salmonella* Typhimurium BRD509ΔaroA infection.

IFN-γ, IL-6 MIG, MCP-1, MIP-1α, MIP-1β, RANTES, TNF and IL-12 p40 levels were measured in tissue homogenates of liver and spleen from wt (depicted WT) and caspase-1/11/12/8 RipK3$^{-/-}$ mice. *p<0.05, Graph shows mean ± SEM, statistical analysis performed with 2way ANOVA. n=3 mice per genotype.

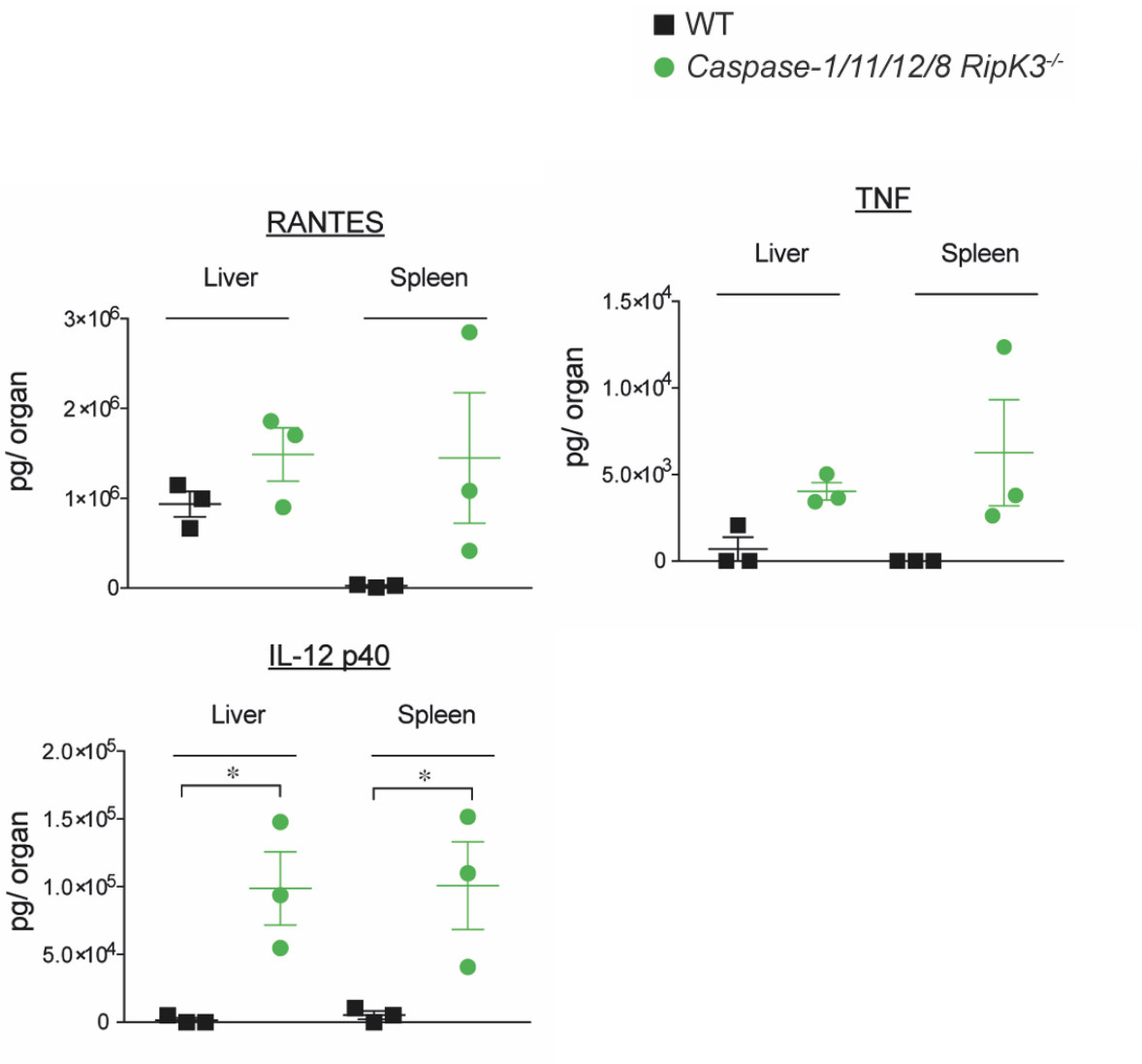

Figure 4-4 continued.

4.2.3 Deficiency of the adaptor protein TRIF has only relatively minor impact on *Salmonella* Typhimurium clearance

In an approach to identify a master regulator capable of switching the cellular response between necroptosis, apoptosis and pyroptosis during *S*. Typhimurium infection, we tested TRIF as a potential candidate. As in section 4.2.1 the caspase-1/11/12/8 RipK3 ko BMDMs showed substantially increased survival capacity compared to the wildtype and caspase-1/11/12 deficient cells following *S*. Typhimurium SL1344 infection at all timepoints and all MOIs tested (Figure 4-5). However, when the TRIF ko cells were assessed they had a similar phenotype to the wildtype cells and exhibited no increased survival capacity, in striking contrast to the caspase-1/11/12/8 RipK3 ko cells (Figure 4-5).

To exclude a role for TRIF as a master regulator during *S*. Typhimurium infection, we conducted *in vivo* infection experiments with the vaccine strain BRD509ΔaroA. The bacterial counts in the spleen, liver and gall bladder revealed no overwhelming defect in bacterial clearance of TRIF ko mice (Figure 4-2). However, the bacterial burden in the spleen, liver and gall bladder was approximately 10-fold higher compared to the wildtype animals but did not reach the levels seen for the caspase-1/11/12/8 RipK3 knockout mice (Figure 4-2).

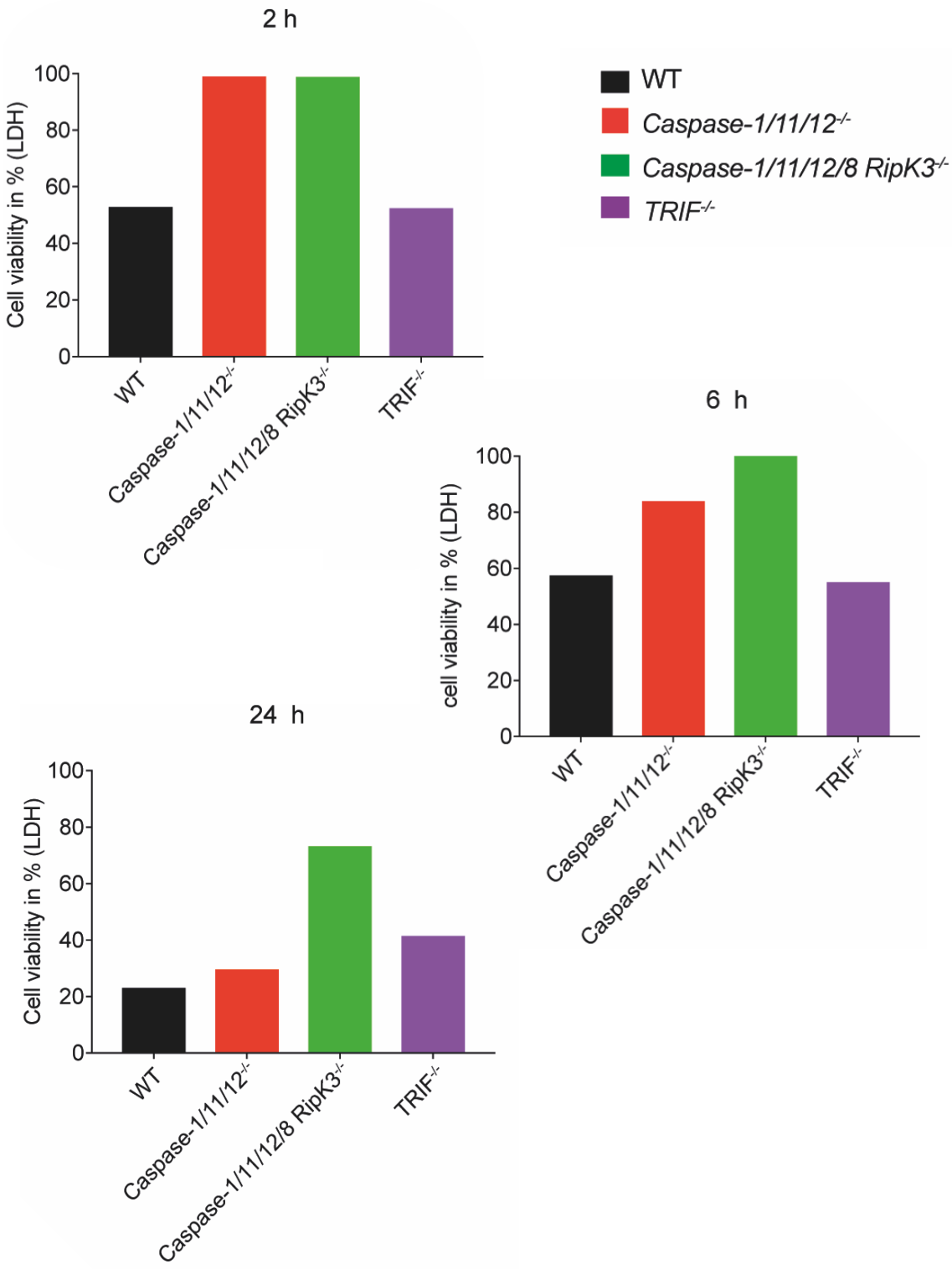

Figure 4-5: A minor role for TRIF during *Salmonella* Typhimurium infection. Infection of BMDMs derived from mice of the indicated genotypes with *S.* Typhimurium SL1344 at MOI of 50. Cell survival was analysed at 2, 6 and 24 h post-infection. Graphs show one experiment, triplicate wells. 2way ANOVA.

4.2.4 The flagella mutant Δ*fliC*Δ*fljB* *Salmonella* Typhimurium strain can still induce cell death in BMDMs *in vitro*

To investigate which bacterial components can activate cell death during *S.* Typhimurium infection we assessed the impact of a non-flagellated mutant on the viability of BMDMs. Using the *S*. Typhimurium mutant Δ*fliC*Δ*fljB* strain we infected wildtype, caspase-1/11/12/2$^{-/-}$, caspase-8 RipK3 and caspase-1/11/12/8 RipK3 knockout BMDMs. Since the exact functions of caspase-2 alone or in combination with inflammatory caspases-1, -11 and 12 are poorly understood, we crossed caspase-2$^{-/-}$ mice with our caspase-1/11/12$^{-/-}$ triple knockout mice to obtain caspase-1/11/12/2 quadruple knockout mice. In the following assay we included primary myeloid cells from these mice to screen for any crucial functions of caspase-2 in combination with caspases-1, -11 and -12 during *S*. Typhimurium infection. There was no difference in cell viability between cells infected with either SL1344 or the Δ*fliC*ΔfljB mutant assessed for the BMDMs derived from the various knockout mice (Figure 4-6). Furthermore, the caspase-1/11/12/2$^{-/-}$ cells showed no difference in cell survival when compared to caspase-1/11/12 triple knockout mice from previous assays (see Figure 4-1a and 4-6). Only the MOI of 10 was used for the Δ*fliC*Δ*fljB* infections. Possibly higher (MOI 50 and MOI 500) infections are required, as a low MOI such as MOI 10 may mask a role played by flagella in the induction of inflammasome driven cell death.

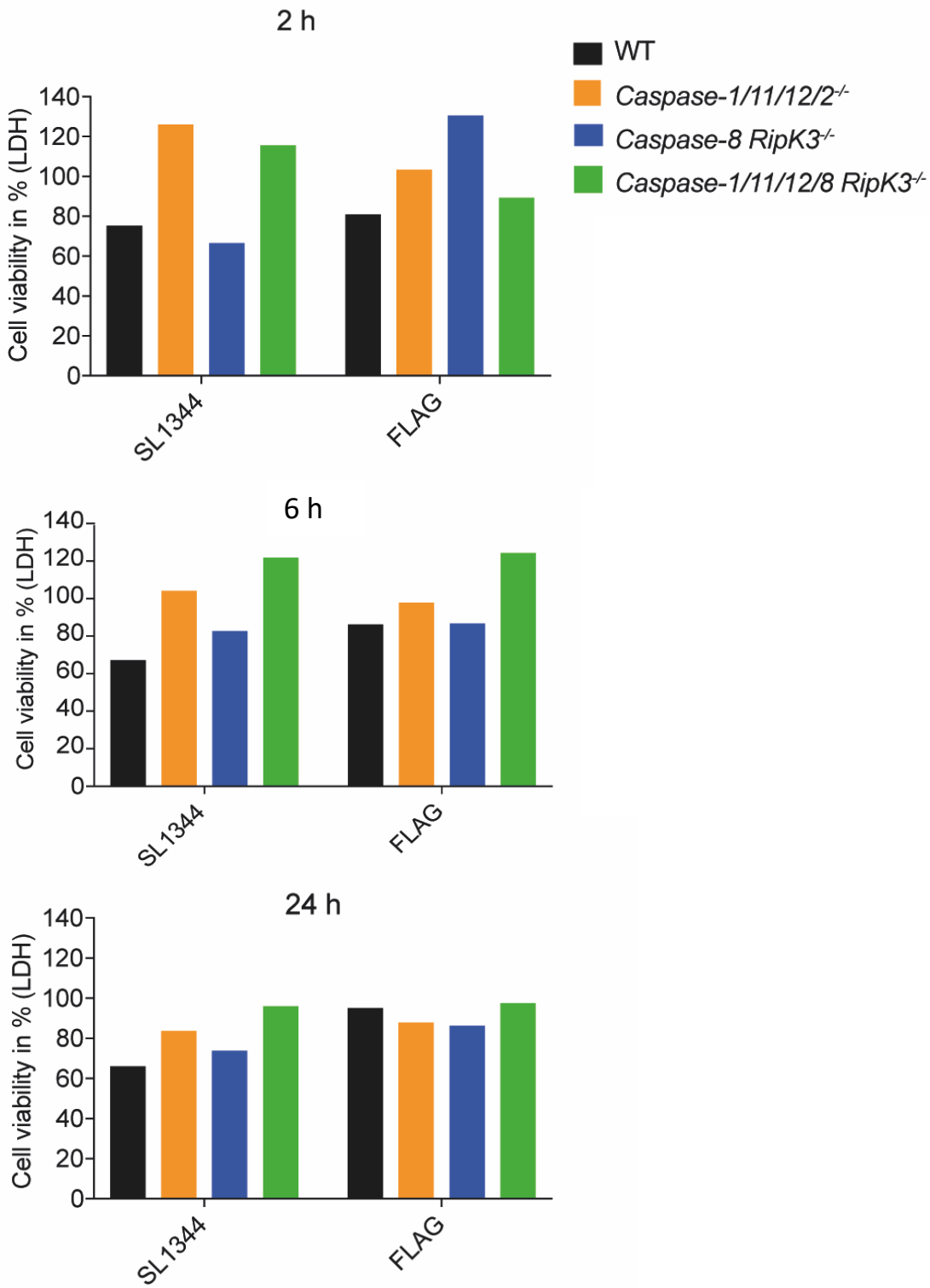

Figure 4-6: The flagella mutant *Salmonella* Typhimurium strain ΔfliCΔfljB can kill BMDMs *in vitro.*

Infection of BMDMs of the indicated genotypes with *S.* Typhimurium SL1344 or the flagellin mutant Δ*fliC*Δ*fljB* (labelled FLAG) at an MOI of 10. Cell survival was analysed at 2, 6 and 24 h post-infection. Data shown represent one experiment with n=1 mouse per strain, triplicate wells.

4.3 Discussion

This chapter focused on the hypothesis that a large degree of functional overlap exists amongst the caspase family, and hence amongst different cell death pathways, in the response of cells to pathogen infection. To examine individual and overlapping roles of the different cell death pathways involved in the clearance of pathogens, we generated a mouse strain deficient for three major cell death pathways, namely death receptor-induced apoptosis, necroptosis and pyroptosis. By generating mice lacking caspases-1, -11, -12 and -8 as well as RipK3 we aimed to determine if any other cell death mediators play a role during *S.* Typhimurium clearance and if further cell killing mechanisms are involved to ensure adequate the removal of infected cells.

We infected primary BMDMs derived from the caspase-1/11/12/8 RipK3$^{-/-}$ mice, caspase-1/11/12$^{-/-}$, caspase-8 RipK3 knock out as well as wildtype control mice with *S.* Typhimurium SL1344 strain and analysed cell survival, cytokine secretion and bacterial counts. Interestingly, BMDMs lacking caspases-1, -11, -12, -8 and RipK3 were highly resistant to infection with the *S.* Typhimurium SL1344 strain *in vitro*, even at MOIs as high as 500 (Figure 4-1a). Consistent with previous reports on the caspase-1/11 double knockout BMDMs, our caspase-1/11/12$^{-/-}$ BMDMs showed increased survival compared to *S.* Typhimurium SL1344 strain infected wildtype BMDMs [189], but their survival was still much less impressive compared to the caspase-1/11/12/8 RipK3 BMDMs. This reveals that death receptor-induced apoptosis, necroptosis and pyroptosis have major functional overlap in the killing of *S.* Typhimurium SL1344 infected cells.

Caspases-1 and -11 are well established mediators of pyroptosis with caspase-11 sensing Gram-negative bacteria [121]. However, deleting the inflammatory caspases-1, -11 and -12 only showed a delay, albeit significant, in *S.* Typhimurium SL1344 strain-induced cell killing compared to wildtype cells, but no full protection (Figure 4-1a). Furthermore, the cytokine production in the caspase-1/11/12/8 RipK3 knockout cells was completely absent (Figure 4-1b). In the caspase-1/11/12$^{-/-}$ cells, the cytokine secretion was significantly reduced but still detectable at low levels, as

expected from previous reports on caspase-1/11$^{-/-}$ BMDMs [121]. It has been shown previously that the deletion of caspase-8 causes a significant reduction in IL-1β production after infection with *Salmonella* or LPS stimulation [6, 190]. Interestingly, Il-1β production in caspase-8 RipK3 deficient cells was even lower than the levels detected in caspase-1/11/12 triple knockout cells at 24 hours post-infection (Figure 4-1b). One possible explanation for this observation could be due to low n numbers of caspase-8 RipK3 deficient BMDMs or potential inaccuracy of the ELISA assay at these low concentrations. However, the difference in IL-1β levels between caspase-8 RipK3$^{-/-}$ and caspase-1/11/12$^{-/-}$ are not statistically significant. To be able to further address this observation, more biological repeats with caspase-8 RipK3 deficient BMDMs are necessary.

Interestingly, deleting caspase-8 and RipK3 in combination with the pyroptotic mediator's caspase-1 and -11 prevented IL-1β production entirely (Figure 4-1b). It is possible that the secretion of other cytokines additional to IL-1β are eliminated or at least reduced in the caspase-1/11/12/8 RipK3 knockout cells which can impact on inflammation. Cytokines are key components during inflammation and cell death [191].

Interfering with cytokine secretion and consequently the cross talk between cells upon insult can have an impact on the inflammatory response, thus it is probable that a reduced cytokine secretion in the caspase-1/11/12/8 RipK3 quintuple knockout cells contributes to the higher resistance to cell death upon *S.* Typhimurium SL1344 strain infection.

These results indicate that the combined absence of caspases-1, -11, -12 and -8 in conjunction with the loss of RipK3 is able to almost completely abrogate *S.* Typhimurium SL1344 strain-induced cell death and abolish IL-1β secretion. Moreover, these results highlight that other mechanisms appear to play only a very minor role or no role at all in *S.* Typhimurium-induced killing. Three major cell killing pathways are deleted in caspase-1/11/12/8 RipK3$^{-/-}$ cells: death receptor-induced apoptosis (caspase-8 dependent), necroptosis (RipK3 dependent) and pyroptosis (caspase-1/11/(12) dependent) (Figure 4-1a). Thus, these three cell death pathways appear to account for most of *S.* Typhimurium SL1344-induced cell killing. The reason why some caspase-1/11/12/8 RipK3$^{-/-}$ cells can die in response

to infection with *S.* Typhimurium SL1344 strain at high MOI at later timepoints is not clear. This may involve other programmed cell death pathways, such as BAX/BAK-dependent intrinsic apoptotic pathway or it could be due to non-programmed (catastrophic) death due to the bacteria shutting down essential cellular processes.

To investigate how the intracellular growth of the Gram-negative bacteria is affected by defects in the diverse cell death pathways, we analysed the lysed cells for intracellular bacteria by plating the contents of cellular lysates on agar plates. This analysis revealed higher bacterial numbers in both the caspase-1/11/12$^{-/-}$ and caspase-1/11/12/8 RipK3$^{-/-}$ BMDMs compared to wildtype or caspase-8 RipK3$^{-/-}$ BMDMs (Figure 4-1c). This indicates that the prolonged survival of the caspase-1/11/12/8 RipK3$^{-/-}$ BMDMs facilitates increased replication of intracellular bacteria (Figure 4-1c). However, further investigation is required to fully understand the relationship between the number of live BMDMs and the numbers of intracellular bacteria. For the reason that there are generally less viable cells remaining in each well (after 2, 6 or 24 h post-infection) for the wildtype and caspase-8 RipK3 cells (Figure 4-1a) it is plausible that there are consequently less cells for the bacteria to replicate in. Thus, the protocol used might not be the most appropriate to quantitate intracellular bacterial numbers because it does not account for the number of dying cells in each individual genotype. To address this issue, an assay quantitating the viable cell count remaining at a specific timepoint as well as bacterial count for each well and genotype will be set up in the future; in this way the bacterial load can be measured per surviving cell. Additionally, we were only able to obtain 2 biological repeats for the caspase-8 RipK3$^{-/-}$ BMDMs due to limited availability of caspase-8 RipK3 deficient mice at the time. More repeats and an improved assay to measure intracellular bacterial counts are required to fully resolve this issue.

Next, we investigated how the loss of caspases-1, -11, -12, -8 together with the loss of RipK3 affects *S.* Typhimurium clearance *in vivo.* When infecting caspase-1/11/12/8 RipK3$^{-/-}$ mice with the vaccine *S.* Typhimurium strain BRD509ΔaroA, these animals showed very high (up to 1000-fold increase compared to wildtype animals) bacterial burdens in their livers, spleens and gall bladders (Figure 4-2),

suggesting severe defects in bacterial clearance. *S.* Typhimurium can establish a systemic infection by crossing the epithelial barrier in the gastrointestinal tract and spread to the liver and successively infect other major organs, such as the spleen and gall bladder. In our systemic infection model, all the major organs targeted by *S.* Typhimurium BRD509ΔaroA during infection (spleen, liver, gall bladder) showed substantially higher bacterial counts in the caspase-1/11/12/8 RipK3$^{-/-}$ mice compared to wildtype controls (Figure 4-2). Caspase-8 RipK3$^{-/-}$ mice as well as caspase-1$^{-/-}$ and caspase-1/11$^{-/-}$ mice have been reported to be more susceptible to pathogens than wildtype animals [170].

As expected, the caspase-1/11$^{-/-}$ mice show a comparatively minor increase in bacterial burden in the organs tested with the highest burden of around 5-fold in liver and gall bladder (Figure 4-2).

However, in our study, the combined deletion of caspases-1, -11, -12, -8 together with RipK3 increased the clearance defect up to 1000-fold compared to that of the already known knockout phenotypes (for caspase-1$^{-/-}$, caspase-1/11$^{-/-}$ or caspase-8 RipK3$^{-/-}$ mice) [170]. This reveals that disabling all three cell death pathways, namely death receptor-induced apoptosis, necroptosis and pyroptosis impairs the ability to clear *S*. Typhimurium infection much more severely than the loss of only one or even two of these cell death pathways (Figure 4-2).

Interestingly, the absence of caspase-12 appears to affect the ability of mice to clear bacteria from the gall bladder; since higher numbers of *S.* Typhimurium were observed in the gall bladders of the caspase-1/11/12 triple knockout mice when compared to caspase-1/11 double ko animals even though the bacterial counts in the other tissues tested were comparable between these two strains (Figure 4-2). This suggests a role for caspase-12 in the clearance or release of bacteria from the gall bladder (Figure 4-2). Our data might show a role for caspase-12 in an inflammatory process, which agrees with previous reports, that suggest a role for the human *caspase-12s* gene in the inflammatory response in human retinal cells [69]. Also, another study suggested caspase-12 functions as a dominant negative regulator of the inflammasome [70], however this was in dispute with other published results [71].

Therefore, our findings are in line with reports of caspase-12 functions during inflammation. Additionally, to this previously proposed role, for the first time, our

data might indicate a novel role for caspase-12 (and potentially other caspases) in bacterial sequestering in the gall bladder and bacterial shedding.

As mentioned above, the *caspase-12* gene contains a premature stop codon in most humans, making it non-functional [52]. Thus, this function may exist in humans only in those people of African descent who can express full-length caspase-12.

One may speculate that during the course of human evolution and their migration out of Africa, humans encountered a variety of different pathogens in Asia and Europe that needed to be dealt with in a new manner [67]. It is conceivable that the shedding of certain bacteria (e.g. *Salmonella*) from the gall bladder and possibly other tissues may have been disadvantageous to humans, because in this manner the pathogen could be passed on to offspring and others in the community. This could have engendered a selective advantage for individuals that lack full-length (enzymatically active) caspase-12. However, further investigations are required to fully understand the roles of caspase-12.

Furthermore, we quantified the cytokine levels in liver and spleen of wildtype and caspase-1/11/12/8 RipK3 knockout mice on day 21 post *S.* Typhimurium BRD509ΔaroA strain infection (Figure 4-4). We analysed an array of major cytokines including IFN-γ MIG, IL-12 p40 and TNF. Nearly all cytokines showed a slight increase in both, liver and spleen of the caspase-1/11/12/8 RipK3 knockout mice (Figure 4-4). The organs were harvested at the ethical endpoint of the experiment (day 21). At this timepoint the bacteria already established a systemic infection in the major organs of the mouse (Figure 4-2). Since the caspase-1/11/12/8 RipK3 knockout mice are unable to clear the infection in these organs (Figure 4-2), it appears that the organs are secreting high levels of cytokines in an attempt to combat the infection. This cytokine storm is indicative of a potential septic shock building up due to an overload of bacterial burden thus resulting in an overaction of the body's immune response.

We further investigated the role of the multifunctional adaptor protein TRIF in *S.* Typhimurium infection as it has been implicated in the induction of apoptosis, necroptosis and pyroptosis. TRIF is required during TLR3 and TLR4 receptor-mediated necroptosis [192] but can also cause cellular apoptosis via caspase-8 activation [182] and additionally has indirect functions during pyroptosis [186]. Thus,

TRIF was a likely candidate to serve as a potential master regulator that decides between the three programmed cell death pathways (i.e. apoptosis, necroptosis and proptosis).

We infected TRIF deleted myeloid cells *in vitro* and TRIF deficient mice *in vivo* with *S.* Typhimurium to investigate its role. Infecting TRIF deficient BMDMs at an MOI of 50 with the *S.* Typhimurium strain SL1344 showed no protection from cell death (Figure 4-5). The levels of cell death after 24 h were similar to those seen in wildtype BMDMs (Figure 4-5). If TRIF was essential for the coordination of all three cell death pathways (death receptor-induced apoptosis, necroptosis and pyroptosis), one would expect similar protection from *S.* Typhimurium SL1344 strain-induced cell killing compared with the caspase-1/11/12/8 RipK3$^{-/-}$ BMDMs. We also tested the consequence of TRIF deficiency on the response of mice to infection with *S.* Typhimurium vaccine strain BRD509ΔaroA. We did not observe significant differences in the clearance of bacteria from any of the organs tested compared to wildtype mice (Figure 4-2). However, it remains possible that TRIF has a regulatory role in these cell death pathways during bacterial infection, but these functions can also be executed by additional (yet to be identified) adaptor protein. Such redundancy in the regulation of cell death pathways might well be advantageous, since activation of these three pathways upon infection or cellular damage is crucial for the survival and wellbeing of the host. Based on our results it is unlikely that TRIF acts on its own as a master regulator of different cell death pathways upon pathogen infection.

To clear an infection, signaling cascades have to be triggered by PAMPs or DAMPs. Some of the major PAMPs are LPS, flagellin or proteins from the type III secretion system [49]. *Salmonella* derived flagellin is one of the major PAMPs recognised by TLR5 in host cells [193]. *S.* Typhimurium expresses two major flagellin proteins, fljB and fliC [194]. To investigate the implications of this ligand-TLR system in *S.* Typhimurium-induced cell killing, we tested the impact of the loss of these PAMPs on a cellular immune response. For this, we used a *S*. Typhimurium mutant Δ*fliC*Δ*fljB* (labelled FLAG) that lacks the two flagellin proteins fljB and fliC, which are expressed in *S*. Typhimurium.

One could predict that the loss of fliC and fljB, two major flagellum components, could reduce detection of intracellular *S.* Typhimurium and thereby reduce cell death induction. However, there was no difference in cell viability between cells infected with flagellin deficient *S.* Typhimurium vs those infected with the SL1344 strain, at least at MOI of 10 (Figure 4-6). However, additional experiments with the Δ*fliC*Δ*fljB* using also infections at higher MOI are required to draw definitive conclusions.

In conclusion, our findings provide evidence that multiple cell death pathways (i.e. apoptosis, necroptosis, pyroptosis) are involved in the response to infection with Gram-negative bacteria and possibly other pathogens. The findings also show substantial extents of functional overlap between several caspases in bacterial clearance. It appears likely that this extensive functional overlap has been selected for to ensure survival of the host in case one process is dysfunctional. This would ensure adequate clearance even if an effector in one signaling pathway is defective or a pathway has been disabled by a pathogen. This insight is interesting in the context of future drug design. A better understanding of the host's signaling networks in response to infection might be exploited therapeutically. Understanding these complex molecular networks and trying to understand how the switching between the pathways is controlled could be used to take advantage of these mechanism in dealing with infections.

For example, one could design drugs to activate a back-up cell death pathway if another one is dysregulated, thereby initiate bacterial clearance. By targeting specific caspases, such as caspase-8, if pyroptosis is defective for example, one could switch on caspase-8 dependent clearance upon infection. Since a lot of anti-cancer drugs already are targeted at programmed cell death, these could theoretically be repurposed, and also be used as antimicrobials by activating specific cell death pathways in order to clear an infection.

Thus, we aim to use the caspase-1/11/12/8 RipK3 deletion model to explore if we can pre-treat these mice with cell death-inducing drugs, so-called BH3 mimetics, to test, whether we can reduce the bacterial burden in the organs upon infection.

Furthermore, a better understanding of caspase functions, utilisation and activation during clearance will give us a better understanding about the complex system of redundancy that hosts employ to deal with pathogens.

Interestingly, our studies suggest a novel and thus far not yet described role for caspase-12 in the dissemination of bacteria from the gall bladder and a potential explanation for the selective mutation of human *caspase-12l* as a protective mechanism against certain microbial burdens during the course of human evolution.

Here, we generated and described a novel mouse model deficient for three major cell death pathways (apoptosis, pyroptosis and necroptosis) by the deletion of caspases-1, -11, -12 -8 and RipK3; which will be useful to study different cell death pathways and their role upon pathogen clearance.

Chapter 5: Impact of deleting all murine CARD containing caspases on different cell death pathways

5.1 Introduction

The apoptotic machinery and some of its key players, such as proteins belonging to the death domain (DD) superfamily, are highly conserved from the nematode *Caenorhabditis elegans* to mammals [33, 94]. One subgroup of the DD superfamily is the CARD subfamily, which contains amongst other proteins the caspases-1, -2, -4, -5, -9, -11, and -12.

In *C. elegans*, the caspase CED-3 is required for developmentally programmed cell death, apoptosis, acting as both, initiator as well as effector caspase [195, 196]. CED-3 carries an N-terminal domain with extensive sequence homology to the mammalian CARD domain [195, 197, 198].

DD superfamily members are found in many species; however, generally a smaller number of members are found in simpler organisms, such as Drosophila or nematodes, compared to mammals [54]. The fact that mammals have many DD superfamily members, including many CARD containing caspases could indicate a degree of functional redundancy. Given that all members of the DD superfamily share the death fold motif, it is interesting to speculate about the potential evolutionary relationship among the subfamilies within the DD superfamily and whether their similarities imply similar functions; i.e. such as deleting the CARD member CED-3 in *C. elegans* having the same effect as deleting all CARD containing caspases in mammals.

It was shown that mice deficient for caspase-9 die around embryonic day 15/16 due to exencephaly that resulted from reduced apoptosis of neuronal cells during development [87, 199, 200]. However, it is important to note, that even though this

abnormality in caspase-9 deficient mice is prominent on a mixed C57BL/6 x 129SV background, it is much less pronounced on an inbred C57BL/6 background where many caspase-$9^{-/-}$ mice make it to birth and even beyond [196] (our own unpublished data).

The loss of caspase-9 was shown to only delay apoptosis of haematopoietic cells and fibroblasts after cytokine withdrawal or treatment with cytotoxic stimuli but does not prevent cell death [148]. Furthermore the loss of caspase-9 did not result in accumulation of haematopoietic cells [87, 148], in striking contrast to the loss of BIM, combined loss of BAX and BAK or BCL-2 overexpression [87, 201].

The programmed death of caspase-9 deficient cells does not efficiently dispose of cellular constituents during cell demolition. This leads for example to the egress of mitochondrial DNA into the cytoplasm [202] that drives a type 1 interferon response that causes defects in haematopoietic stem and progenitor cells [203, 204].

A plethora of single caspase knockout mice (including caspase-1, -2, -11 and -12) have been generated and haematopoiesis in these mice appeared normal [19, 87, 205, 206]**.** Apart from the important roles of caspase-9 during brain development and the indirect impact of its loss on haematopoietic stem/progenitor cells, little is known about the roles of caspases, especially their overlapping functions, during embryonic development and adult life [19, 87, 148, 204, 205, 206]. Since caspases play key roles in various processes, it seems likely that redundancy exists to ensure correct embryonic development, immunity and haematopoiesis. We therefore generated mice deficient for all CARD containing caspases, i.e. lacking caspases-1, -11, -12, -2 and -9. To be able to generate such animals we had to deal with the embryonic lethality caused by the loss of caspase-9. We did this by analysing embryos at day E14.5, thus prior to the death of caspase-9 deficient mice. To investigate the impact of the combined loss of caspases-1, -11, -12, -2, -9 on haematopoiesis and apoptotic cell death, we lethally irradiated wt recipient mice and reconstituted them with haematopoietic stem/progenitor cells from the foetal livers of caspase-1/11/12/2/$9^{-/-}$ E14.5 embryos.

5.2 Results

5.2.1 The role of CARD containing caspases during embryonic development.

To assess whether the additional deletion of caspases-1, -11, -12 an -2 would impact embryonic development even more than loss of caspase-9 alone, we crossed our caspase-1/11/12$^{-/-}$ mice described in Chapter 3 with caspase-2$^{-/-}$/ 9$^{+/-}$ mice. The caspase-1/11/12/2$^{-/-}$/9$^{+/-}$ mice, which are viable and fertile, resulting from two backcrosses were inter-crossed to obtain quintuple knockout mice deficient for caspases-1, -11, -12, -2 and -9. Mice lacking caspase-9 die perinatally as a result of reduced apoptosis during brain development causing exencephaly (enlargement and protrusion of the forebrain) [87, 199, 200].

To confirm a caspase-1/11/12/2/9$^{-/-}$ quintuple ko deletion, embryos were harvested at day E14.5 and genomic DNA from digested tail clippings was examined by PCR (Figure 5-1). Successful deletion of the *caspase-1/11/12* locus results in a knockout band of 413 bp. The *caspase-2* ko PCR product runs at 500 bp and deletion of *caspase-9* results in a band of around 500 bp in size. The genotyping for all three loci of a caspase-1/11/12/2/9$^{-/-}$ embryo (denoted KO3) is shown in Figure 5-1.

Embryos were harvested and analysed at embryonic day E14.5. The two caspase-1/11/12/2/9$^{-/-}$ embryos depicted appear normal and display no obvious deformities (Figure 5-2). However, these results are very preliminary, and more mouse crosses are required to increase the numbers of embryos for analysis. For comparison, a caspase-1/11/12$^{+/-}$2$^{-/-}$/9$^{+/+}$ embryo is shown since caspase-1/11/12$^{-/-}$ and caspase-2$^{-/-}$ mice develop normally [205] (see Chapter 3) and unfortunately no image of a wt embryos was taken at the time.

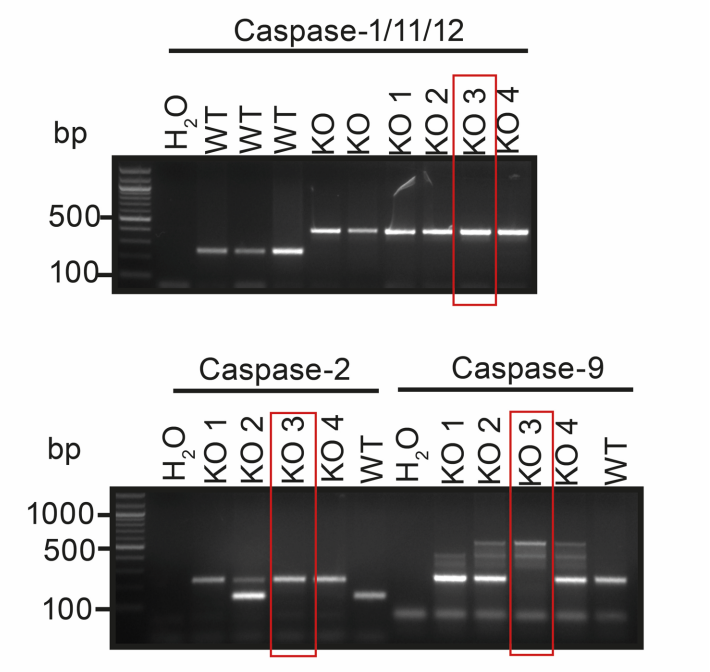

Figure 5-1: Genotyping of embryos to confirm deletion of caspases-1, -11, -12, -2 and -9.

Top agarose gel: For the *caspase-1/11/12* locus, a knockout band is amplified by PCR at 413 bp whereas the wildtype fragment runs at 245 bp. Bottom agarose gel, left lanes: PCR for *caspase-2* gene amplifies a wildtype band of 150 bp and a knockout band at 250 bp. Bottom agarose gel, right lanes: *Caspase-9* genotyping results in a band of 250 bp for the wildtype allele and 500 bp for the knockout allele. A caspase-1/11/12/2/9$^{-/-}$quintuple ko embryo is denoted KO3 and the results from its genotyping are highlighted with red boxes for each locus. The genotyping data shown are representative of all genotyping analyses performed for the generation of caspase-1/11/12/2/9$^{-/-}$ embryos. H_2O served as a negative control, KO indicates knockout controls (if available) and WT is a wildtype control.

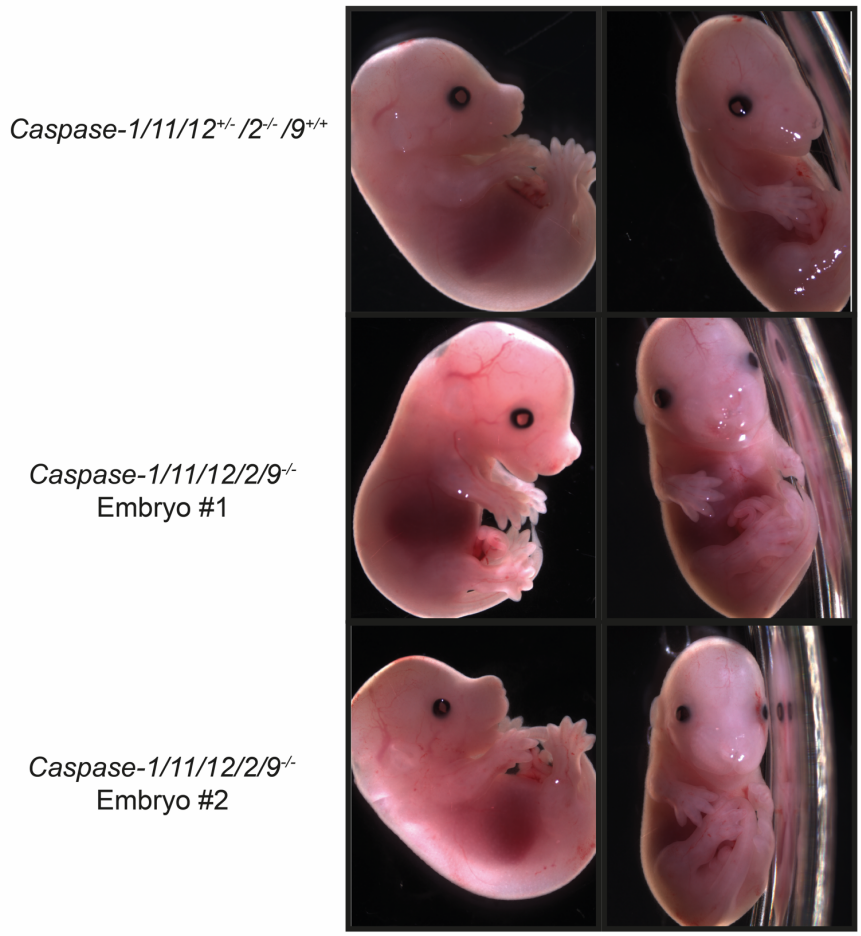

Figure 5-2: Deletion of all murine CARD containing caspases (-1, -11, -12, -2 and -9) does not affect embryonic development up to day E14.5.

Embryos taken at E14.5. One caspase-1/11/12$^{+/-}$ 2$^{-/-}$ /9$^{+/+}$ embryo is shown as control and two caspase-1/11/12/2/9$^{-/-}$ embryos (labelled #1 and #2, respectively). Images taken at a Zeiss Stemi 2000-C microscope. Caspase-1/11/12$^{+/-}$ 2$^{-/-}$ /9$^{+/+}$ embryo is shown for comparison as they are developmentally like wt embryos.

5.2.2 Impact of combined loss of caspases-1, -11, -12, -2 and -9 on the haematopoietic system

To investigate the impact of the combined loss of all murine CARD containing caspases, namely caspase-1, -11, -12, -2 and -9, on haematopoiesis, we reconstituted lethally irradiated wildtype mice with HSPCs derived from the foetal liver of caspase-1/11/12/2/9$^{-/-}$ E14.5 embryos, using mice reconstituted with wt foetal liver derived HSPCs as controls (Figure 5-3 and 5-4). After 8-10 weeks, we analysed the different haematopoietic cell subsets of the caspase-1/11/12/2/9$^{-/-}$ or wt haematopoietic system reconstituted mice using flow cytometry (Figures 5-3 and 5-4). Analysis of the T cell subsets in the thymus, spleen and lymph nodes showed no significant defects in the CD4 single positive (CD4^{+}), CD8 single positive (CD8^{+}), CD4/CD8 double positive (CD4^{+}CD8^{+}) or double negative (DN, CD4^{-}CD8^{-}) T lymphocyte subsets in the thymus between the caspase-1/11/12/2/9$^{-/-}$ vs the wt reconstituted mice (Figures 5-3a and 5-4a). Furthermore, we did not observe any differences in the frequencies of the peripheral naïve (CD44^{low}) or activated/memory T cells (CD44^{high}) between the caspase-1/11/12/2/9$^{-/-}$ vs the wt HSPC reconstituted mice (Figures 5-3b and 5-4b).

Interestingly, however, we found increased numbers of peripheral CD4^{+} T cells in the lymph nodes of the caspase-1/11/12/2/9$^{-/-}$ reconstituted mice (Figure 5-4b), which is probably due to an increase in the naïve CD4^{+} T cells. There was no difference in the regulatory T cell populations (T_{regs}), defined as CD4^{+}CD25^{+}FOXP3^{+}, in the lymph nodes and spleen between mice reconstituted with caspase-1/11/12/2/9$^{-/-}$ or wt HSPCs. Interestingly, we observed a marked increase in the percentages of thymic T_{reg} cells in mice reconstituted with caspase-1/11/12/2/9$^{-/-}$ HSPCs compared to those reconstituted with wt HSPCs (Figures 5-3c).

The follicular (IgD^{+}IgD^{lo}), B-1 (IgM^{+}CD5^{+}B220^{-}) and marginal zone (IgM^{+}B220^{+}CD5^{-}) B cell populations were comparable in percentages and total cell numbers between mice reconstituted with caspase-1/11/12/2/9$^{-/-}$ or wildtype HSPCs (Figure 5-3d, 5-4d). Furthermore, the pro-B/pre-B (B220^{+}IgM^{-}), immature B (B220^{low} IgM^{+}), transitional B (B220^{+}IgM^{high}), and mature B (B220^{high}IgM^{+}), cells in the bone marrow were not affected by the combined loss of caspases-1, -11, -12, -2 and -9 (Figures 5-

3e and 5-4e). We observed a trend towards increased numbers of B cells in the lymph nodes of the caspase-1/11/12/2/9$^{-/-}$ reconstituted mice, but the difference to mice reconstituted with a wt haematopoietic system was not statistically significant.
Quantifying neutrophil (Mac1^{+}/GR1^{+}) and monocyte/macrophage (Mac1^{+}) cell numbers and percentages in the lymph nodes and bone marrow revealed no differences between the mice reconstituted with caspase-1/11/12/2/9$^{-/-}$ HSPCs compared to control mice reconstituted with wt HSPCs (Figures 5-3f and 5-4f).

Admittedly, the data shown are preliminary and we will need to examine more reconstituted mice but based on the findings so far, we conclude that the combined loss of all CARD containing caspases does not cause major abnormalities in the haematopoietic system of mice under steady state conditions.

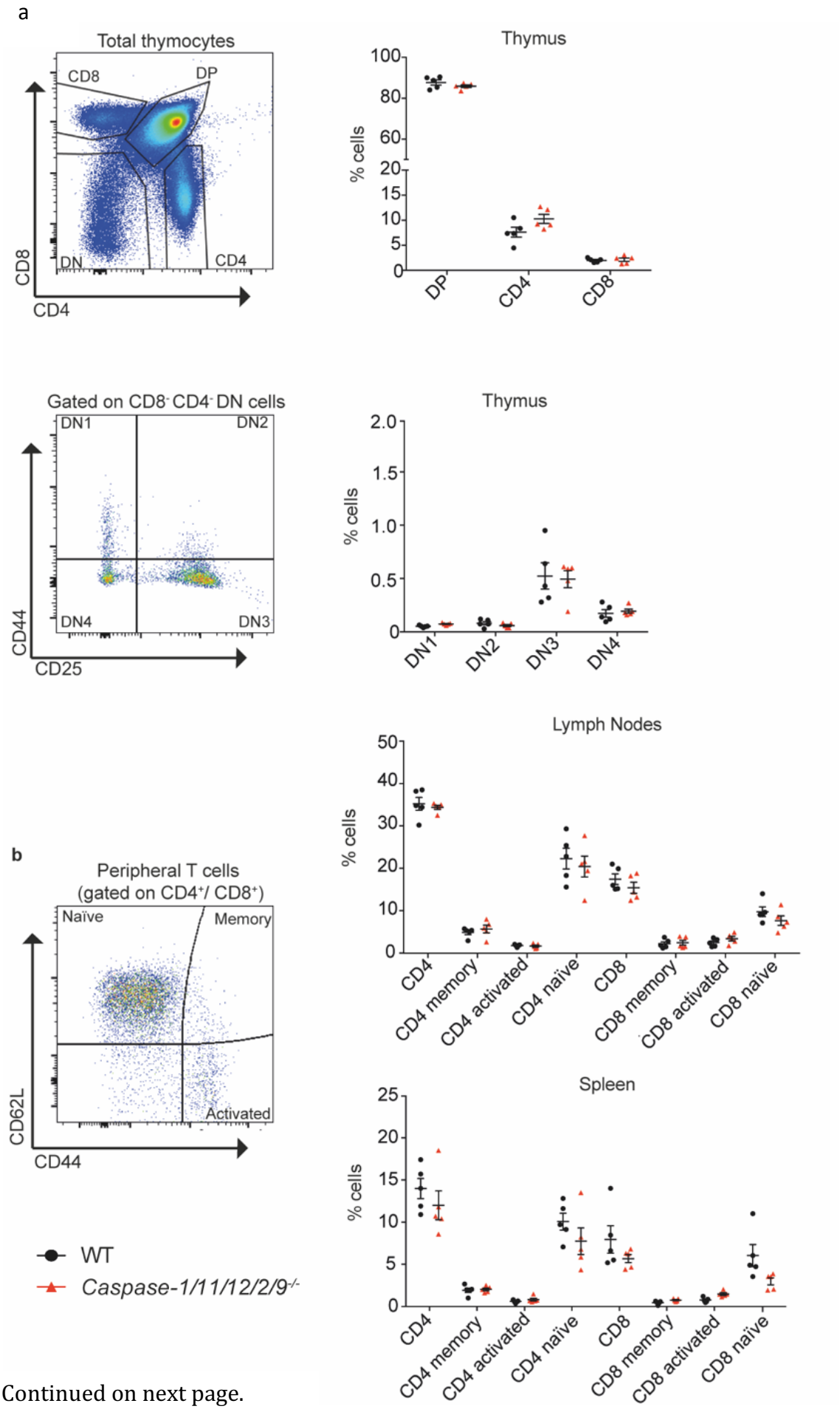

Continued on next page.

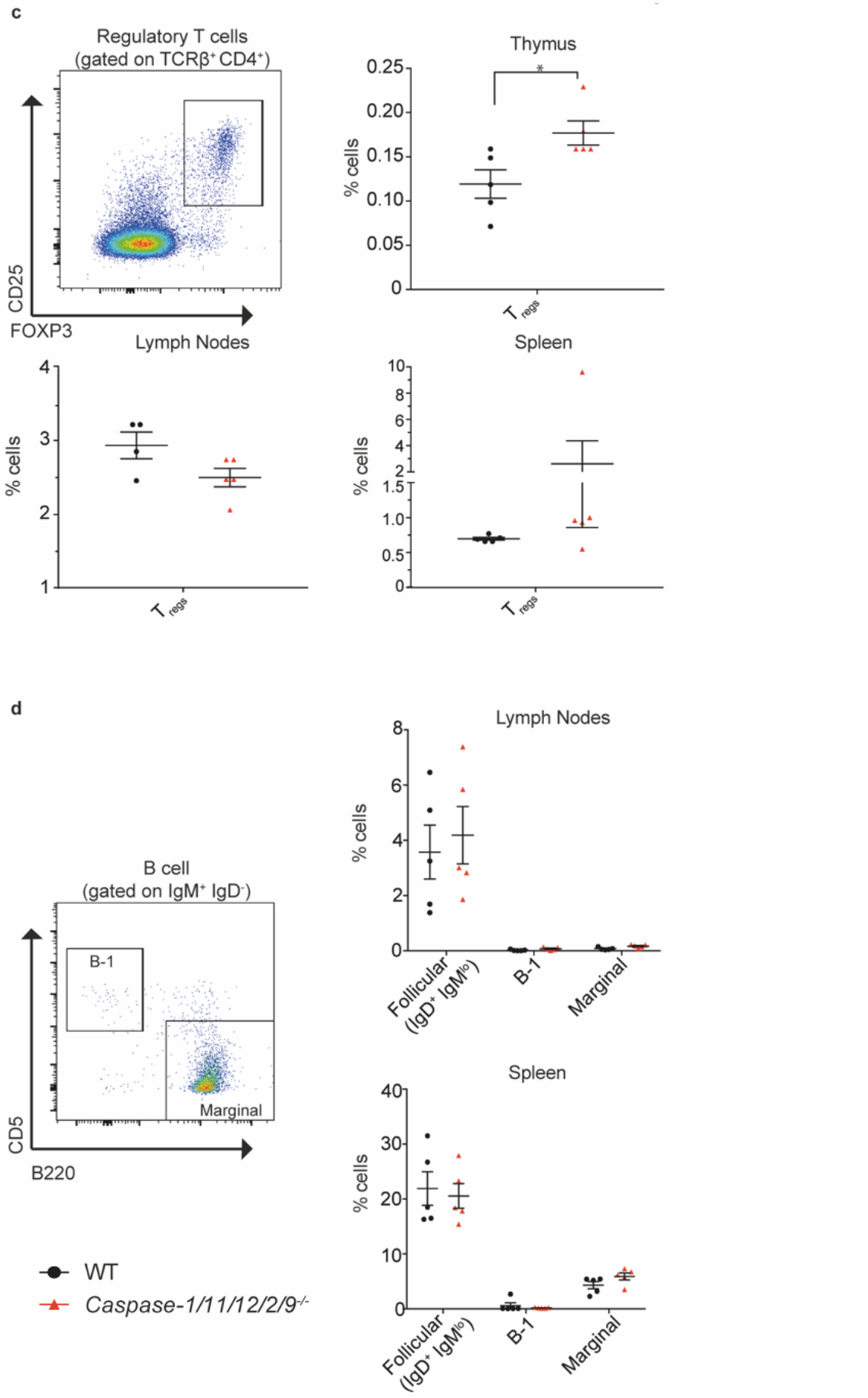

Continued on next page.

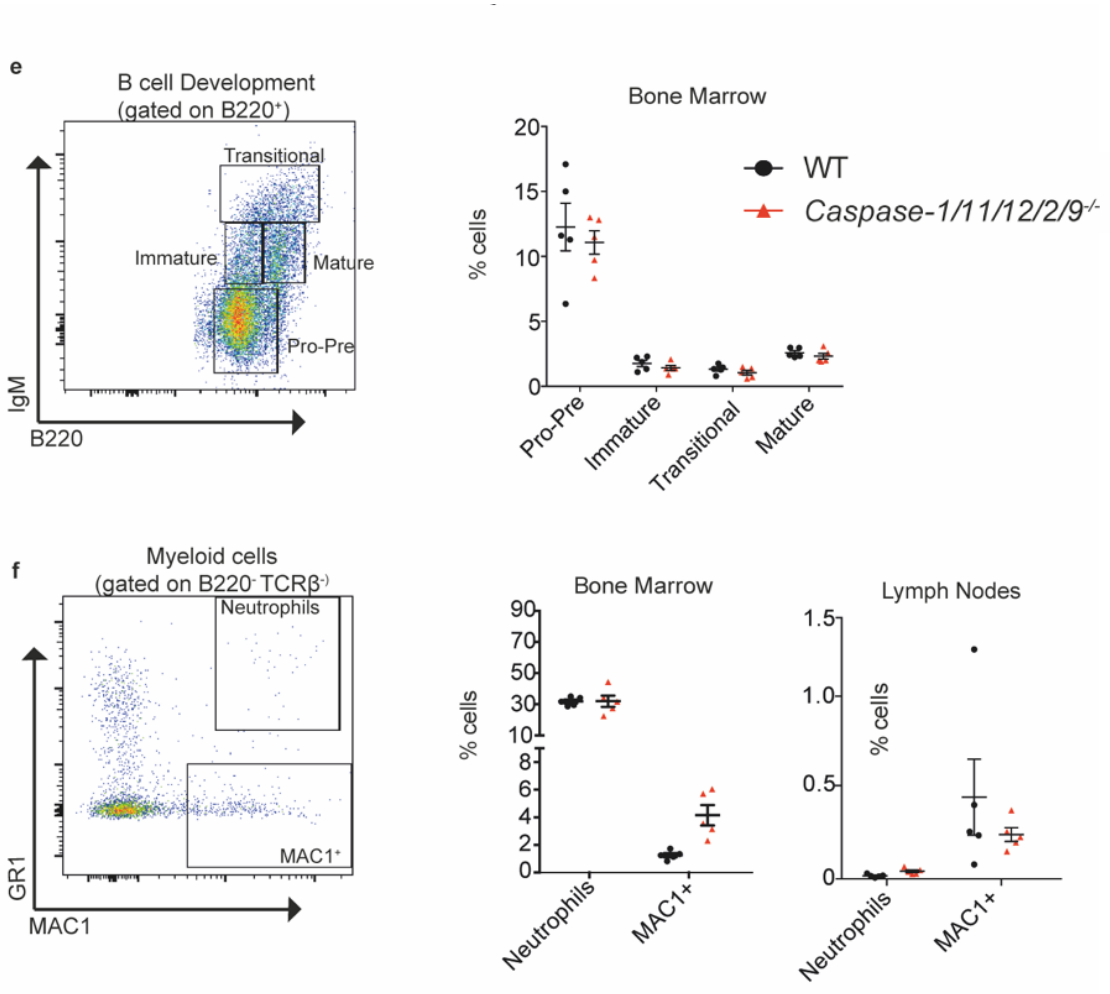

Figure 5-3: The deletion of caspases-1, -11, -12, -2 and -9 has no major impact on haematopoiesis in mice.

Flow cytometric analysis of the haematopoietic system of mice reconstituted with caspase-1/11/12/2/9$^{-/-}$ or control (wt) HSPCs. Gating strategies of cell subsets are depicted in the left column; the percentages of cells are shown in the right panels. **a** T cell development in the thymus. Depicted populations are CD8^{+}, CD4^{+} and DP for CD4^{+}CD8^{+} double positive T cells. The double negative (CD8^{-}CD4^{-}) progenitor cells (DN) were further subdivided using staining for CD25 and CD44. The gating strategy for DN progenitor cells is depicted in the second plot down from the top on the left. Cells are defined as: DN1 (CD44^{+}CD25^{-}), DN2 (CD44^{+}CD25^{+}), DN3 (CD44^{-}CD25^{+}) and DN4 (CD44^{-}CD25^{-}). **a** (bottom right) wt and caspase-1/11/12/2/9 quintuple knockout DN 1-4 stages shown as percentages. **b** (left column) Representative gating strategy for the activation status of CD4^{+} T cells. T cells that do not express the CD44 surface marker are considered naïve T cells, gate in top left quadrant. Upon

activation, T cells upregulate CD44 expression (right panels). These activated T cells can be further sub-divided into memory (upregulated CD62L expression) and activated $CD4^+$ T cells ($CD44^{hi}$ $CD62L^{lo}$). Percentages in the spleen (bottom right) and lymph nodes (top right) of naïve, memory and activated $CD4^+$ T cells from mice reconstituted with caspase-$1/11/12/2/9^{-/-}$ or wt HSPCs. **c** The top left plot shows representative flow cytometry gating strategy for T cell populations in the different lymphoid organs. **c** (top right and two bottom panels) Determination of the percentages of regulatory T cells (T_{regs}) ($CD4^+CD25^+FOXP3^+$) in the thymus (top right), lymph nodes (bottom left) and spleen (bottom right) using flow cytometry. **d** (left) Representation of flow cytometric gating of B cell populations in the lymph nodes (top right) and spleen (bottom right). **d** (right) The percentages are shown for follicular B cells (IgD^+IgD^{lo}), B-1 B cells ($IgM^+CD5^+B220^-$) and marginal zone B cells ($IgM^+B220^+CD5^-$). **e** (left) Representative gating strategy used to analyse B cell development. Representative plots showing pro-B/pre-B ($B220^+IgM^-$), immature B ($B220^+IgM^{lo}$), transitional B ($B220^+IgM^{hi}$) and mature B cells ($B220^{hi}IgM^{lo}$) in the bone marrow. **e** (right) Percentages of B cell populations in the bone marrow of mice reconstituted with caspase-$1/11/12/2/9^{-/-}$ or wt HSPCs. **f** (left) Gating strategy for myeloid cell populations analysed by flow cytometry. Neutrophils ($GR\text{-}1^+MAC\text{-}1^+$) are shown on the top right, monocytes ($GR\text{-}1^-MAC\text{-}1^+$) are shown on the bottom right. **f** (right) Percentages of these cell populations in the bone marrow and lymph nodes (axial, brachial and inguinal) of mice reconstituted with caspase-$1/11/12/2/9^{-/-}$ or wt HSPCs are shown. Each symbol represents one reconstituted mouse. $n \geq 4$. Graphs show mean ± SEM. Results tested with 2-way ANOVA or unpaired two-tailed Students t-test.

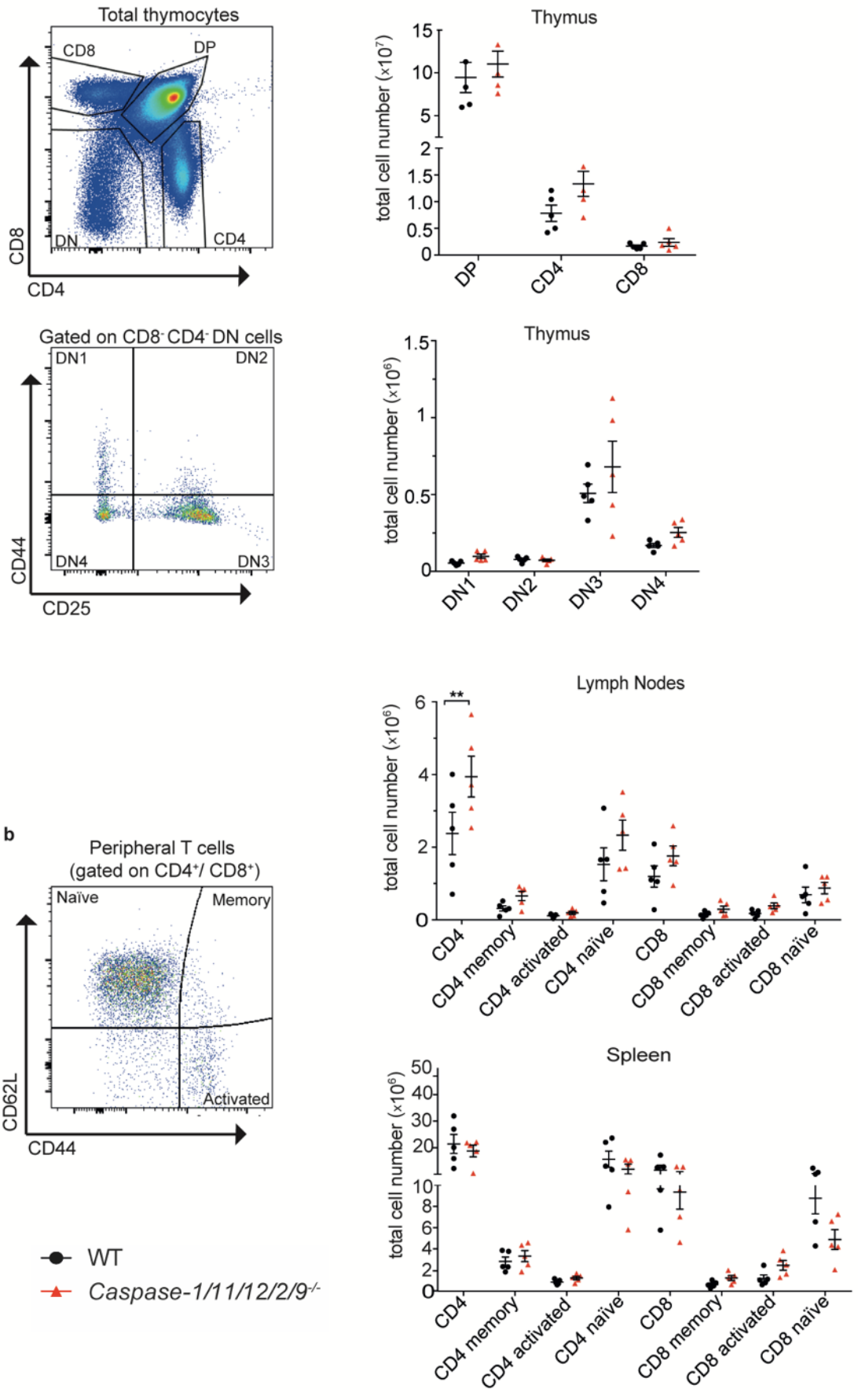

Continued on next page.

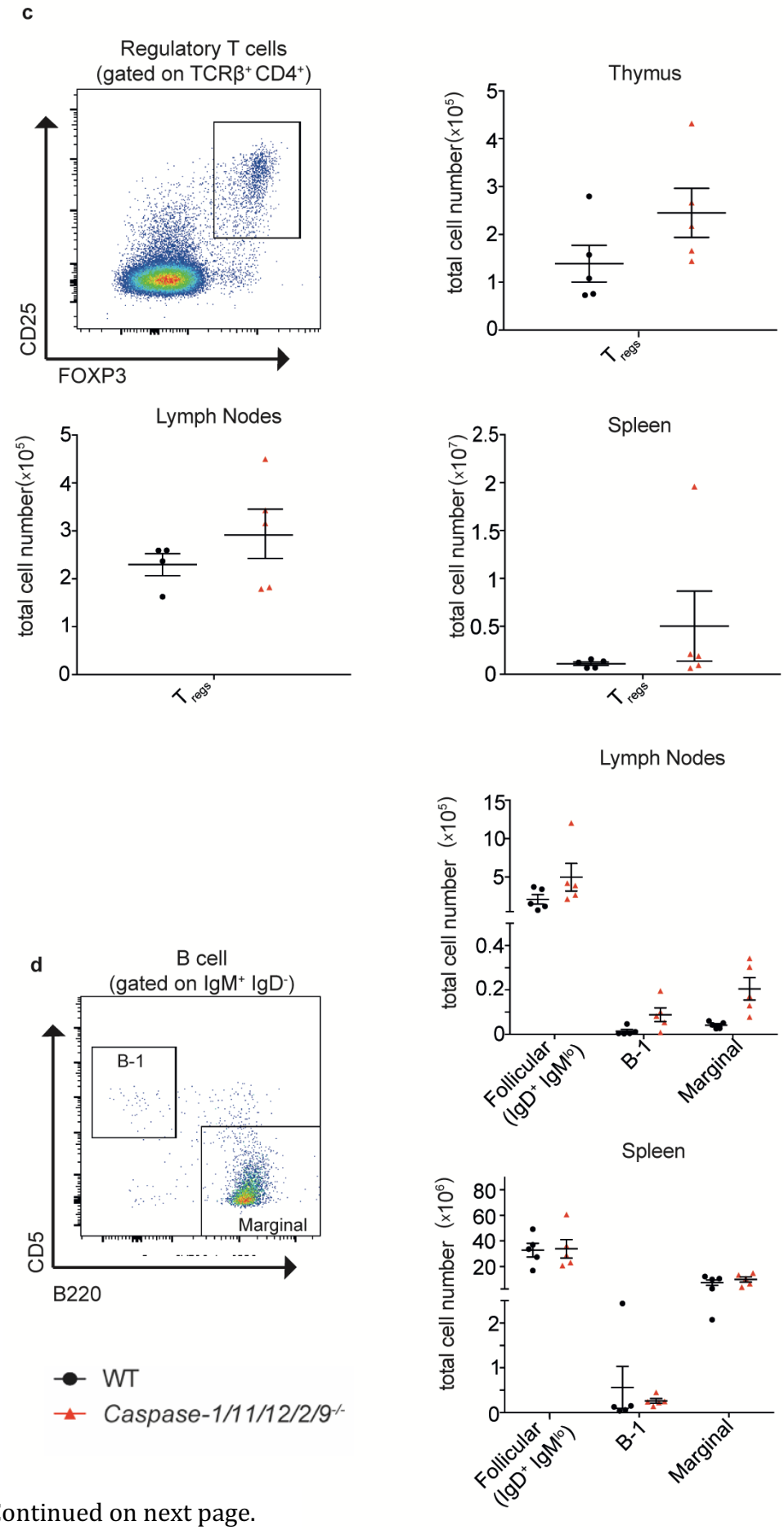

Continued on next page.

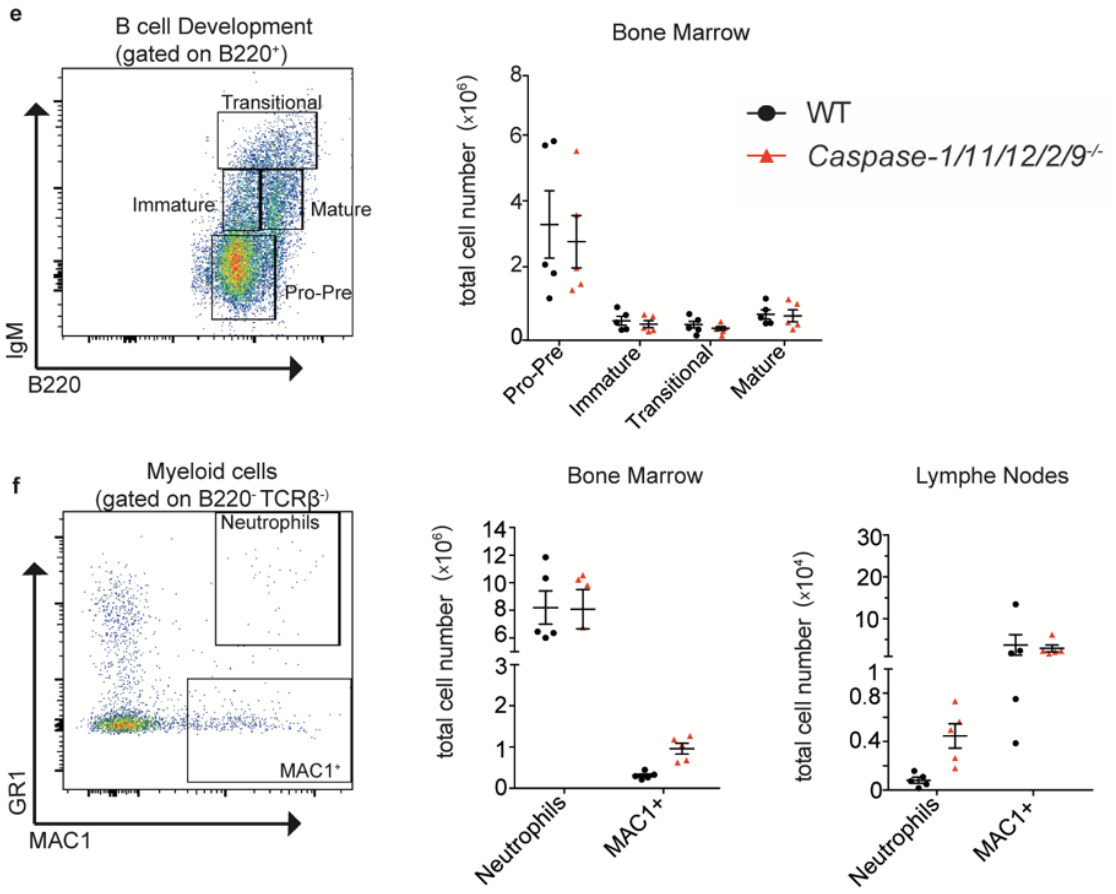

Figure 5-4 : Caspase-1/11/12/2/9$^{-/-}$ mice show normal overall numbers of haematopoietic cell subsets.

Subsets analysed and depicted the same as in Figure 5-3. Cell subsets from bone marrow (both tibia and femur), lymph nodes (axial, brachial and inguinal), thymus and spleen of caspase-1/11/12/2/9 quintuple knockout and wt control mice.

a-f Cell subsets are shown and quantified in total numbers with gating strategy representations in left column. Graphs show means ± SEM. n≥4. Symbols represent individual mice. Results tested with 2way ANOVA or unpaired two-tailed Students t-test.

5.2.3 T lymphoid cells deficient for caspases-1, -11, -12, -2 and -9 show similar susceptibility as wildtype cells towards different apoptotic stimuli.

In order to determine whether the deletion of all murine CARD containing caspases (caspases-1, -11, -12, -2 and -9) had an effect on apoptosis, we isolated caspase-1/11/12/2/9 deficient thymocytes (or as a control wt thymocytes) from the reconstituted animals and examined their spontaneous death and ionomycin-induced apoptosis. The percentages of live and dead cells were determined over 3 days using staining for Annexin V plus PI followed by flow cytometric analysis (Figure 5-5). As depicted in Figure 5-5, the untreated wildtype and caspase-1/11/12/2/9$^{-/-}$ thymocytes underwent spontaneous apoptosis at a similar rate with approximately 50% of cells remaining alive after 72 h of culture. Upon treatment with ionomycin, a delay in the apoptosis of the caspase-1/11/12/2/9 deficient thymocytes compared to the wt thymocytes was observed (Figure 5-5, right panel). However, the death of the caspase-1/11/12/2/9 deficient thymocytes was not prevented but only delayed, and at 72 h all ionomycin treated caspase-1/11/12/2/9 deficient thymocytes were dead. These data reveal that the apoptosis of thymocytes is only delayed, but not prevented in the absence of all CARD containing caspases.

Upon infection, T lymphocytes will expand and differentiate into activated T cells to fight pathogenic infection. Once the infection is resolved, large number of immune cells (especially effector type cells) are no longer required and are therefore removed by apoptosis [207]. To investigate whether the loss of all murine CARD containing caspases impacts on the apoptosis of activated T cell blasts, we isolated spleen cells from mice reconstituted with caspase-1/11/12/2/9$^{-/-}$ or wt (control) HSPCs and stimulated them with ConA plus IL-2. After 4 days of culture we detected ~80 % T cell blasts (Figure 5-5b, 0 h timepoint), with no differences apparent between wildtype and caspase-1/11/12/2/9 deficient cells (Figure 5-5b). As these T cell blasts depend on IL-2 for their survival and proliferation, we wanted to test whether the absence of all CARD containing caspases might reduce the apoptosis

caused by IL-2 withdrawal from the medium. To this end, we washed the T cell blasts to remove IL-2, plated these cells in simple medium (no added IL-2) and measured their survival over time using PI plus Annexin V staining followed by flow cytometric analysis. Interestingly, we observed no difference in the rate of cell death between the caspase-1/11/12/2/9$^{-/-}$ vs the wt T cell blasts (Figure 5-5b).

These experiments demonstrate that cells lacking all CARD containing caspases have no long-term survival advantage over wildtype cells, with only a relatively minor delay in ionomycin-induced apoptosis seen in thymocytes and no protection in activated T cell blasts deprived of IL-2.

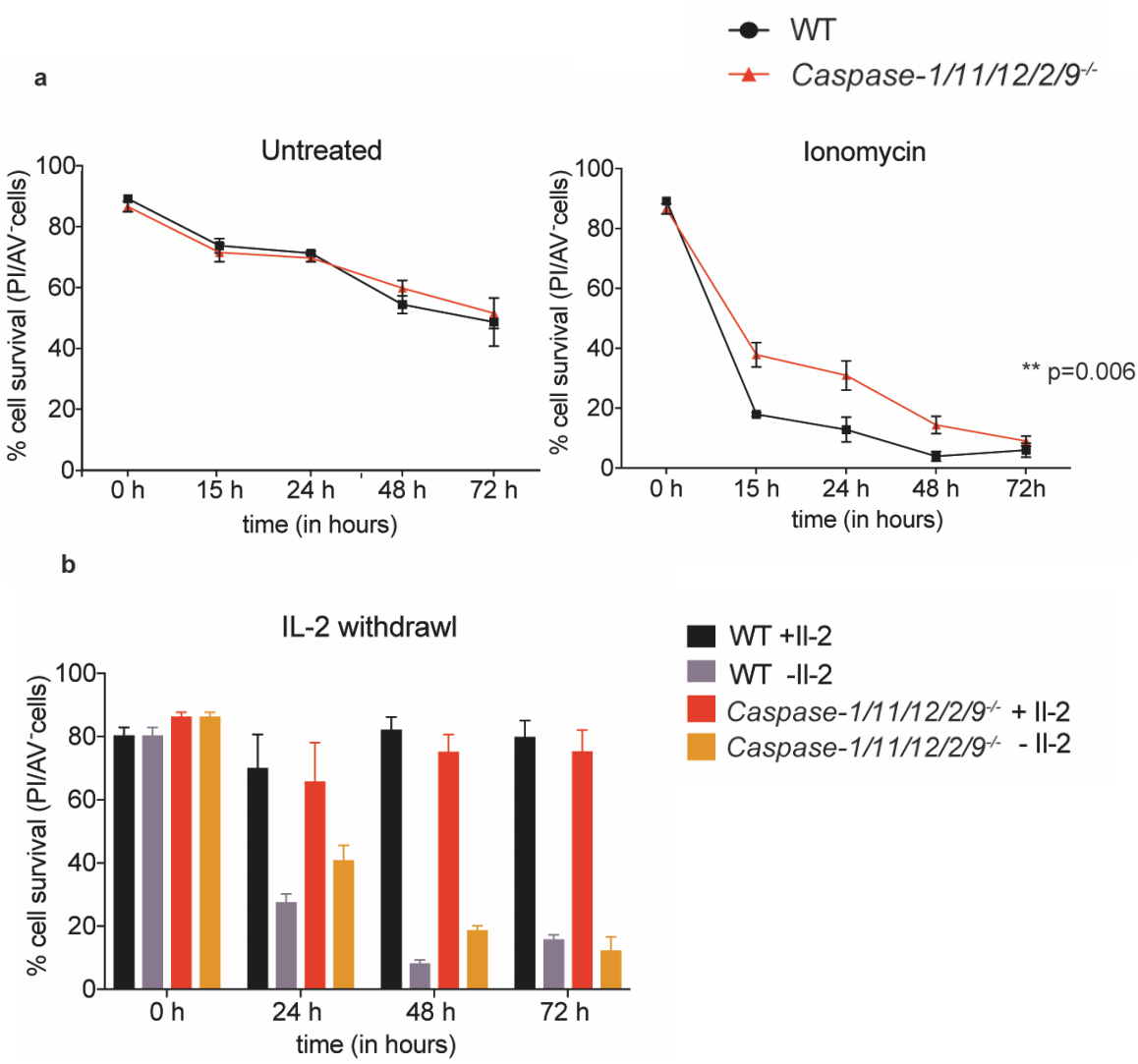

Figure 5-5: The combined loss of all murine CARD caspases-1, -11, -12, -2 and -9 does not protect lymphocytes from cell death *in vitro*.

a: Unsorted thymocytes isolated from mice reconstituted with HSPCs derived from wt or caspase-1/11/12/2/9$^{-/-}$ E14.5 foetal liver cells. Left panel: Untreated thymocytes grown in medium for 3 days. Right panel: Ionomycin-treated thymocytes (1 µg/mL), (% survival normalised to untreated). Cell viability was quantified by measuring PI$^-$ Annexin V$^-$ (live) cells at a flow cytometer. **b** Unsorted T cells from spleen isolated from mice reconstituted with HSPCs derived from wt (control) or caspase-1/11/12/2/9$^{-/-}$ E14.5 foetal liver cells. Cells were stimulated with ConA plus IL-2 for 4 days. On day 4, cells were washed and subsequently cultured in the presence or absence of IL-2 for the indicated timepoints. Cell survival was measured by PI plus Annexin V staining followed by flow cytometric analysis. n=4 across 2 independent experiments, statistical analysis: 2way ANOVA, p value as indicated.

5.2 Discussion

Although the essential roles of the caspase family of proteases during embryogenesis, inflammation and cell death in general have long been recognised [22, 110], there are still many unanswered questions about their exact and potentially overlapping functions. The question of functional overlap within the caspase family has not yet been rigorously addressed. One reason for the limited data on this topic might be explained by the lack of mouse strains deficient for multiple caspases (more than 2) or even deleted for an entire caspase sub-family (e.g. the CARD sub-family). It is undisputed that the initiator caspase, caspase-9, plays an important role in the intrinsic apoptotic pathway [25]. However, caspase-9 deficient cells and even cells deficient for both caspase-9 and caspase-2 still die in response to cytotoxic insults that are known to induce the intrinsic apoptotic pathway (Figure 5-5) [87, 148]. How is this cell killing achieved even with the lack of this key initiator caspase? The BCL-2-regulated or mitochondrial apoptotic pathway leads to the destruction of the outer mitochondrial membrane, which is considered the point of no return in the apoptotic pathway [80, 94]. It would be possible that downstream of MOMP other factors, such as other proteases, lead to the activation of executioner caspases and hence demolition of the cell. Also, the existence of a completely caspase-independent, yet to be discovered cell demolition cannot be excluded.

An interesting explanation might be that in the absence of caspase-9 (or absence of both caspase-9 and caspase-2) other CARD containing caspases can compensate and mediate the activation of the effector caspases. It is interesting to contemplate that all CARD containing caspases may have overlapping roles in the intrinsic apoptotic pathway upstream of the effector caspases. Notably, the function of caspase-2 is not yet fully resolved although a role in mitotic cell division has recently been reported [9, 208, 209, 210, 211]. Given that caspase-2/9 double deficient cells remained sensitive to apoptosis triggered by diverse cytotoxic stimuli [148], we wondered whether all CARD containing caspases (i.e. caspases-1, -11, -12, -2 and -9) might have substantially overlapping roles in apoptosis. We therefore generated a mouse strain lacking all murine CARD containing caspases. In preliminary studies we were unable to identify obvious abnormalities in the embryos lacking caspases-1, -11, -12, -2 and -9 (Figure 5-2). This may appear to be an unexpected finding given that caspase9$^{-/-}$

embryos were shown to exhibit exencephaly with high incidence. However, it must be noted that this high incidence in exencephaly was seen in caspase-$9^{-/-}$ embryos only on a mixed C57BL/6 x 129SV background [199, 200], whereas this developmental abnormality was less prevalent on a pure C57BL/6 background [196] (unpublished observations from our own work). Of note, the caspase-$1/11/12/2/9^{-/-}$ embryos analysed in the present study are on a C57BL/6 background, which may explain why we have not seen any cases with exencephaly so far. In any case, we have not yet screened sufficient numbers of embryos (thus far we only obtained 2 caspase-$1/11/12/2/9^{-/-}$ embryos) to provide conclusive insight into the impact of the loss of all CARD containing caspases on embryonic development. It is also possible that abnormalities in embryonic development could only become apparent at later stages, such as E16.5 or E18.5. Conversely, it is possible that the loss of all CARD containing caspases causes lethal defects at earlier stages of embryogenesis with all affected embryos having disappeared before E14.5 the stage of development when we performed our analysis. Thus, many more embryos need to be generated and examined at various stages of development to gain an understanding of the overlapping functions of caspases-1, -11, -12, -2 and -9 in embryogenesis. It is also interesting to contemplate that all initiator caspases, i.e. all CARD containing caspases and the DED containing caspase, caspase-8, have critical overlapping roles in embryogenesis. Thus, it will also be of interest to generate embryos deficient for caspases-1, -11, -12, -2 and -9 as well as caspase-8 (plus loss of MLKL or RipK3 to prevent the embryonic lethality at E10.5 that is caused by the aberrant necroptosis arising from the absence of caspase-8).

The BCL-2 regulated apoptotic pathway plays a crucial role in the development and functioning of the haematopoietic system [212]. Abrogation of apoptosis, due to the combined loss of BAX and BAK [213, 214, 215] the combined loss of several BH3-only proteins (e.g. BIM and PUMA) [216, 217, 218] or the over-expression of BCL-2 [219, 220, 221] cause substantial increases in lymphoid or myeloid cells. Interestingly, we found that the loss of all CARD containing caspases (using a haematopoietic reconstitution system) did not cause a notable increase in any lymphoid or myeloid cell populations examined. This is consistent with the previous finding that the combined loss of caspases-2 and -9 does not cause a notable accumulation of lymphoid or myeloid cells [148]. This suggests that the activation of MOMP in the cells

programmed to die, for example lymphocytes lacking antigen receptors due to failed *Tcr* or *Ig* gene rearrangement, the induction of MOMP, even in the complete absence of all CARD containing caspases, is sufficient for cell killing. It will still be interesting to generate mice lacking in their haematopoietic compartment not only all CARD containing caspases, but also the DED containing initiator caspase-8 (with additional loss of MLKL or RipK3 to prevent aberrant necroptosis). This would reveal whether developmentally programmed death of lymphoid and myeloid cells can proceed in the absence of all initiator caspases. Ultimately, it would be exciting to generate cell lines or mice lacking in their haematopoietic system all caspases. This would allow to rigorously address the postulated roles of caspases in processes other than apoptosis, pyroptosis, inflammation and prevention of necroptosis, such as cell division [222, 223, 224].

Interestingly, it has been reported that the absence of caspase-9 impairs the normally "neat" demolition of cells undergoing apoptosis and that the leakage of mitochondrial DNA into the cytoplasm causes aberrant activation of type 1 interferon signalling. This, in turn, causes a mobilisation of haematopoietic stem cells [203, 225]. It will be interesting to determine whether the loss of all CARD containing caspases will cause even more severe defects in the dismantling of cells undergoing apoptosis, resulting in greater inflammatory signalling with further impact on haematopoietic stem and progenitor cells. Following on from this, it would also be interesting to determine whether the loss of all initiator caspases (i.e. loss of all CARD containing caspases plus loss of caspase-8) would cause greater aberrations in the dismantling of cells undergoing apoptosis, than loss of caspase-9 alone, and whether this might result in greater inflammatory signalling with impact on the haematopoietic stem and progenitor cells.

To investigate the impact of the combined loss of all murine CARD containing caspases on apoptosis of cells *in vitro*, we analysed spontaneous and ionomycin-induced apoptosis of thymocytes and the IL-2 deprivation-induced apoptosis of mitogen activated T cell blasts derived from lethally irradiated wt mice that had been reconstituted with caspase-1/11/12/2/9$^{-/-}$ or wt HSPCs from foetal livers of E14.5 embryos. These studies showed that the caspase-1/11/12/2/9$^{-/-}$ cells still die to the same extent as wt cells, although some delay in cell killing was seen in thymocytes treated with ionomycin. This delayed cell death was not unexpected

given that previous analysis revealed a similar delay in cytokine deprivation-induced apoptosis in cells lacking caspase-9 [87] or both caspase-2 and -9 [148]. Thus, the additional loss of caspases-1, -11, -12 plus caspase-2 provides no further protection against cytokine deprivation or ionomycin-induced apoptosis beyond the minor delay in apoptosis afforded by the loss of caspase-9.

Taken together, our results show that caspase-1/11/12/2/9$^{-/-}$ cells can still undergo a form of cell death that appears to resemble, at least in certain aspects, apoptosis. Whether this suggests a fully caspase-independent way of cell killing, or activation of downstream effector caspases (caspase-3, -6 and -7) in an atypical initiator caspase-independent manner remains to be elucidated. Since caspase-8 also functions as an initiator caspase, traditionally in response to the ligation of death receptors within an activation platform, called DISC, one could hypothesise that it acts redundantly with caspases-1, -11, -12, -2 and -9 to activate the effector caspases and initiate apoptosis. Of note, recent reports suggested a role for caspase-8, downstream of death receptors, in apoptosis triggered by DNA damage inducing agents [226] or ER stress inducing agents [227]. Although these findings could not be reproduced in a follow-up study [228], it will be interesting to examine the overall impact of the loss of all initiator caspases (i.e. caspases-1, -11, -12, -2, -9 plus caspase-8) on cytokine deprivation as well as cytotoxic drug-induced cell killing *in vitro*. It will be particularly exciting to investigate the morphological and biochemical changes of cells undergoing apoptosis in the absence of all of these caspases.

Certain pathogens express inhibitors of caspases, such as CrmA. The ability of cells to undergo cell death that still resembles apoptosis in at least certain aspects, may be related to this; i.e. the death of pathogen infected cells, even when caspases are disabled, will be advantageous for the host, enabling it to clear the infection.

In conclusion, the studies presented in this chapter reveal that there appears not to be substantial functional overlap between the different CARD containing caspases in embryonic development, development and function of the haematopoietic system and apoptotic death of cells triggered by developmental cues, cytokine deprivation or cytotoxic insults. However, the work presented here is only a starting point and much more exciting work can be done to investigate the overlapping roles of initiator caspases or all caspases in these processes.

Chapter 6: Conclusion

Programmed cell death (PCD) is pivotal during embryonic development, inflammation and the fight against invading pathogens. Over the past three decades, the key regulators and executioners of both PCD and inflammation have been discovered and the latter include the superfamily of caspases.

The three major PCD pathways are apoptosis, necroptosis and pyroptosis. Caspases play critical roles in all of these pathways, in the case of apoptosis and pyroptosis as critical executioners of cellular demolition and in the case of necroptosis as critical inhibitors (caspase-8) of pathway activation. Caspases are highly conserved across the entire metazoan lineage consistent with their critical roles in diverse biological processes [1, 229]. Even though some caspases are known to exert critical functions in the regulation of life vs death decisions of cells and inflammation; the roles of some other caspases, such as caspases-2 and -12, are still only poorly understood. Moreover, the overlapping roles of the many caspases and the complexity of the connections between the different cell death pathways in which the caspases function need to be dissected carefully. This may seem surprising, considering how fundamentally important the correct regulation of cell death and inflammation are for multicellular organisms, but the generation of mice deficient for three or more caspases must have been a significant deterrence from conducting relevant studies in this area.

The work of my thesis focused on unravelling the overlapping functions of the different CARD containing caspases, caspases-1, -11, -12, -2 and -9, and the greater overlapping functions of all initiator (i.e. long pro-domain containing) caspases, i.e. caspases-1, -11, -12, -2, -9 and -8. My work aimed to explore the complex interplay and possible overlapping functions in embryogenesis, inflammation and different cell death pathways, including apoptosis, pyroptosis and necroptosis. Such knowledge is essential to fully understand the underlying causes of many diseases that are thought to be caused, at least in part, by defects in cell death, including neurodegenerative disorders, cancer, aberrant inflammation, infection and sepsis.

Additionally, the knockout mouse strains lacking 3 or more caspases generated during my PhD can be used in the future for further investigations in developmental biology, cancer, infectious diseases or general immunology.

In my PhD studies I characterised a mouse strain deficient for the inflammatory caspases-1, -11 and -12 and I found that the absence of these three caspases had no major impact on haematopoiesis or embryonic development. Interestingly, caspase-12 did not appear to contribute to the septic shock response in mice, as the caspase-1/11/12 triple knockout mice did not display additional protection from LPS injection-induced septic shock compared to the caspase-1/11 double knockout mice that had previously been reported [121]. Additionally, we failed to confirm a role of caspase-12 during endoplasmic reticulum stress-induced cell death in contrast to what was previously published [206], but consistent with other studies [52]. However, we did discover a potentially novel role for caspase-12 in the clearance of *Salmonella* Typhimurium vaccine strain BRD509ΔaroA from the gall bladder. Mice lacking caspase-12 on top of either caspases-1 and -11 or caspases-1, -11, -8 and RipK3 showed an increased number of bacteria in their gall bladder upon *S.* Typhimurium vaccine strain BRD509ΔaroA infection compared to the relevant control mice containing caspase-12. This provides the first indication for a role for caspase-12 in the clearance of bacterial infections. Therefore, in the future we aim to generate and study caspase-12 single knockout mice to determine precisely the indispensable function of caspase-12 during infection with Gram-negative bacteria and other pathogens (e.g. viruses).

Furthermore, I generated mice deficient for caspases-1, -11, -12 and-8 with additional loss of RipK3, which is necessary to prevent the embryonic lethality (E10.5) that is caused by the loss of caspase-8. These quintuple knockout animals were subjected to *Salmonella* Typhimurium vaccine strain BRD509ΔaroA infection and, interestingly, this revealed severe defects in bacterial clearance from major organs, such as the liver, spleen and gall bladder. This indicates that the deficiency in these caspases and hence the loss of death receptor-induced apoptosis, necroptosis and pyroptosis causes severe defects in the clearance of intracellular bacteria. It remains open, whether this is a specific feature for infection with

Salmonella Typhimurium or whether the lack of these cell death pathways also leads to defects in the clearance of other pathogens.

In my final chapter, I show preliminary data describing a mouse strain in which we have deleted all CARD containing caspases, namely caspases-1, -11, -12, -2, -9. As caspase-9 deficient animals display developmental abnormalities (with severity greatly affected by genetic background), I was investigating whether other CARD containing caspases could have overlapping functions with caspase-9 in embryonic development; i.e. I predicted that mice lacking all CARD containing caspases might have more pronounced developmental abnormalities than mice lacking only caspase-9. Surprisingly, the mice lacking all CARD containing caspases displayed no additional overt phenotypes during embryogenesis compared to the caspase-$9^{-/-}$ mice, at least as shown in preliminary experiments at embryonic day E14. Additionally, we used HSPCs from E14 foetal livers from caspase-$1/11/12/2/9^{-/-}$ mice to reconstitute lethally irradiated wt mice to determine the overlapping roles of all CARD containing caspases in haematopoietic development and the response of haematopoietic cells to diverse apoptotic stimuli. I found no significant abnormalities in the haematopoietic subsets analysed in the mice lacking all CARD containing caspases. Furthermore, when subjecting thymocytes lacking all CARD containing caspases to different apoptotic stimuli *in vitro*, I observed only a delay in the rate of cell death but no long-term survival phenotype, comparable to that observed for the cells lacking only caspase-9. This suggests that the cells must die by a CARD caspase independent cell death pathway, which likely involves BAX/BAK mediated permeabilisation of the outer mitochondrial membrane (MOMP), just without full activation of the downstream caspase cascade.

Chapter 7: Appendix

MOI 10	Significant?	Adjusted p value
2 h		
WT vs Caspase-1/11/12$^{-/-}$	**	0.0014
WT vs Caspase-1/11/12/8 RipK3$^{-/-}$	****	<0.0001
6 h		
WT vs Caspase-1/11/12/8 RipK3$^{-/-}$	***	0.0001
Caspase-1/11/12$^{-/-}$ vs Caspase-1/11/12/8 RipK3$^{-/-}$	*	0.0443
24 h		
WT vs Caspase-1/11/12/8 RipK3$^{-/-}$	*	0.0319
Caspase-1/11/12$^{-/-}$ vs Caspase-1/11/12/8 RipK3$^{-/-}$	*	0.0138

MOI 50	Significant?	Adjusted p value
2 h		
WT vs Caspase-1/11/12$^{-/-}$	****	<0.0001
WT vs Caspase-1/11/12/8 RipK3$^{-/-}$	****	<0.0001
Caspase-8 RipK3$^{-/-}$ vs Caspase-1/11/12$^{-/-}$	****	<0.0001
Caspase-8 RipK3$^{-/-}$ vs Caspase-1/11/12/8 RipK3$^{-/-}$	****	<0.0001
6 h		
WT vs Caspase-1/11/12$^{-/-}$	*	0.0154
WT vs Caspase-1/11/12/8 RipK3$^{-/-}$	****	<0.0001
Caspase-8 RipK3$^{-/-}$ vs Caspase-1/11/12/8 RipK3$^{-/-}$	****	<0.0001
Caspase-1/11/12$^{-/-}$ vs Caspase-1/11/12/8 RipK3$^{-/-}$	****	<0.0001
24 h		
WT vs Caspase-1/11/12/8 RipK3$^{-/-}$	****	<0.0001
Caspase-8 RipK3$^{-/-}$ vs Caspase-1/11/12/8 RipK3$^{-/-}$	**	0.0058
Caspase-1/11/12$^{-/-}$ vs Caspase-1/11/12/8 RipK3$^{-/-}$	****	<0.0001

MOI 500	Significant?	Adjusted p value
2 h		
WT vs Caspase-1/11/12$^{-/-}$	****	<0.0001
WT vs Caspase-1/11/12/8 RipK3$^{-/-}$	****	<0.0001
Caspase-8 RipK3$^{-/-}$ vs Caspase-1/11/12$^{-/-}$	****	<0.0001
Caspase-8 RipK3$^{-/-}$ vs Caspase-1/11/12/8 RIPK3$^{-/-}$	****	<0.0001
6 h		
WT vs Caspase-1/11/12/8 RipK3$^{-/-}$	****	<0.0001
Caspase-8 RipK3$^{-/-}$ vs Caspase-1/11/12/8 RipK3$^{-/-}$	****	<0.0001
Caspase-1/11/12$^{-/-}$ vs Caspase-1/11/12/8 RipK3$^{-/-}$	****	<0.0001
24 h		
WT vs Caspase-1/11/12/8 RipK3$^{-/-}$	**	0.0025
Caspase-8 RipK3$^{-/-}$ vs Caspase-1/11/12/8 RipK3$^{-/-}$	**	0.0084
Caspase-1/11/12$^{-/-}$ vs Caspase-1/11/12/8 RipK3$^{-/-}$	*	0.0125

Table 7-1: Adjusted p values and statistical significances of cell viability shown in Figure 4-1 a. Cell viability of BMDMs measured by GPA assay after infection with *S.* Typhimurium SL1344 strain of the indicated MOI. Viability measured at indicated timepoints post-infection. C1/11/12$^{-/-}$ depicts BMDMs from caspase-1/11/12$^{-/-}$ mice, C8 RipK3 represents caspase-8 RipK3 deficient BMDMs and C1/11/12/8 RipK3 depicts BMDMs taken from caspase-1/11/12/8 and RipK3-deficient mice.

MOI 10	Significant?	Adjusted p value
6 h		
WT vs Caspase-8 RipK3$^{-/-}$	*	0.0146
WT vs Caspase-1/11/12$^{-/-}$	**	0.0019
WT vs Caspase-1/11/12/8 RipK3$^{-/-}$	****	<0.0001
24 h		
WT vs Caspase-8 RipK3$^{-/-}$	*	0.0135
WT vs Caspase-1/11/12$^{-/-}$	*	0.02
WT vs Caspase-1/11/12/8 RipK3$^{-/-}$	***	0.0002
MOI 50	**Significant?**	**Adjusted p value**
6 h		
WT vs Caspase-1/11/12/8 RipK3$^{-/-}$	*	0.0153
24 h		
WT vs Caspase-1/11/12/8 RipK3$^{-/-}$	**	0.002

Table 7-2: Adjusted p values for IL-1β secretion data shown in Figure 4-1b.
Cytokines measured in supernatant of BMDMs upon *S.* Typhimurium SL1344 strain infection of the indicated MOIs. Cytokines measured at indicated timepoints after infection. C1/11/12$^{-/-}$ depicts BMDMs from caspase-1/11/12$^{-/-}$ mice, C8 RipK3 represents caspase-8 RipK3 deficient BMDMs and C1/11/12/8 RipK3 depicts BMDMs taken from caspase-1/11/12/8 and RipK3-deficient mice.

MOI 10	Significant?	Adjusted p value
24 h		
C8 RipK3$^{-/-}$ vs C1/11/12$^{-/-}$	*	0.0319

MOI 50	Significant?	Adjusted p value
24 h		
C8 RipK3$^{-/-}$ vs C1/11/12$^{-/-}$	*	0.0486

MOI 500	Significant?	Adjusted p value
2 h		
WT vs C1/11/12/8 RipK3$^{-/-}$	*	0.0304
C8 RipK3$^{-/-}$ vs C1/11/12$^{-/-}$	*	0.0359
C8 RipK3$^{-/-}$ vs C1/11/12/8 RipK3 $^{-/-}$	*	0.0209
6 h		
WT vs C1/11/12/8 RipK3 $^{-/-}$	*	0.0213

Table 7-3: Adjusted p values for CFUs depicted in Figure 4c.

C1/11/12$^{-/-}$ depicts BMDMs from caspase-1/11/12$^{-/-}$ mice, C8 RipK3 represents caspase-8 RipK3 deficient BMDMs and C1/11/12/8 RipK3 depicts BMDMs taken from caspase-1/11/12/8 and RipK3 deficient mice.

Spleen	Significant?	Adjusted p value
WT vs C1/11/12/8 RipK3$^{-/-}$	****	<0.0001
C1/11/12/8 RipK3$^{-/-}$ vs C1/11$^{-/-}$	****	<0.0001
C1/11/12/8 RipK3$^{-/-}$ vs C8 RipK3$^{-/-}$	**	0.0038
C1/11/12/8 RipK3$^{-/-}$ vs C1/11/12$^{-/-}$	***	0.0003
C1/11/12/8 RipK3$^{-/-}$ vs TRIF	***	0.0001

Liver	Significant?	Adjusted p value
WT vs C1/11/12/8 RipK3$^{-/-}$	****	<0.0001
WT vs C8 RipK3$^{-/-}$	**	0.0013
WT vs C1/11/12 $^{-/-}$	**	0.0083
WT vs C1/11/12 RipK3$^{-/-}$	*	0.0453
WT vs TRIF	*	0.0413
C1/11/12/8 RipK3$^{-/-}$ vs C1/11$^{-/-}$	****	<0.0001
C1/11/12/8 RipK3$^{-/-}$ vs C8 RipK3$^{-/-}$	***	0.0003
C1/11/12/8 RipK3$^{-/-}$ vs C1/11/12 $^{-/-}$	****	<0.0001
C1/11/12/8 RipK3$^{-/-}$ vs C1/11/12 RipK3$^{-/-}$	*	0.0122
C1/11/12/8 RipK3$^{-/-}$ vs TRIF	***	0.0002

Gall bladder	Significant?	Adjusted p value
WT vs C1/11/12/8 RipK3$^{-/-}$	****	<0.0001
WT vs C8 RipK3$^{-/-}$	****	<0.0001
WT vs C1/11/12$^{-/-}$	**	0.0017
C1/11/12/8 RipK3$^{-/-}$ vs C1/11$^{-/-}$	****	<0.0001
C1/11/12/8 RipK3$^{-/-}$ vs. C8 RipK3$^{-/-}$	*	0.0215
C1/11/12/8 RipK3$^{-/-}$ vs C1/11/12$^{-/-}$	****	<0.0001
C1/11/12/8 RipK3$^{-/-}$ vs C1/11/12 RipK3$^{-/-}$	**	0.0022
C1/11/12/8 RipK3$^{-/-}$ vs TRIF	****	<0.0001
C1/11$^{-/-}$ vs C8 RipK3$^{-/-}$	**	0.0017
C8 RipK3$^{-/-}$ vs TRIF	*	0.0112

Table 7-4: Adjusted p values and statistical significances for indicated organ CFUs in mice of the indicated genotypes after injection with *S.* Typhimurium vaccine strain BRD509 ΔaroA depicted in Figure 4-2. C1/11/12$^{-/-}$ depicts BMDMs from caspase-1/11/12$^{-/-}$ mice, C8 RipK3 represents caspase-8 RipK3 deficient BMDMs and C1/11/12/8 RipK3 depicts BMDMs taken from caspase-1/11/12/8 and RipK3-deficient mice.

References

1. Lamkanfi M, Declercq W, Kalai M, Saelens X, Vandenabeele P. Alice in caspase land. A phylogenetic analysis of caspases from worm to man. *Cell Death Differ* 2002, **9**(4)**:** 358-361.

2. Shalini S, Dorstyn L, Dawar S, Kumar S. Old, new and emerging functions of caspases. *Cell Death Differ* 2015, **22**(4)**:** 526-539.

3. Miura M, Zhu H, Rotello R, Hartwieg EA, Yuan J. Induction of apoptosis in fibroblasts by IL-1 beta-converting enzyme, a mammalian homolog of the C. elegans cell death gene ced-3. *Cell* 1993, **75**(4)**:** 653-660.

4. Lamkanfi M, Festjens N, Declercq W, Vanden Berghe T, Vandenabeele P. Caspases in cell survival, proliferation and differentiation. *Cell Death Differ* 2007, **14**(1)**:** 44-55.

5. Ramirez MLG, Salvesen GS. A primer on caspase mechanisms. *Semin Cell Dev Biol* 2018.

6. Man SM, Tourlomousis P, Hopkins L, Monie TP, Fitzgerald KA, Bryant CE. Salmonella infection induces recruitment of Caspase-8 to the inflammasome to modulate IL-1beta production. *J Immunol* 2013, **191**(10)**:** 5239-5246.

7. Lawlor KE, Khan N, Mildenhall A, Gerlic M, Croker BA, D'Cruz AA*, et al.* RIPK3 promotes cell death and NLRP3 inflammasome activation in the absence of MLKL. *Nat Commun* 2015, **6:** 6282.

8. Ho LH, Taylor R, Dorstyn L, Cakouros D, Bouillet P, Kumar S. A tumor suppressor function for caspase-2. *Proc Natl Acad Sci U S A* 2009, **106**(13)**:** 5336-5341.

9. Fava LL, Schuler F, Sladky V, Haschka MD, Soratroi C, Eiterer L*, et al.* The PIDDosome activates p53 in response to supernumerary centrosomes. *Genes Dev* 2017, **31**(1)**:** 34-45.

10. Dorstyn L, Kumar S. Putative functions of caspase-2. *F1000 Biol Rep* 2009, **1:** 96.

11. Bouchier-Hayes L, Green DR. Caspase-2: the orphan caspase. *Cell Death Differ* 2012, **19**(1)**:** 51-57.

12. Lippens S, Kockx M, Knaapen M, Mortier L, Polakowska R, Verheyen A*, et al.* Epidermal differentiation does not involve the pro-apoptotic executioner caspases, but is associated with caspase-14 induction and processing. *Cell Death Differ* 2000, **7**(12)**:** 1218-1224.

13. Li J, Yuan J. Caspases in apoptosis and beyond. *Oncogene* 2008, **27**(48)**:** 6194-6206.

14. Fuentes-Prior P, Salvesen GS. The protein structures that shape caspase activity, specificity, activation and inhibition. *Biochem J* 2004, **384**(Pt 2)**:** 201-232.

15. Lahm A, Paradisi A, Green DR, Melino G. Death fold domain interaction in apoptosis. *Cell Death Differ* 2003, **10**(1)**:** 10-12.

16. Wachmann K, Pop C, van Raam BJ, Drag M, Mace PD, Snipas SJ*, et al.* Activation and specificity of human caspase-10. *Biochemistry* 2010, **49**(38)**:** 8307-8315.

17. Julien O, Wells JA. Caspases and their substrates. *Cell Death Differ* 2017, **24**(8)**:** 1380-1389.

18. Sakamaki K, Imai K, Tomii K, Miller DJ. Evolutionary analyses of caspase-8 and its paralogs: Deep origins of the apoptotic signaling pathways. *Bioessays* 2015, **37**(7)**:** 767-776.

19. Wang S, Miura M, Jung YK, Zhu H, Li E, Yuan J. Murine caspase-11, an ICE-interacting protease, is essential for the activation of ICE. *Cell* 1998, **92**(4)**:** 501-509.

20. Reed JC, Doctor K, Rojas A, Zapata JM, Stehlik C, Fiorentino L*, et al.* Comparative analysis of apoptosis and inflammation genes of mice and humans. *Genome Res* 2003, **13**(6B)**:** 1376-1388.

21. Koenig U, Eckhart L, Tschachler E. Evidence that caspase-13 is not a human but a bovine gene. *Biochem Biophys Res Commun* 2001, **285**(5)**:** 1150-1154.

22. Pop C, Salvesen GS. Human caspases: activation, specificity, and regulation. *J Biol Chem* 2009, **284**(33)**:** 21777-21781.

23. Parrish AB, Freel CD, Kornbluth S. Cellular mechanisms controlling caspase activation and function. *Cold Spring Harb Perspect Biol* 2013, **5**(6).

24. Earnshaw WC, Martins LM, Kaufmann SH. Mammalian caspases: structure, activation, substrates, and functions during apoptosis. *Annu Rev Biochem* 1999, **68:** 383-424.

25. Boatright KM, Renatus M, Scott FL, Sperandio S, Shin H, Pedersen IM*, et al.* A unified model for apical caspase activation. *Mol Cell* 2003, **11**(2)**:** 529-541.

26. Pop C, Timmer J, Sperandio S, Salvesen GS. The apoptosome activates caspase-9 by dimerization. *Mol Cell* 2006, **22**(2)**:** 269-275.

27. Riedl SJ, Salvesen GS. The apoptosome: signalling platform of cell death. *Nat Rev Mol Cell Biol* 2007, **8**(5)**:** 405-413.

28. Shearwin-Whyatt LM, Kumar S. Caspases in developmental cell death. *IUBMB Life* 1999, **48**(2)**:** 143-150.

29. Bratton SB, Salvesen GS. Regulation of the Apaf-1-caspase-9 apoptosome. *J Cell Sci* 2010, **123**(Pt 19)**:** 3209-3214.

30. Stennicke HR, Deveraux QL, Humke EW, Reed JC, Dixit VM, Salvesen GS. Caspase-9 can be activated without proteolytic processing. *J Biol Chem* 1999, **274**(13)**:** 8359-8362.

31. Rodriguez J, Lazebnik Y. Caspase-9 and APAF-1 form an active holoenzyme. *Genes Dev* 1999, **13**(24)**:** 3179-3184.

32. Zamaraev AV, Kopeina GS, Prokhorova EA, Zhivotovsky B, Lavrik IN. Post-translational Modification of Caspases: The Other Side of Apoptosis Regulation. *Trends Cell Biol* 2017, **27**(5)**:** 322-339.

33. Riley JS, Malik A, Holohan C, Longley DB. DED or alive: assembly and regulation of the death effector domain complexes. *Cell Death Dis* 2015, **6:** e1866.

34. Pop C, Fitzgerald P, Green DR, Salvesen GS. Role of proteolysis in caspase-8 activation and stabilization. *Biochemistry* 2007, **46**(14)**:** 4398-4407.

35. Oberst A, Pop C, Tremblay AG, Blais V, Denault JB, Salvesen GS*, et al.* Inducible dimerization and inducible cleavage reveal a requirement for both processes in caspase-8 activation. *J Biol Chem* 2010, **285**(22)**:** 16632-16642.

36. Fischer U, Janicke RU, Schulze-Osthoff K. Many cuts to ruin: a comprehensive update of caspase substrates. *Cell Death Differ* 2003, **10**(1)**:** 76-100.

37. Takahashi A, Hirata H, Yonehara S, Imai Y, Lee KK, Moyer RW*, et al.* Affinity labeling displays the stepwise activation of ICE-related proteases by Fas, staurosporine, and CrmA-sensitive caspase-8. *Oncogene* 1997, **14**(23)**:** 2741-2752.

38. Srinivasula SM, Ahmad M, Fernandes-Alnemri T, Litwack G, Alnemri ES. Molecular ordering of the Fas-apoptotic pathway: the Fas/APO-1 protease Mch5 is a CrmA-inhibitable protease that activates multiple Ced-3/ICE-like cysteine proteases. *Proc Natl Acad Sci U S A* 1996, **93**(25)**:** 14486-14491.

39. Muzio M, Salvesen GS, Dixit VM. FLICE induced apoptosis in a cell-free system. Cleavage of caspase zymogens. *J Biol Chem* 1997, **272**(5)**:** 2952-2956.

40. Riedl SJ, Shi Y. Molecular mechanisms of caspase regulation during apoptosis. *Nat Rev Mol Cell Biol* 2004, **5**(11)**:** 897-907.

41. Taylor RC, Cullen SP, Martin SJ. Apoptosis: controlled demolition at the cellular level. *Nat Rev Mol Cell Biol* 2008, **9**(3)**:** 231-241.

42. Kersse K, Vanden Berghe T, Lamkanfi M, Vandenabeele P. A phylogenetic and functional overview of inflammatory caspases and caspase-1-related CARD-only proteins. *Biochem Soc Trans* 2007, **35**(Pt 6)**:** 1508-1511.

43. Van de Craen M, Vandenabeele P, Declercq W, Van den Brande I, Van Loo G, Molemans F*, et al.* Characterization of seven murine caspase family members. *FEBS Lett* 1997, **403**(1)**:** 61-69.

44. Wang S, Miura M, Jung Y, Zhu H, Gagliardini V, Shi L*, et al.* Identification and characterization of Ich-3, a member of the interleukin-1beta converting enzyme (ICE)/Ced-3 family and an upstream regulator of ICE. *J Biol Chem* 1996, **271**(34)**:** 20580-20587.

45. Sollberger G, Strittmatter GE, Garstkiewicz M, Sand J, Beer HD. Caspase-1: the inflammasome and beyond. *Innate Immun* 2014, **20**(2)**:** 115-125.

46. Baker PJ, Boucher D, Bierschenk D, Tebartz C, Whitney PG, D'Silva DB*, et al.* NLRP3 inflammasome activation downstream of cytoplasmic LPS recognition by both caspase-4 and caspase-5. *Eur J Immunol* 2015, **45**(10)**:** 2918-2926.

47. Zhao Y, Shi J, Shao F. Inflammatory Caspases: Activation and Cleavage of Gasdermin-D In Vitro and During Pyroptosis. *Methods Mol Biol* 2018, **1714:** 131-148.

48. Shi J, Gao W, Shao F. Pyroptosis: Gasdermin-Mediated Programmed Necrotic Cell Death. *Trends Biochem Sci* 2017, **42**(4)**:** 245-254.

49. Lamkanfi M, Dixit VM. Mechanisms and functions of inflammasomes. *Cell* 2014, **157**(5)**:** 1013-1022.

50. Latz E, Xiao TS, Stutz A. Activation and regulation of the inflammasomes. *Nat Rev Immunol* 2013, **13**(6)**:** 397-411.

51. Shi J, Zhao Y, Wang Y, Gao W, Ding J, Li P*, et al.* Inflammatory caspases are innate immune receptors for intracellular LPS. *Nature* 2014, **514**(7521)**:** 187-192.

52. Lamkanfi M, Kalai M, Vandenabeele P. Caspase-12: an overview. *Cell Death Differ* 2004, **11**(4)**:** 365-368.

53. Vince JE, Wong WW, Gentle I, Lawlor KE, Allam R, O'Reilly L*, et al.* Inhibitor of apoptosis proteins limit RIP3 kinase-dependent interleukin-1 activation. *Immunity* 2012, **36**(2)**:** 215-227.

54. Park HH, Lo YC, Lin SC, Wang L, Yang JK, Wu H. The death domain superfamily in intracellular signaling of apoptosis and inflammation. *Annu Rev Immunol* 2007, **25:** 561-586.

55. Degterev A, Boyce M, Yuan J. A decade of caspases. *Oncogene* 2003, **22**(53)**:** 8543-8567.

56. Creagh EM. Caspase crosstalk: integration of apoptotic and innate immune signalling pathways. *Trends Immunol* 2014, **35**(12)**:** 631-640.

57. Chu LH, Gangopadhyay A, Dorfleutner A, Stehlik C. An updated view on the structure and function of PYRIN domains. *Apoptosis* 2015, **20**(2)**:** 157-173.

58. Vanaja SK, Rathinam VA, Fitzgerald KA. Mechanisms of inflammasome activation: recent advances and novel insights. *Trends Cell Biol* 2015, **25**(5)**:** 308-315.

59. Cui J, Li Y, Zhu L, Liu D, Songyang Z, Wang HY*, et al.* NLRP4 negatively regulates type I interferon signaling by targeting the kinase TBK1 for degradation via the ubiquitin ligase DTX4. *Nat Immunol* 2012, **13**(4)**:** 387-395.

60. Allen IC, Wilson JE, Schneider M, Lich JD, Roberts RA, Arthur JC*, et al.* NLRP12 suppresses colon inflammation and tumorigenesis through the negative regulation of noncanonical NF-kappaB signaling. *Immunity* 2012, **36**(5)**:** 742-754.

61. Periasamy S, Porter KA, Atianand MK, H TL, Earley S, Duffy EB*, et al.* Pyrin-only protein 2 limits inflammation but improves protection against bacteria. *Nat Commun* 2017, **8:** 15564.

62. Khare S, Ratsimandresey RA, de Almeida L, Cuda CM, Rellick SL, Misharin AV*, et al.* The PYRIN domain-only protein POP3 inhibits ALR inflammasomes and regulates responses to infection with DNA viruses. *Nat Immunol* 2014, **15**(4)**:** 343-353.

63. Dorfleutner A, Bryan NB, Talbott SJ, Funya KN, Rellick SL, Reed JC*, et al.* Cellular pyrin domain-only protein 2 is a candidate regulator of inflammasome activation. *Infect Immun* 2007, **75**(3)**:** 1484-1492.

64. Stehlik C, Krajewska M, Welsh K, Krajewski S, Godzik A, Reed JC. The PAAD/PYRIN-only protein POP1/ASC2 is a modulator of ASC-mediated nuclear-factor-kappa B and pro-caspase-1 regulation. *Biochem J* 2003, **373**(Pt 1)**:** 101-113.

65. Rathinam VA, Vanaja SK, Fitzgerald KA. Regulation of inflammasome signaling. *Nat Immunol* 2012, **13**(4)**:** 333-342.

66. Hermel E, Klapstein KD. A possible mechanism for maintenance of the deleterious allele of human CASPASE-12. *Med Hypotheses* 2011, **77**(5)**:** 803-806.

67. Xue Y, Daly A, Yngvadottir B, Liu M, Coop G, Kim Y*, et al.* Spread of an inactive form of caspase-12 in humans is due to recent positive selection. *Am J Hum Genet* 2006, **78**(4)**:** 659-670.

68. Stehlik C, Dorfleutner A. COPs and POPs: modulators of inflammasome activity. *J Immunol* 2007, **179**(12)**:** 7993-7998.

69. Bian ZM, Elner SG, Elner VM. Regulated expression of caspase-12 gene in human retinal pigment epithelial cells suggests its immunomodulating role. *Invest Ophthalmol Vis Sci* 2008, **49**(12)**:** 5593-5601.

70. Saleh M, Mathison JC, Wolinski MK, Bensinger SJ, Fitzgerald P, Droin N*, et al.* Enhanced bacterial clearance and sepsis resistance in caspase-12-deficient mice. *Nature* 2006, **440**(7087)**:** 1064-1068.

71. Vande Walle L, Jimenez Fernandez D, Demon D, Van Laethem N, Van Hauwermeiren F, Van Gorp H*, et al.* Does caspase-12 suppress inflammasome activation? *Nature* 2016, **534**(7605)**:** E1-4.

72. Matusiak M, Van Opdenbosch N, Lamkanfi M. CARD- and pyrin-only proteins regulating inflammasome activation and immunity. *Immunol Rev* 2015, **265**(1)**:** 217-230.

73. Le HT, Harton JA. Pyrin- and CARD-only Proteins as Regulators of NLR Functions. *Front Immunol* 2013, **4:** 275.

74. Lee SH, Stehlik C, Reed JC. Cop, a caspase recruitment domain-containing protein and inhibitor of caspase-1 activation processing. *J Biol Chem* 2001, **276**(37)**:** 34495-34500.

75. Humke EW, Shriver SK, Starovasnik MA, Fairbrother WJ, Dixit VM. ICEBERG: a novel inhibitor of interleukin-1beta generation. *Cell* 2000, **103**(1)**:** 99-111.

76. Hotchkiss RS, Strasser A, McDunn JE, Swanson PE. Cell death. *N Engl J Med* 2009, **361**(16)**:** 1570-1583.

77. Kerr JF, Wyllie AH, Currie AR. Apoptosis: a basic biological phenomenon with wide-ranging implications in tissue kinetics. *Br J Cancer* 1972, **26**(4)**:** 239-257.

78. Strasser A, Cory S, Adams JM. Deciphering the rules of programmed cell death to improve therapy of cancer and other diseases. *EMBO J* 2011, **30**(18)**:** 3667-3683.

79. Enari M, Hug H, Hayakawa M, Ito F, Nishimura Y, Nagata S. Different apoptotic pathways mediated by Fas and the tumor-necrosis-factor receptor. Cytosolic phospholipase A2 is not involved in Fas-mediated apoptosis. *Eur J Biochem* 1996, **236**(2)**:** 533-538.

80. Vaux DL, Strasser A. The molecular biology of apoptosis. *Proc Natl Acad Sci U S A* 1996, **93**(6)**:** 2239-2244.

81. Youle RJ, Strasser A. The BCL-2 protein family: opposing activities that mediate cell death. *Nat Rev Mol Cell Biol* 2008, **9**(1)**:** 47-59.

82. Placzek WJ, Wei J, Kitada S, Zhai D, Reed JC, Pellecchia M. A survey of the anti-apoptotic Bcl-2 subfamily expression in cancer types provides a platform to predict the efficacy of Bcl-2 antagonists in cancer therapy. *Cell Death Dis* 2010, **1:** e40.

83. Herman MD, Nyman T, Welin M, Lehtio L, Flodin S, Tresaugues L*, et al.* Completing the family portrait of the anti-apoptotic Bcl-2 proteins: crystal structure of human Bfl-1 in complex with Bim. *FEBS Lett* 2008, **582**(25-26)**:** 3590-3594.

84. Adams JM, Cory S. The Bcl-2 apoptotic switch in cancer development and therapy. *Oncogene* 2007, **26**(9)**:** 1324-1337.

85. Cosentino K, Garcia-Saez AJ. Bax and Bak Pores: Are We Closing the Circle? *Trends Cell Biol* 2017, **27**(4)**:** 266-275.

86. Uren RT, Iyer S, Kluck RM. Pore formation by dimeric Bak and Bax: an unusual pore? *Philos Trans R Soc Lond B Biol Sci* 2017, **372**(1726).

87. Marsden VS, O'Connor L, O'Reilly LA, Silke J, Metcalf D, Ekert PG*, et al.* Apoptosis initiated by Bcl-2-regulated caspase activation independently of the cytochrome c/Apaf-1/caspase-9 apoptosome. *Nature* 2002, **419**(6907)**:** 634-637.

88. Strasser A, O'Connor L, Dixit VM. Apoptosis signaling. *Annu Rev Biochem* 2000, **69:** 217-245.

89. Jost PJ, Grabow S, Gray D, McKenzie MD, Nachbur U, Huang DC*, et al.* XIAP discriminates between type I and type II FAS-induced apoptosis. *Nature* 2009, **460**(7258)**:** 1035-1039.

90. Larsen BD, Sorensen CS. The caspase-activated DNase: apoptosis and beyond. *FEBS J* 2017, **284**(8)**:** 1160-1170.

91. Dixit S, Dhar P, Mehra RD. Alpha lipoic acid (ALA) modulates expression of apoptosis associated proteins in hippocampus of rats exposed during postnatal period to sodium arsenite (NaAsO2). *Toxicol Rep* 2015, **2:** 78-87.

92. Segawa K, Nagata S. An Apoptotic 'Eat Me' Signal: Phosphatidylserine Exposure. *Trends Cell Biol* 2015, **25**(11)**:** 639-650.

93. Nagata S, Hanayama R, Kawane K. Autoimmunity and the clearance of dead cells. *Cell* 2010, **140**(5)**:** 619-630.

94. Nagata S. Apoptosis and Clearance of Apoptotic Cells. *Annu Rev Immunol* 2018, **36:** 489-517.

95. Shaltouki A, Freer M, Mei Y, Weyman CM. Increased expression of the pro-apoptotic Bcl2 family member PUMA is required for mitochondrial release of cytochrome C and the apoptosis associated with skeletal myoblast differentiation. *Apoptosis* 2007, **12**(12)**:** 2143-2154.

96. Weinlich R, Oberst A, Beere HM, Green DR. Necroptosis in development, inflammation and disease. *Nat Rev Mol Cell Biol* 2017, **18**(2)**:** 127-136.

97. Vandenabeele P, Galluzzi L, Vanden Berghe T, Kroemer G. Molecular mechanisms of necroptosis: an ordered cellular explosion. *Nat Rev Mol Cell Biol* 2010, **11**(10)**:** 700-714.

98. Newton K, Manning G. Necroptosis and Inflammation. *Annu Rev Biochem* 2016, **85:** 743-763.

99. Wu XN, Yang ZH, Wang XK, Zhang Y, Wan H, Song Y*, et al.* Distinct roles of RIP1-RIP3 hetero- and RIP3-RIP3 homo-interaction in mediating necroptosis. *Cell Death Differ* 2014, **21**(11)**:** 1709-1720.

100. Sun L, Wang H, Wang Z, He S, Chen S, Liao D*, et al.* Mixed lineage kinase domain-like protein mediates necrosis signaling downstream of RIP3 kinase. *Cell* 2012, **148**(1-2)**:** 213-227.

101. Chen W, Zhou Z, Li L, Zhong CQ, Zheng X, Wu X*, et al.* Diverse sequence determinants control human and mouse receptor interacting protein 3 (RIP3) and mixed lineage kinase domain-like (MLKL) interaction in necroptotic signaling. *J Biol Chem* 2013, **288**(23)**:** 16247-16261.

102. Wang H, Sun L, Su L, Rizo J, Liu L, Wang LF*, et al.* Mixed lineage kinase domain-like protein MLKL causes necrotic membrane disruption upon phosphorylation by RIP3. *Mol Cell* 2014, **54**(1)**:** 133-146.

103. Su L, Quade B, Wang H, Sun L, Wang X, Rizo J. A plug release mechanism for membrane permeation by MLKL. *Structure* 2014, **22**(10)**:** 1489-1500.

104. Cai Z, Jitkaew S, Zhao J, Chiang HC, Choksi S, Liu J*, et al.* Plasma membrane translocation of trimerized MLKL protein is required for TNF-induced necroptosis. *Nat Cell Biol* 2014, **16**(1)**:** 55-65.

105. Dondelinger Y, Declercq W, Montessuit S, Roelandt R, Goncalves A, Bruggeman I*, et al.* MLKL compromises plasma membrane integrity by binding to phosphatidylinositol phosphates. *Cell Rep* 2014, **7**(4)**:** 971-981.

106. Tanzer MC, Tripaydonis A, Webb AI, Young SN, Varghese LN, Hall C*, et al.* Necroptosis signalling is tuned by phosphorylation of MLKL residues outside the pseudokinase domain activation loop. *Biochem J* 2015, **471**(2)**:** 255-265.

107. Hildebrand JM, Tanzer MC, Lucet IS, Young SN, Spall SK, Sharma P*, et al.* Activation of the pseudokinase MLKL unleashes the four-helix bundle domain to induce membrane localization and necroptotic cell death. *Proc Natl Acad Sci U S A* 2014, **111**(42)**:** 15072-15077.

108. Chen X, Li W, Ren J, Huang D, He WT, Song Y*, et al.* Translocation of mixed lineage kinase domain-like protein to plasma membrane leads to necrotic cell death. *Cell Res* 2014, **24**(1)**:** 105-121.

109. de Zoete MR, Palm NW, Zhu S, Flavell RA. Inflammasomes. *Cold Spring Harb Perspect Biol* 2014, **6**(12)**:** a016287.

110. Vince JE, Silke J. The intersection of cell death and inflammasome activation. *Cell Mol Life Sci* 2016, **73**(11-12)**:** 2349-2367.

111. Martinon F, Tschopp J. Inflammatory caspases and inflammasomes: master switches of inflammation. *Cell Death Differ* 2007, **14**(1)**:** 10-22.

112. Man SM, Kanneganti TD. Gasdermin D: the long-awaited executioner of pyroptosis. *Cell Res* 2015, **25**(11)**:** 1183-1184.

113. Feng S, Fox D, Man SM. Mechanisms of Gasdermin Family Members in Inflammasome Signaling and Cell Death. *J Mol Biol* 2018.

114. Kayagaki N, Stowe IB, Lee BL, O'Rourke K, Anderson K, Warming S*, et al.* Caspase-11 cleaves gasdermin D for non-canonical inflammasome signalling. *Nature* 2015, **526**(7575)**:** 666-671.

115. Takeuchi O, Akira S. Pattern recognition receptors and inflammation. *Cell* 2010, **140**(6)**:** 805-820.

116. Dubois H, Wullaert A, Lamkanfi M. General Strategies in Inflammasome Biology. *Curr Top Microbiol Immunol* 2016, **397:** 1-22.

117. Man SM, Karki R, Kanneganti TD. Molecular mechanisms and functions of pyroptosis, inflammatory caspases and inflammasomes in infectious diseases. *Immunol Rev* 2017, **277**(1)**:** 61-75.

118. Lamkanfi M, Dixit VM. Inflammasomes and their roles in health and disease. *Annu Rev Cell Dev Biol* 2012, **28:** 137-161.

119. Kawai T, Akira S. The roles of TLRs, RLRs and NLRs in pathogen recognition. *Int Immunol* 2009, **21**(4)**:** 317-337.

120. Bortoluci KR, Medzhitov R. Control of infection by pyroptosis and autophagy: role of TLR and NLR. *Cell Mol Life Sci* 2010, **67**(10)**:** 1643-1651.

121. Kayagaki N, Warming S, Lamkanfi M, Vande Walle L, Louie S, Dong J*, et al.* Non-canonical inflammasome activation targets caspase-11. *Nature* 2011, **479**(7371)**:** 117-121.

122. Kayagaki N, Wong MT, Stowe IB, Ramani SR, Gonzalez LC, Akashi-Takamura S*, et al.* Noncanonical inflammasome activation by intracellular LPS independent of TLR4. *Science* 2013, **341**(6151)**:** 1246-1249.

123. Schauvliege R, Vanrobaeys J, Schotte P, Beyaert R. Caspase-11 gene expression in response to lipopolysaccharide and interferon-gamma requires nuclear factor-kappa B and signal transducer and activator of transcription (STAT) 1. *J Biol Chem* 2002, **277**(44)**:** 41624-41630.

124. Bauernfeind FG, Horvath G, Stutz A, Alnemri ES, MacDonald K, Speert D*, et al.* Cutting edge: NF-kappaB activating pattern recognition and cytokine receptors license NLRP3 inflammasome activation by regulating NLRP3 expression. *J Immunol* 2009, **183**(2)**:** 787-791.

125. Hagar JA, Powell DA, Aachoui Y, Ernst RK, Miao EA. Cytoplasmic LPS activates caspase-11: implications in TLR4-independent endotoxic shock. *Science* 2013, **341**(6151)**:** 1250-1253.

126. Ayala JM, Yamin TT, Egger LA, Chin J, Kostura MJ, Miller DK. IL-1 beta-converting enzyme is present in monocytic cells as an inactive 45-kDa precursor. *J Immunol* 1994, **153**(6)**:** 2592-2599.

127. Martinon F, Burns K, Tschopp J. The inflammasome: a molecular platform triggering activation of inflammatory caspases and processing of proIL-beta. *Mol Cell* 2002, **10**(2)**:** 417-426.

128. Kostura MJ, Tocci MJ, Limjuco G, Chin J, Cameron P, Hillman AG*, et al.* Identification of a monocyte specific pre-interleukin 1 beta convertase activity. *Proc Natl Acad Sci U S A* 1989, **86**(14)**:** 5227-5231.

129. Shi J, Zhao Y, Wang K, Shi X, Wang Y, Huang H*, et al.* Cleavage of GSDMD by inflammatory caspases determines pyroptotic cell death. *Nature* 2015, **526**(7575)**:** 660-665.

130. Ding J, Wang K, Liu W, She Y, Sun Q, Shi J*, et al.* Pore-forming activity and structural autoinhibition of the gasdermin family. *Nature* 2016, **535**(7610)**:** 111-116.

131. Sakamaki K, Satou Y. Caspases: evolutionary aspects of their functions in vertebrates. *J Fish Biol* 2009, **74**(4)**:** 727-753.

132. Shaw PJ, McDermott MF, Kanneganti TD. Inflammasomes and autoimmunity. *Trends Mol Med* 2011, **17**(2)**:** 57-64.

133. Kuemmerle-Deschner JB, Verma D, Endres T, Broderick L, de Jesus AA, Hofer F*, et al.* Clinical and Molecular Phenotypes of Low-Penetrance Variants of NLRP3: Diagnostic and Therapeutic Challenges. *Arthritis Rheumatol* 2017, **69**(11)**:** 2233-2240.

134. Aksentijevich I, Putnam CD, Remmers EF, Mueller JL, Le J, Kolodner RD*, et al.* The clinical continuum of cryopyrinopathies: novel CIAS1 mutations in North American patients and a new cryopyrin model. *Arthritis Rheum* 2007, **56**(4)**:** 1273-1285.

135. Shinkai K, McCalmont TH, Leslie KS. Cryopyrin-associated periodic syndromes and autoinflammation. *Clin Exp Dermatol* 2008, **33**(1)**:** 1-9.

136. O'Brien T, Lee D. Prospects for caspase inhibitors. *Mini Rev Med Chem* 2004, **4**(2)**:** 153-165.

137. Uren AG, Vaux DL. Molecular and clinical aspects of apoptosis. *Pharmacol Ther* 1996, **72**(1)**:** 37-50.

138. Frenette CT, Morelli G, Shiffman ML, Frederick RT, Rubin RA, Fallon MB*, et al.* Emricasan Improves Liver Function in Patients With Cirrhosis and High Model for End-stage Liver Disease Scores Compared With Placebo. *Clin Gastroenterol Hepatol* 2018.

139. Brumatti G, Ma C, Lalaoui N, Nguyen NY, Navarro M, Tanzer MC*, et al.* The caspase-8 inhibitor emricasan combines with the SMAC mimetic birinapant to induce necroptosis and treat acute myeloid leukemia. *Sci Transl Med* 2016, **8**(339)**:** 339ra369.

140. Dubois EA, Rissmann R, Cohen AF. Rilonacept and canakinumab. *Br J Clin Pharmacol* 2011, **71**(5)**:** 639-641.

141. Dinarello CA, Simon A, van der Meer JW. Treating inflammation by blocking interleukin-1 in a broad spectrum of diseases. *Nat Rev Drug Discov* 2012, **11**(8)**:** 633-652.

142. Dinarello CA. Blocking interleukin-1beta in acute and chronic autoinflammatory diseases. *J Intern Med* 2011, **269**(1)**:** 16-28.

143. Spohn G, Schori C, Keller I, Sladko K, Sina C, Guler R*, et al.* Preclinical efficacy and safety of an anti-IL-1beta vaccine for the treatment of type 2 diabetes. *Mol Ther Methods Clin Dev* 2014, **1:** 14048.

144. Fulda S. Therapeutic opportunities based on caspase modulation. *Semin Cell Dev Biol* 2017.

145. Howley B, Fearnhead HO. Caspases as therapeutic targets. *J Cell Mol Med* 2008, **12**(5A)**:** 1502-1516.

146. Callus BA, Vaux DL. Caspase inhibitors: viral, cellular and chemical. *Cell Death Differ* 2007, **14**(1)**:** 73-78.

147. Rickard JA, O'Donnell JA, Evans JM, Lalaoui N, Poh AR, Rogers T*, et al.* RIPK1 regulates RIPK3-MLKL-driven systemic inflammation and emergency hematopoiesis. *Cell* 2014, **157**(5)**:** 1175-1188.

148. Marsden VS, Ekert PG, Van Delft M, Vaux DL, Adams JM, Strasser A. Bcl-2-regulated apoptosis and cytochrome c release can occur independently of both caspase-2 and caspase-9. *J Cell Biol* 2004, **165**(6)**:** 775-780.

149. Yamamoto M, Sato S, Hemmi H, Hoshino K, Kaisho T, Sanjo H*, et al.* Role of adaptor TRIF in the MyD88-independent toll-like receptor signaling pathway. *Science* 2003, **301**(5633)**:** 640-643.

150. Schott WH, Haskell BD, Tse HM, Milton MJ, Piganelli JD, Choisy-Rossi CM*, et al.* Caspase-1 is not required for type 1 diabetes in the NOD mouse. *Diabetes* 2004, **53**(1)**:** 99-104.

151. De Nardo D, Kalvakolanu DV, Latz E. Immortalization of Murine Bone Marrow-Derived Macrophages. *Methods Mol Biol* 2018, **1784:** 35-49.

152. Rapp UR, Cleveland JL, Fredrickson TN, Holmes KL, Morse HC, 3rd, Jansen HW*, et al.* Rapid induction of hemopoietic neoplasms in newborn mice by a raf(mil)/myc recombinant murine retrovirus. *J Virol* 1985, **55**(1)**:** 23-33.

153. Karasuyama H, Melchers F. Establishment of mouse cell lines which constitutively secrete large quantities of interleukin 2, 3, 4 or 5, using modified cDNA expression vectors. *Eur J Immunol* 1988, **18**(1)**:** 97-104.

154. Salvamoser R, Brinkmann K, O'Reilly LA, Whitehead L, Strasser A, Herold MJ. Characterisation of mice lacking the inflammatory caspases-1/11/12 reveals no contribution of caspase-12 to cell death and sepsis. *Cell Death Differ* 2018.

155. Schindelin J, Arganda-Carreras I, Frise E, Kaynig V, Longair M, Pietzsch T*, et al.* Fiji: an open-source platform for biological-image analysis. *Nat Methods* 2012, **9**(7)**:** 676-682.

156. O'Reilly LA, Cullen L, Moriishi K, O'Connor L, Huang DC, Strasser A. Rapid hybridoma screening method for the identification of monoclonal antibodies to low-abundance cytoplasmic proteins. *Biotechniques* 1998, **25**(5)**:** 824-830.

157. O'Reilly LA, Cullen L, Visvader J, Lindeman GJ, Print C, Bath ML*, et al.* The proapoptotic BH3-only protein bim is expressed in hematopoietic, epithelial, neuronal, and germ cells. *Am J Pathol* 2000, **157**(2)**:** 449-461.

158. Schmittgen TD, Livak KJ. Analyzing real-time PCR data by the comparative C(T) method. *Nat Protoc* 2008, **3**(6)**:** 1101-1108.

159. Majowicz SE, Musto J, Scallan E, Angulo FJ, Kirk M, O'Brien SJ*, et al.* The global burden of nontyphoidal Salmonella gastroenteritis. *Clin Infect Dis* 2010, **50**(6)**:** 882-889.

160. Coburn B, Grassl GA, Finlay BB. Salmonella, the host and disease: a brief review. *Immunol Cell Biol* 2007, **85**(2)**:** 112-118.

161. Bhetwal A, Maharjan A, Khanal PR, Parajuli NP. Enteric Fever Caused by Salmonella enterica Serovars with Reduced Susceptibility of Fluoroquinolones at a Community Based Teaching Hospital of Nepal. *Int J Microbiol* 2017, **2017:** 2869458.

162. de Jong HK, Parry CM, van der Poll T, Wiersinga WJ. Host-pathogen interaction in invasive Salmonellosis. *PLoS Pathog* 2012, **8**(10)**:** e1002933.

163. Steele-Mortimer O. The Salmonella-containing vacuole: moving with the times. *Curr Opin Microbiol* 2008, **11**(1)**:** 38-45.

164. Gordon MA. Salmonella infections in immunocompromised adults. *J Infect* 2008, **56**(6)**:** 413-422.

165. Eng SK, Pusparajah P, Ab Mutalib NS, Ser HL, Chan KG, Lee LH. Salmonella: A review on pathogenesis, epidemiology and antibiotic resistance. *Front Life Sci* 2015, **8**(3)**:** 284-293.

166. Gal-Mor O, Boyle EC, Grassl GA. Same species, different diseases: how and why typhoidal and non-typhoidal Salmonella enterica serovars differ. *Front Microbiol* 2014, **5:** 391.

167. Franchi L. Role of inflammasomes in salmonella infection. *Front Microbiol* 2011, **2:** 8.

168. Broz P, Newton K, Lamkanfi M, Mariathasan S, Dixit VM, Monack DM. Redundant roles for inflammasome receptors NLRP3 and NLRC4 in host defense against Salmonella. *J Exp Med* 2010, **207**(8)**:** 1745-1755.

169. Antonopoulos C, Russo HM, El Sanadi C, Martin BN, Li X, Kaiser WJ*, et al.* Caspase-8 as an Effector and Regulator of NLRP3 Inflammasome Signaling. *J Biol Chem* 2015, **290**(33)**:** 20167-20184.

170. Jorgensen I, Rayamajhi M, Miao EA. Programmed cell death as a defence against infection. *Nat Rev Immunol* 2017, **17**(3)**:** 151-164.

171. Golstein P, Kroemer G. Redundant cell death mechanisms as relics and backups. *Cell Death Differ* 2005, **12 Suppl 2:** 1490-1496.

172. Shlomovitz I, Zargrian S, Gerlic M. Mechanisms of RIPK3-induced inflammation. *Immunol Cell Biol* 2017, **95**(2)**:** 166-172.

173. Wang X, Jiang W, Yan Y, Gong T, Han J, Tian Z*, et al.* RNA viruses promote activation of the NLRP3 inflammasome through a RIP1-RIP3-DRP1 signaling pathway. *Nat Immunol* 2014, **15**(12)**:** 1126-1133.

174. Feuillet V, Medjane S, Mondor I, Demaria O, Pagni PP, Galan JE*, et al.* Involvement of Toll-like receptor 5 in the recognition of flagellated bacteria. *Proc Natl Acad Sci U S A* 2006, **103**(33)**:** 12487-12492.

175. Akira S, Uematsu S, Takeuchi O. Pathogen recognition and innate immunity. *Cell* 2006, **124**(4)**:** 783-801.

176. Royle MC, Totemeyer S, Alldridge LC, Maskell DJ, Bryant CE. Stimulation of Toll-like receptor 4 by lipopolysaccharide during cellular invasion by live Salmonella typhimurium is a critical but not exclusive event leading to macrophage responses. *J Immunol* 2003, **170**(11)**:** 5445-5454.

177. Arpaia N, Godec J, Lau L, Sivick KE, McLaughlin LM, Jones MB*, et al.* TLR signaling is required for Salmonella typhimurium virulence. *Cell* 2011, **144**(5)**:** 675-688.

178. Eom JS, Seok Kim J, Im Jang J, Kim BH, Young Yoo S, Hyeon Choi J*, et al.* Enhancement of host immune responses by oral vaccination to Salmonella enterica serovar Typhimurium harboring both FliC and FljB flagella. *PLoS One* 2013, **8**(9)**:** e74850.

179. Yamamoto M, Sato S, Mori K, Hoshino K, Takeuchi O, Takeda K*, et al.* Cutting edge: a novel Toll/IL-1 receptor domain-containing adapter that preferentially activates the IFN-beta promoter in the Toll-like receptor signaling. *J Immunol* 2002, **169**(12)**:** 6668-6672.

180. Oshiumi H, Matsumoto M, Funami K, Akazawa T, Seya T. TICAM-1, an adaptor molecule that participates in Toll-like receptor 3-mediated interferon-beta induction. *Nat Immunol* 2003, **4**(2)**:** 161-167.

181. De Trez C, Pajak B, Brait M, Glaichenhaus N, Urbain J, Moser M*, et al.* TLR4 and Toll-IL-1 receptor domain-containing adapter-inducing IFN-beta, but not MyD88, regulate Escherichia coli-induced dendritic cell maturation and apoptosis in vivo. *J Immunol* 2005, **175**(2)**:** 839-846.

182. Kaiser WJ, Offermann MK. Apoptosis induced by the toll-like receptor adaptor TRIF is dependent on its receptor interacting protein homotypic interaction motif. *J Immunol* 2005, **174**(8)**:** 4942-4952.

183. Han KJ, Su X, Xu LG, Bin LH, Zhang J, Shu HB. Mechanisms of the TRIF-induced interferon-stimulated response element and NF-kappaB activation and apoptosis pathways. *J Biol Chem* 2004, **279**(15)**:** 15652-15661.

184. Gaidt MM, Ebert TS, Chauhan D, Schmidt T, Schmid-Burgk JL, Rapino F*, et al.* Human Monocytes Engage an Alternative Inflammasome Pathway. *Immunity* 2016, **44**(4)**:** 833-846.

185. Linkermann A, Green DR. Necroptosis. *N Engl J Med* 2014, **370**(5)**:** 455-465.

186. Rathinam VA, Vanaja SK, Waggoner L, Sokolovska A, Becker C, Stuart LM*, et al.* TRIF licenses caspase-11-dependent NLRP3 inflammasome activation by gram-negative bacteria. *Cell* 2012, **150**(3)**:** 606-619.

187. Zhivotovsky B, Orrenius S. Cell death mechanisms: cross-talk and role in disease. *Exp Cell Res* 2010, **316**(8)**:** 1374-1383.

188. Feltham R, Vince JE, Lawlor KE. Caspase-8: not so silently deadly. *Clin Transl Immunology* 2017, **6**(1)**:** e124.

189. Broz P, Ruby T, Belhocine K, Bouley DM, Kayagaki N, Dixit VM*, et al.* Caspase-11 increases susceptibility to Salmonella infection in the absence of caspase-1. *Nature* 2012, **490**(7419)**:** 288-291.

190. Mandal P, Feng Y, Lyons JD, Berger SB, Otani S, DeLaney A*, et al.* Caspase-8 Collaborates with Caspase-11 to Drive Tissue Damage and Execution of Endotoxic Shock. *Immunity* 2018, **49**(1)**:** 42-55 e46.

191. Rock KL, Kono H. The inflammatory response to cell death. *Annu Rev Pathol* 2008, **3:** 99-126.

192. Moreno-Gonzalez G, Vandenabeele P, Krysko DV. Necroptosis: A Novel Cell Death Modality and Its Potential Relevance for Critical Care Medicine. *Am J Respir Crit Care Med* 2016, **194**(4)**:** 415-428.

193. Salazar-Gonzalez RM, McSorley SJ. Salmonella flagellin, a microbial target of the innate and adaptive immune system. *Immunol Lett* 2005, **101**(2)**:** 117-122.

194. Elhadad D, Desai P, Rahav G, McClelland M, Gal-Mor O. Flagellin Is Required for Host Cell Invasion and Normal Salmonella Pathogenicity Island 1 Expression by Salmonella enterica Serovar Paratyphi A. *Infect Immun* 2015, **83**(9)**:** 3355-3368.

195. Horvitz HR. Genetic control of programmed cell death in the nematode Caenorhabditis elegans. *Cancer Res* 1999, **59**(7 Suppl)**:** 1701s-1706s.

196. Kumar S. Caspase function in programmed cell death. *Cell Death Differ* 2007, **14**(1)**:** 32-43.

197. Malin JZ, Shaham S. Cell Death in C. elegans Development. *Curr Top Dev Biol* 2015, **114:** 1-42.

198. Shaham S. Identification of multiple Caenorhabditis elegans caspases and their potential roles in proteolytic cascades. *J Biol Chem* 1998, **273**(52)**:** 35109-35117.

199. Kuida K, Haydar TF, Kuan CY, Gu Y, Taya C, Karasuyama H*, et al.* Reduced apoptosis and cytochrome c-mediated caspase activation in mice lacking caspase 9. *Cell* 1998, **94**(3)**:** 325-337.

200. Hakem R, Hakem A, Duncan GS, Henderson JT, Woo M, Soengas MS*, et al.* Differential requirement for caspase 9 in apoptotic pathways in vivo. *Cell* 1998, **94**(3)**:** 339-352.

201. Villunger A, Marsden VS, Zhan Y, Erlacher M, Lew AM, Bouillet P*, et al.* Negative selection of semimature CD4(+)8(-)HSA+ thymocytes requires the BH3-only protein Bim but is independent of death receptor signaling. *Proc Natl Acad Sci U S A* 2004, **101**(18)**:** 7052-7057.

202. McArthur K, Whitehead LW, Heddleston JM, Li L, Padman BS, Oorschot V*, et al.* BAK/BAX macropores facilitate mitochondrial herniation and mtDNA efflux during apoptosis. *Science* 2018, **359**(6378).

203. White MJ, McArthur K, Metcalf D, Lane RM, Cambier JC, Herold MJ*, et al.* Apoptotic caspases suppress mtDNA-induced STING-mediated type I IFN production. *Cell* 2014, **159**(7)**:** 1549-1562.

204. Lu EP, McLellan M, Ding L, Fulton R, Mardis ER, Wilson RK*, et al.* Caspase-9 is required for normal hematopoietic development and protection from alkylator-induced DNA damage in mice. *Blood* 2014, **124**(26)**:** 3887-3895.

205. Bergeron L, Perez GI, Macdonald G, Shi L, Sun Y, Jurisicova A*, et al.* Defects in regulation of apoptosis in caspase-2-deficient mice. *Genes Dev* 1998, **12**(9)**:** 1304-1314.

206. Nakagawa T, Zhu H, Morishima N, Li E, Xu J, Yankner BA*, et al.* Caspase-12 mediates endoplasmic-reticulum-specific apoptosis and cytotoxicity by amyloid-beta. *Nature* 2000, **403**(6765)**:** 98-103.

207. Strasser A, Pellegrini M. T-lymphocyte death during shutdown of an immune response. *Trends Immunol* 2004, **25**(11)**:** 610-615.

208. Manzl C, Fava LL, Krumschnabel G, Peintner L, Tanzer MC, Soratroi C*, et al.* Death of p53-defective cells triggered by forced mitotic entry in the presence of DNA damage is not uniquely dependent on Caspase-2 or the PIDDosome. *Cell Death Dis* 2013, **4:** e942.

209. Lim Y, De Bellis D, Dorstyn L, Kumar S. p53 accumulation following cytokinesis failure in the absence of caspase-2. *Cell Death Differ* 2018.

210. Dawar S, Lim Y, Puccini J, White M, Thomas P, Bouchier-Hayes L*, et al.* Caspase-2-mediated cell death is required for deleting aneuploid cells. *Oncogene* 2017, **36**(19)**:** 2704-2714.

211. Sladky V, Schuler F, Fava LL, Villunger A. The resurrection of the PIDDosome - emerging roles in the DNA-damage response and centrosome surveillance. *J Cell Sci* 2017, **130**(22)**:** 3779-3787.

212. Marsden VS, Strasser A. Control of apoptosis in the immune system: Bcl-2, BH3-only proteins and more. *Annu Rev Immunol* 2003, **21:** 71-105.

213. Lindsten T, Ross AJ, King A, Zong WX, Rathmell JC, Shiels HA*, et al.* The combined functions of proapoptotic Bcl-2 family members bak and bax are essential for normal development of multiple tissues. *Mol Cell* 2000, **6**(6)**:** 1389-1399.

214. Rathmell JC, Lindsten T, Zong WX, Cinalli RM, Thompson CB. Deficiency in Bak and Bax perturbs thymic selection and lymphoid homeostasis. *Nat Immunol* 2002, **3**(10)**:** 932-939.

215. Mason KD, Lin A, Robb L, Josefsson EC, Henley KJ, Gray DH*, et al.* Proapoptotic Bak and Bax guard against fatal systemic and organ-specific autoimmune disease. *Proc Natl Acad Sci U S A* 2013, **110**(7)**:** 2599-2604.

216. Erlacher M, Labi V, Manzl C, Bock G, Tzankov A, Hacker G*, et al.* Puma cooperates with Bim, the rate-limiting BH3-only protein in cell death during lymphocyte development, in apoptosis induction. *J Exp Med* 2006, **203**(13)**:** 2939-2951.

217. Bean GR, Ganesan YT, Dong Y, Takeda S, Liu H, Chan PM*, et al.* PUMA and BIM are required for oncogene inactivation-induced apoptosis. *Sci Signal* 2013, **6**(268)**:** ra20.

218. Ren D, Tu HC, Kim H, Wang GX, Bean GR, Takeuchi O*, et al.* BID, BIM, and PUMA are essential for activation of the BAX- and BAK-dependent cell death program. *Science* 2010, **330**(6009)**:** 1390-1393.

219. Strasser A, Harris AW, von Boehmer H, Cory S. Positive and negative selection of T cells in T-cell receptor transgenic mice expressing a bcl-2 transgene. *Proc Natl Acad Sci U S A* 1994, **91**(4)**:** 1376-1380.

220. Strasser A, Harris AW, Cory S. bcl-2 transgene inhibits T cell death and perturbs thymic self-censorship. *Cell* 1991, **67**(5)**:** 889-899.

221. Ogilvy S, Metcalf D, Print CG, Bath ML, Harris AW, Adams JM. Constitutive Bcl-2 expression throughout the hematopoietic compartment affects multiple lineages and enhances progenitor cell survival. *Proc Natl Acad Sci U S A* 1999, **96**(26)**:** 14943-14948.

222. Hashimoto T, Kikkawa U, Kamada S. Contribution of caspase(s) to the cell cycle regulation at mitotic phase. *PLoS One* 2011, **6**(3)**:** e18449.

223. Woo M, Hakem R, Furlonger C, Hakem A, Duncan GS, Sasaki T*, et al.* Caspase-3 regulates cell cycle in B cells: a consequence of substrate specificity. *Nat Immunol* 2003, **4**(10)**:** 1016-1022.

224. Woo M, Hakem R, Soengas MS, Duncan GS, Shahinian A, Kagi D*, et al.* Essential contribution of caspase 3/CPP32 to apoptosis and its associated nuclear changes. *Genes Dev* 1998, **12**(6)**:** 806-819.

225. Zhou X, Franklin RA, Adler M, Jacox JB, Bailis W, Shyer JA*, et al.* Circuit Design Features of a Stable Two-Cell System. *Cell* 2018, **172**(4)**:** 744-757 e717.

226. Biton S, Ashkenazi A. NEMO and RIP1 control cell fate in response to extensive DNA damage via TNF-alpha feedforward signaling. *Cell* 2011, **145**(1)**:** 92-103.

227. Lu M, Lawrence DA, Marsters S, Acosta-Alvear D, Kimmig P, Mendez AS*, et al.* Opposing unfolded-protein-response signals converge on death receptor 5 to control apoptosis. *Science* 2014, **345**(6192)**:** 98-101.

228. Glab JA, Doerflinger M, Nedeva C, Jose I, Mbogo GW, Paton JC*, et al.* DR5 and caspase-8 are dispensable in ER stress-induced apoptosis. *Cell Death Differ* 2017, **24**(5)**:** 944-950.

229. Crawford ED, Seaman JE, Barber AE, 2nd, David DC, Babbitt PC, Burlingame AL*, et al.* Conservation of caspase substrates across metazoans suggests

hierarchical importance of signaling pathways over specific targets and cleavage site motifs in apoptosis. *Cell Death Differ* 2012, **19**(12)**:** 2040-2048.

Author/s:
Salvamoser, Ranja

Title:
Analysing the impact of the absence of CARD containing caspases on different forms of cell death

Date:
2018

Persistent Link:
http://hdl.handle.net/11343/218091

File Description:
Analysing the impact of the absence of CARD containing caspases on different forms of cell death